JPRS-UMS-93-002
5 March 1993

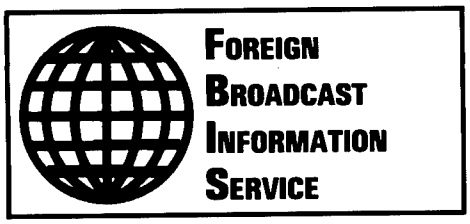

JPRS Report

Science & Technology

Central Eurasia: Materials Science

Science & Technology
Central Eurasia: Materials Science

JPRS-UMS-93-002

CONTENTS

5 March 1993

Analysis, Testing

Coatings

Composite Materials

Corrosion

Ferrous Metals

Nonferrous Metals, Alloys, Brazes, Solders

Nonmetallic Materials

Preparations

Treatments

Welding, Brazing, Soldering

Extractive Metallurgy, Mining

Miscellaneous

Study of Friction Coefficient of Composite 01 on Hardened Steel ShKh15

937D0042G Kiev SVERKHTVERDYYE MATERIALY in Russian No 5 (80), Sep-Oct 92 pp 47-50

[Article by G.S. Zheleznov, S.A. Singeyev, Syzran Branch of Samara Polytechnic Institute; UDC 621.91.01]

[Abstract] The friction coefficient of composite 01 on hardened steel ShKh15 with an HRC 60-62 hardness is examined in a model 16K20 lathe using a special simulator and cylindrical steel samples with a 150 mm diameter. The test rig consists of an indentor with a built-in thermocouple, a two-component strain gauge dynamometer, regulated power supply, a strain gauge amplifier, an oscilloscope, and a holder with the composite. A block diagram of the test rig for measuring the friction coefficient is cited and the design and operation of its components is outlined. The holder makes it possible to ensure cutting in direct proximity to the friction spot and preserve the juvenile surface already formed on the blank. The dependence of the friction coefficient on the contact temperature at various normal contact stresses and on the normal contact stress at various temperatures is plotted and the mean friction coefficient is found as a ratio of the friction force to normal force. An expression is derived for calculating the friction coefficient of composite 01 and hardened steel ShKh15; it can be recommended for calculating the friction coefficient as a function of cutting factors during machining of hardened steels by tools equipped with composite 01 under similar contact temperatures and stresses. Figures 4; references 1.

Force and Friction Coefficient Measurement During Optical Glass Polishing With Aquapol Tool

937D0042H Kiev SVERKHTVERDYYE MATERIALY in Russian No 5 (80), Sep-Oct 92 pp 52-55

[Article by V.V. Rogov, V.V. Shchipanov, A.V. Shchipanov, Superhard Materials Institute at the Ukrainian Academy of Sciences, Kiev and Tolyatti Polytechnic Institute; UDC 681.4.022.2]

[Abstract] The lack of theoretical and experimental data on the mechanism of removing the machining allowance from optical glass parts polished by suspensions containing rare earth polishing powders prompted a study of optical glass polishing with the Aquapol tool developed at the Superhard Materials Institute (ISM) at the Ukrainian Academy of Sciences on the basis of a composition of bound rare earth polishing powders. The study is conducted from a viewpoint of the molecular-adhesive (adhesive-deformation) theory of friction. The experimental procedure and units for determining the friction tool/glass interaction parameters are outlined and the dependence of the shear strength of the molecular bond on the actual pressure in the tool/optical glass contact zone is plotted. An analysis shows that the friction force which normally has two components—deformation and adhesion (or molecular)—is largely determined by the adhesion component and that fatigue wear is the dominant machining allowance removal mechanism. Figures 2; tables 1; references 6.

Dynamics of Magnetic Behavior of Alloy $Co_{0.53}Ga_{0.47}$ at Low Temperatures

937D0046A St. Petersburg FIZIKA TVERDOGO TELA in Russian Vol 34 No 5, May 92 pp 1332-1337

[Article by N. A. Belous, I. A. Zorin, N. V. Kulich, I. V. Lezhnenko, and A. 5I. Tovstolytkin, Institute of Physics of Metals, Ukrainian Academy of Sciences, Kiev; UDC 548:537.621]

[Abstract] Temperature and time dependences of $Co_{0.53}Ga_{0.47}$ alloy's magnetization were investigated. It was found that aging effects strongly alter the character of relaxation curves at temperatures below T_1 = 8.5 K (the transition temperature to the spin glass state is T_f = 10 K). The effect of slight temperature variations on aging processes was investigated. It was concluded that the maximum time τ_{max} in the spectrum of relaxation times for the alloy in question is less than 200 seconds at $T > 8.5$ K. Peculiarities of the magnetic behavior of $Co_{0.53}Ga_{0.47}$ alloy are due to random local anisotropy of antistructural formations of cobalt.

High-Temperature Plastic Deformation and Luminescence Properties of GaAs

937D0046B St. Petersburg FIZIKA TVERDOGO TELA in Russian Vol 34 No 5, May 92 pp 1390-1394

[Article by O. K. Gorodnichenko, V. F. Kovalenko, and A. V. Prokhorovich, Institute of Semiconductors, Ukrainian Academy of Sciences, Kiev; UDC 621.315.592]

[Abstract] In a photoluminescence investigation of the effect of high-temperature (800-1100° C) plastic deformation on the properties of strongly doped crystals of *n*-GaAs(Sn), the effect of deformation-induced disintegration of complex groups at elevated deformation temperatures was discovered for the first time. This effect is due to a decrease in the concentration of groups of the type impurity-intrinsic defect, which are centers of radiative recombination, as a result of their interaction with elastic fields of dislocation stresses.

On the Magnetic Structure of Y_2BaCuO_5

937D0046C St. Petersburg FIZIKA TVERDOGO TELA in Russian Vol 34 No 5, May 92 pp 1460-1464

[Article by O. D. Kolotiy and V. A. Blinkin, Institute of Single Crystals, Ukrainian Academy of Sciences, Kharkov; UDC 537.611.45]

[Abstract] The magnetic structure of Y_2BaCuO_5 was analyzed on the basis of neutron-measuring data obtained in an earlier work by T. Chattopadhyay, P. J. Brown, U. Kobler and M. Wilhelm. It was demonstrated that the data from that work do not permit an unequivocal conclusion about the character of antiferromagnetic ordering. More likely there is another, collinear type of ordering of magnetic moments of Cu^{2+} ions corresponding to the only wave vector k_1 = (00 1/2). A second magnetic reflex at θ = 28.8° which was noted in the earlier work and attributed to a second wave vector k_2 = (1/2 0 1/2) can probably be explained also by scattering of neutrons by antiferromagnetically ordered Cu^{2+} ions of the impurity phase $YBa_2Cu_3O_6 + x$.

Magnetic and Crystal Structure of Rare-Earth Cuprates Re_2BaCuO_5

937D0046D St. Petersburg FIZIKA TVERDOGO TELA in Russian Vol 34 No 5, May 92 pp 1473-1481

[Article by I. V. Golosovskiy, V. P. Plakhtiy, V. P. Kharchenkov, Ya. Zoubkova, B. V. Mill, M. Bonne, and Ye. Rudo, Nuclear Physics Institute im. B. P. Konstantinov, Russian Academy of Sciences, St. Petersburg]

[Abstract] Based on results of neutron diffraction in polycrystalline specimens, magnetic order was determined in the cuprates Re_2BaCuO_5, where Re = Dy, Ho, Er, Tm and Yb at different temperatures. Parameters of crystal structure in the paramagnetic phase were obtained. Different antiferromagnetic structures were observed in all of the investigated compounds, and spin-reorientation transitions at different temperatures were detected for Dy_2BaCuO_5 and Ho_2BaCuO_5.

Low-Temperature Magnetic Phase Transition in $YBa_2(Cu_{1-x}Fe_x)_3O_7 + \delta$ ($0.15 \leq x \leq 0.30$) Accompanied by Change in Electron Structure of Fe Atoms

937D0046E St. Petersburg FIZIKA TVERDOGO TELA in Russian Vol 34 No 5, May 92 pp 1482-1485

[Article by I. S. Lyubutin, V. G. Terziyev, T. V. Dmitriyeva, and A. Ya. Shapiro, Crystallography Institute, Russian Academy of Sciences, Moscow]

[Abstract] In $YBa_2(Cu_{1-x}Fe_x)_3O_7 + \delta$ for $0.15 \leq x \leq 0.30$, two magnetic phase transitions were discovered at $T_{m1} \approx 30$ and $T_{m2} \approx 400$ K, in which atoms of iron in different structural positions undergo transition from the magnetically ordered to the paramagnetic state. It was determined that the low-temperature transition is accompanied by a change in the electron structure of iron atoms which is presumed to proceed as follows: $Fe^{4+}_k = 5$ ($S = 2$) $\rightarrow$ $Fe^{3+}_k = 5$ ($S = 3/2$).

Investigation of YBaCuO Ceramics by Positron Annihilation and Rutherford Backscattering Techniques

937D0047A St. Petersburg FIZIKA TVERDOGO TELA in Russian Vol 34 No 5, May 92 pp 1502-1509

[Article by A. Z. Ilyasov, A. V. Mikhaylin, H.-J. Kaufmann, and B. I. Smirnov, Physical-Technical Institute im. A. F. Ioffe, Russian Academy of Sciences, St. Petersburg; UDC 539.124.6.03+62.039.8]

[Abstract] Positron annihilation and Rutherford backscattering techniques were used to investigate ceramics of the system $YBa_2Cu_3O_{7-x}$ for $x = 0.05$, 0.34 and 0.78. Angular correlation curves of annihilation gamma quanta were measured in the temperature range 80-300 K. It was found that in the case of $x = 0.05$ and 0.34, anomalous behavior of the *f*-parameter is observed near 90 K. In all ceramics there is also an *f*-parameter anomaly at higher temperatures, and its position shifts toward lower temperatures as x increases (from 220 K at $x = 0.05$ to 160 K at $x = 0.78$). As oxygen content increases, the magnitude of the *f*-parameter itself decreases. The positron mean lifetime increases and the effective oxygen charge decreases as x increases. The latter indicates a dominant role for Cu(1)-O(4) chains in formation of the superconductive state.

Radiation Defects and Thermoluminescence of Barium Fluoride

937D0047B St. Petersburg FIZIKA TVERDOGO TELA in Russian Vol 34 No 5, May 92 pp 1510-1512

[Article by G. N. Zakharov, A. Kh. Kkhudro, Ye. N. Melchakov, P. A. Rodnyy, and V. V. Yanovskiy, State Technical University, St. Petersburg, and Nuclear Physics Institute, Gatchina; UDC 539.21:535.377]

[Abstract] Characteristics of heat-stimulated luminescence of BaF_2 and BaF_2-LaF_3 crystals irradiated with different types of radiation were determined. Processes of interaction of radiation defects which take part in crystals' radiation were examined.

Thermomagnetic Effect in Inhomogeneous Superconducting Films

937D0047C St. Petersburg FIZIKA TVERDOGO TELA in Russian Vol 34 No 5, May 92 pp 1541-1545

[Article by Yu. M. Galperin and V. I. Kozub, Physical-Technical Institute im. A. F. Ioffe, Russian Academy of Sciences, St. Petersburg]

[Abstract] Possibilities are discussed for noncontact diagnostics of the degree of homogeneity of superconducting films according to the distribution of fluctuation magnetic fields arising at the film surface as a temperature gradient is created along the surface. The nature of these fields, their quantitative characteristics and their dependence on temperature and geometry of the experiment are examined. It is thought that studying the temperature dependence of fluctuation thermomagnetic fields can yield valuable information on the nature and statistics of inhomogeneities of high-temperature superconducting films, especially in the vicinity of the transition point.

NMR Investigation of Magnetic Structure of $Tb_xY_{3-x}Fe_5O_{12}$ Garnets

937D0047D St. Petersburg FIZIKA TVERDOGO TELA in Russian Vol 34 No 5, May 92 pp 1565-1571

[Article by V. D. Doroshev and M. M. Savosta, Donetsk Physical-Technical Institute; UDC 548:537.611.46]

[Abstract] At $T = 4.2$ K, NMR of Fe^{57} was studied in octahedral and tetrahedral sites of $Tb_xY_{3-x}Fe_5O_{12}$ (x = 0.1, 0.26) garnets with an easy direction of magnetization [001]. Analysis of the position of satellite lines in spectra made it possible to determine the magnetic structure of the rare- earth sublattice: $m = 8.53\ (20)\ \mu_b$, $m' \cos \varphi = 5.65\ (20)\ \mu_b$, $\varphi < 30°$. Comparing the results with magnetic measurement data, it was concluded that the magnetic structure of the terbium sublattice is independent of the terbium concentration x (where the easy direction of magnetization is constant). On this basis it was demonstrated that the abrupt change in magnetization of $Tb_3Fe_5O_{12}$ in a magnetic field $\mathbf{H} \parallel [001]$ is due to an orientation phase transition [111] $\rightarrow$ [001] induced by the magnetic field.

Possibility of Determining Type of Josephson Junction by Its Noise Characteristics

937D0047E St. Petersburg FIZIKA TVERDOGO TELA in Russian Vol 34 No 5, May 92 pp 1620-1623

[Article by V. M. Zakosarenko and Ye. V. Ilichov, Institute for Problems of Technology of Microelectronics and Superpure Materials, Russian Academy of Sciences, Chernogolovka]

[Abstract] It is demonstrated that a weak connection can be a source of flicker noise in ceramic high-frequency superconducting quantum interference devices made of high-temperature superconductors. Weighing experimental results against evaluations of noise based on the model of bilevel systems (theory of low-frequency electrical noise), it was determined that this model consistently describes low-frequency noise of a Josephson junction in ceramics, and that the most likely one is a junction of the *S-N-S* type.

Low-Frequency Electromagnetic Losses for the High-Temperature Superconductor $YBa_2Cu_3O_{7-\delta}$ in Magnetic Fields up to H_{c1}

937D0047F St. Petersburg FIZIKA TVERDOGO TELA in Russian Vol 34 No 5, May 92 pp 1625-1627

[Article by D. G. Andrianov, I. V. Matveyev, Ye. A. Khalyavin, S. B. Burgorskiy, I. P. Zautin, and Yu. V. Mezentsev, State Research and Planning Institute of the Rare Metals Industry, Moscow; UDC 537.312.620]

[Abstract] Low-frequency electromagnetic losses for the high-temperature superconductor $YBa_2Cu_3O_{7-\delta}$ were measured by the method of low-temperature adiabatic calorimetry. For such a material the calorimeter was modified for small variable magnetic fields limited by the small value H_{c1}, which is characteristic for high- temperature superconducting materials. All measurements were made at 4.2 K. Analysis of the results indicated that losses in the Moessbauer region had a hysteresis character.

Temper Resistance of Martensite of Cu-Al-Zn Alloys

937D0050 Kiev METALLOFIZIKA in Russian Vol 14 No 6, Jun 92 (manuscript received 13 Mar 92) pp 32-38

[Article by O.G. Zotov and S.Yu. Kondratyev, Technical University, St.Peterburg, Yu.N. Koval, Institute of Metal Physics at Ukrainian Academy of Sciences, Kiev; UDC 669.35'5'71:346.2]

[Abstract] An experimental study of quenched Cu-Al-Zn alloys with a martensite phase was made concerning the kinetics of its breakup and thus its thermodynamic stability during tempering. Alloys with 7.5-10.5 percent wt. Al and 0-17 percent wt. Zn were produced by melting commercially pure metals in a high-frequency induction furnace and then quenched from 700°C in water. The temper resistance of their martensite phase at 250°C and 300°C (below the temperature of beginning of martensite breakup) was estimated on the basis of relative changes in the electrical resistivity and in the Vickers hardness over a 520 min long period and then over an additional 700 min long period. The martensite breakup activation energy was calculated according to the Arrhenius equation. Metallographic examination was performed under a Neophot-21 optical microscope with X100 to X1000 magnifications. The thermal characteristics of martensite breakup were measured with a Chevernard dilatometer. The results indicate existence of two kinds of martensite in the quenched state, depending on the chemical composition of the alloy: 1) teniform (18R) martensite, its weight fraction increasing with higher Al content; 2) spicular (2H) martensite, its weight fraction increasing with higher Zn content. The results also indicate that during tempering of the metastable martensite phase at those temperatures there first takes place diffusionless transformation of its crystalline structure (stage 1), soon attended by preliminary precipitation of stable phases with an increase of hardness (stage 2), and then completed by diffusion throughout the entire volume of an alloy specimen (stage 3). While the preliminary first two stages are of relatively short duration each, the third stage is the longest. The entire breakup was completed in 520 min, extension of the tempering treatment beyond this period having resulted only in coagulation of the stable phases. Increasing the amount of alloying elements was found to lower the thermal stability of the quenched alloy by raising the intensity of structural changes during tempering. Increasing the Zn content had no effect on the trend of this process, while increasing the Al content caused the first two stages to degenerate and the formation of stable phases to be thus accelerated. Calculation of the activation energy for thermally activated diffusional breakup of the martensite has yielded 30-80 kJ/mole, depending on the chemical composition of the alloy. Figures 4; tables 1; references 7.

Magnetic Properties of Amorphous 81.5 Fe-16 P-2.5 V and 81.5 Fe-16 P-2.5 Mo Alloys Produced by Ion-Plasma Sputtering

937D0050B Kiev METALLOFIZIKA in Russian Vol 14 No 6, Jun 92 (manuscript received 10 Mar 92, final version received 6 Jul 92) pp 53-55

[Article by I.V. Sychev, I.V. Zolotukhin, and V.V. Vavilova, Voronezh Polytechnic Institute; UDC 539.213.32]

[Abstract] Magnetic and magnetoelastic properties of amorphous 81.5 Fe-16 P-2.5 V and 81.5 Fe-16 P-2.5 Mo alloys for high-frequency magnetic cores and ultrasonic delay lines were studied, 5-30 μm thick films of both alloys having been produced from Fe + 35 atom. percent P ferrophosphorus targets with 99.9 percent pure Fe and 99.9 percent pure V or 99.98 percent pure Mo admixtures by ion-plasma sputtering. Both alloys were amorphous, according to their X-ray diffraction patterns with, a 0.25 +/- 0.01 nm interatomic distance in each. Their magnetoelastic properties were measured by the resonance-antiresonance method at frequencies covering the 0.1-1 MHz range, the results revealing a very strong ΔE-effect: $(E_H - E_0)/E_0$ = (E_H, E_0-modulus of elasticity in a magnetic field and without a magnetic field respectively). The magnitude of this effect at a 1 MHz field frequency was 0.23 in the Fe-P-V alloy and 0.28 in the Fe-P-Mo alloy. Magnetostriction was measured by the cantilever-capacitance method. The coercive force and the saturation magnetic flux density were measured by the ballistic method in a magnetic fields of up to 200 kA/m intensity, the results

revealing a high magnetic permeability of both alloys: 340 (Fe-P-V) and 850 (Fe-P-Mo) at 1 MHz. Internal friction at frequencies of 300-1500 Hz was measured while the films were heated at a rate of 0.04 K/s. The crystallization temperature, based on these measurements, was 663 +/- 5 K for both alloys. Both alloys are also known to have the same Curie point at 525 K. Tables 1; references 7.

Relaxation Processes during Plastic Deformation of Tungsten

937D0050C Kiev METALLOFIZIKA in Russian Vol 14 No 6, Jun 92 (manuscript received 8 Jul 91, final version received 15 May 92) pp 56-67

[Article by Ye.E. Zasimchuk and V.M. Zamyatnin, Institute of Metal Physics at Ukrainian Academy of Sciences, Kiev; UDC 539.3;548.4]

[Abstract] An experimental study of polycrystalline sintered tungsten was made concerning its structural relaxation during plastic deformation by hot rolling. Powder of 99.95 percent pure tungsten grains of the 12 μm size fraction was compacted into a 27.5 mm thick blank, which was then heated to 1953 K within 5 min in a protective hydrogen atmosphere. It was immediately rolled down to a 4.8 mm thickness in three passes without intermediate reheating so that its temperature dropped to 1273 K at the end of this process, followed by air cooling. A piece was then cut off for examination of the W(1) tungsten structure. The other piece was heated to 1593 K within 4 min in the same protective atmosphere and immediately rolled down further to a 1.65 mm thickness in seven passes without intermediate reheating so that its temperature dropped to 1173 K at the end of this process, again followed by air cooling. A second piece was then cut off for examination of the W(2) tungsten structure. The remaining piece was heated to 893 K within 10 min in the same protective atmosphere and immediately rolled down further to a 1 mm thickness, but this time with intermediate reheating to 893 K within 40-60 s after each pass, then air cooled prior to examination of the W(3) tungsten structure. It could not be rolled down further at temperatures lower than 893 K. A separate plate of also 27.5 mm original thickness was rolled down in identical three stages, but with reheating to 1953 K within 40-60 s in a hydrogen atmosphere after each pass, then also air cooled prior to examination of the W(4) tungsten structure. This structure served as reference for comparative analysis of the other three. Structural examination was done under a transmission electron microscope, also under a scanning electron microscope and an optical one. The images revealed that lowering the rolling temperature had influenced the microstructure in the direction of rolling, two different structures having formed in the process: 1) relaxation structures characterized by equiaxiality, the kinetics of their formation being consistent with the theory of static recrystallization; 2) self-adaptive structures characterized by diffuse microdiffraction in the azimuthal direction, "ripple" and striae, cells with blurry boundaries, and appearance of extinction contours under the transmission electron microscope. Hydrodynamic plastic flow of tungsten in its structurally unstable state can evidently develop into a turbulent one, as also indicated by the "vortex" pattern appearing after recrystallization where a phase transformation had taken place during deformation. Figures 6; references 12.

Structural Transformation in Thin $TiSi_2$ Films

937D0050D Kiev METALLOFIZIKA in Russian Vol 14 No 6, Jun 92 (manuscript received 22 Nov 91) pp 74-80

[Article by Yu.A. Bespalov, Yu.A. Kunitskiy, Yu.N. Makagon, S.I. Sidorenko, A.L. Pryadkina, and Zh.D. Shinkarenko, Kiev Polytechnic Institute; UDC 669.018:539.213]

[Abstract] An experimental study of thin $TiSi_2$ films was made concerning their microscopic structural transformations during heat treatment. The films were 30 nm thick, produced from a bulky target by sputtering in a discharge magnetron with an argon plasma. They were heated at a rate of 6 K/min directly inside the column of an EM-200 electron microscope, while Fraunhofer diffraction patterns on bright-field images of the structure were identified with the aid of a diverging laser beam. Their amorphous initial state at 293 K was characterized by blurry diffraction spectra with a slight elongation of inhomogeneities within the 60-240° sector. Relaxation annealing at 380 K their increased the shape anisotropy of inhomogeneities and the amplitude of peaks on transverse sections through diffraction patterns. The films were also annealed at higher temperatures: 550-570 K, 670 K, 760 K, and 940 K. The optical Fourier spectra as well as the EM-200 images and the electron diffraction patterns indicate that relaxation annealing of these films was attended by a redistribution of silicon and void space, crystallization beginning at 670 K with attendant precipitation of the Ti_5Si_3 phase at boundaries between matrix and structural inhonmogeneities. In order to achieve nucleation of this phase within the matrix too, it was necessary to raise the annealing temperature to 760 K. Subsequent growth of this phase was controlled principally by the diffusion of silicon. The authors thank Professor M.V. Belousov for helpful discussion. Figures 3; tables 3; references 10.

Waveform of Acoustic Emission Signals Generated in Ferromagnetic Materials during Quasi-Static Magnetization Reversal

937D0050E Kiev METALLOFIZIKA in Russian Vol 14 No 6, Jun 92 (manuscript received 8 Oct 91) pp 88-91

[Article by O.A. Bartenev and V.I. Borodin, Izhev State University, V.A. Khamitov, Institute of Engineering Physics at Ural Science Center, Russian Academy of Sciences, Yekaterinburg, A.A. Yudin, Scientific-Industrial Association's Central Scientific Research Institute of Machine Building Technology; UDC 669.1+669.14: 539.374]

[Abstract] The waveform of acoustic emission signals generated in ferromagnetic materials during quasi-static magnetization and magnetization reversal is analyzed, experimental data on changes in their waveform being interpreted on the premise that the cause of magnetoacoustic emission are stress waves generated by the Barkhausen effect. The experiment involved four polycrystalline ferromagnetic materials with widely different domain structures: nickel, 34CrNi3No medium-carbon

alloy steel, 47 Fe-49 Co-4 V Permendur, and 66.67 Fe-24.33 Dy-9 Tb Terfenol. While magnetization was being quasi-statically reversed at a frequency of about 0.05 Hz, the magnetic induction B as well as the magnetostriction coefficient λ and the r.m.s. voltage U of emission signals were measured for an evaluation of their dependence on the magnetic field intensity H. While the B-H curves and the λ-H curves of the four materials were quite similar, their U-H curves differed appreciably. This indicates that the waveform of magnetoacoustic emission signals is quite sensitive to changes of the domain structure. Its effectiveness as a monitor of magnetization and magnetization reversal is demonstrated by an analysis of the data according to the theory of stochastic processes, as has been done for acoustic emission caused by plastic deformation and magnetostrictive deformation being considered here instead. The analysis is, for specificity, applied to a rod in a longitudinal magnetic field. In the case of a long rod inside a solenoid energized by a current with a triangular waveform so that the rate of change of the magnetic field is constant, the power and thus also the r.m.s. voltage of the acoustic emission signal are shown rise to a sharp peak where the λ-H curve passes through its minimum. This analysis needs to be refined by extending the stochastic theory of magnetoacoustic emission to a three-dimensional model of the domain structure. Figures 2; references 5.

Secondary Processes and a Complex Interaction Mechanism During External Friction Between Bodies

937D0052A Minsk TRENIYE I IZNOS in Russian Vol 13 No 5, Sep-Oct 92 pp 816-824

[Article by A. V. Boroday, Novocherkassk Polytechnic Institute imeni Sergo Ordzhonikidze; UDC 539.62]

[Abstract] A generalized model of multi-level primary transverse wave and secondary friction processes was presented. It was concluded that the secondary processes consist of several interrelated diffusion and physico-chemical contact transformations caused by transverse wave energy losses arising from relative tangential contact body displacement. The critical periodic component of the secondary processes is a consequence of the elastic absorption of part of these energy losses. The secondary processes unfold on three basic levels of time and space determined by the distance between the friction surfaces and the layers in which these processes occur and by their thickness. Thus, the friction process also occurs on three levels with different interaction intensities and frequency characteristics. Wear to the mating surfaces is caused by the difference in the levels of energy lost, which is elastically absorbed by the surface layers of the two bodies in contact. The periodic component has a tendency to reduce the average level of complex physico-chemical contact potential, increase the average frequency of the primary process, increase surface barrier strength, and establish negative feedback between the primary and secondary processes, making the entire set of contact processes a unified mechanism of friction interaction. This feedback is constrained by the level of friction loss and wear intensity and can be increased by ensuring that the average absolute rate of change in the physico-chemical potential can increase as a function of the structure and composition of contact zone substances and lubricants which enhance energy loss absorption. The temperature of the contact zone, which is a function of inelastic energy loss absorption, should fall within a range that precludes continuous thermal breakdown of the lubricants and ensures the existence of the periodic component. Thus, speed of contact body interaction is constrained by frictional heating. Figures 4; references 10: Russian.

Development of a Method for the Automated Design of Optimal Sliding Bearings and Their Use in the Bearing Assemblies of Mechanical Sucker-Rod Oil-Pumping Units

937D0052C Minsk TRENIYE I IZNOS in Russian Vol 13 No 5, Sep-Oct 92 pp 848-856

[Article by Z. E. Eyvazova, A. Kh. Dzhanakhmedov, and M. A. Vagidov, the Azerbaijan State Petroleum Academy, Baku; UDC 621.822.5:622.276.53]

[Abstract] An automated design method was developed for the sliding bearings used in the bearing assemblies of oilfield pumping jacks. The problem of optimal bearing design was presented as a third-degree dual integral function expressing lining wear and bearing shaft flexure with constraints expressed in terms of bearing strength and heat resistance criteria and a lubricity criterion. Geometric programming was used to solve the problem, which was then applied to calculate the load placed upon the bearing assembly of a low-speed Ts2NSh-750 reduction gear shaft. The curves thus derived were referenced to a working dynamograph taken from Azizbekovneft Well No. 7297, which is rigged with a 7SK8-3.5-4000 pumping jack. Curves were also calculated for a modern SKD8-3-4000 pumping jack and plotted on the same graph. These calculations made it possible to find the mean integral values for the bearing load, which in both cases was equal to 54.5 kN, and to determine the optimal bearing dimensions, which turned out to be 0.165 m for the bearing diameter and 0.3 m for the lining length. This method was used successfully to design sliding bearing assemblies for the walking beams and the low-speed shafts for standard production Ts2NSh-750B-based reduction gears in 80-kN oil-pumping jacks that will be manufactured by the Sibneftimash [Siberian Oilfield Equipment] plant in Tyumen. Figures 6; references 11: Russian.

Analytical Determination of Wear to Metal Contacting Bodies in Rarefied Gas Media

937D0052D Minsk TRENIYE I IZNOS in Russian Vol 13 No 5, Sep-Oct 1992 pp 857-864

[Article by V. D. Rudyshin and A. K. Dedkov, Khmelnits Technology Institute; UDC 621.891]

[Abstract] A mathematical model was developed to analyze the wear undergone by metal friction systems subject to a normal mechanochemical wear process while working in a rarefied gas medium. The model focuses on the delivery of the active gaseous component to the contact gap, its interaction with the friction surface materials, and the effect of these processes on the friction system. In this model, air is regarded as a binary gaseous mixture, with oxygen being the active component, and nitrogen the inert

one. The model was used to analyze the interaction between a rarefied gaseous medium and the friction surfaces of metal bodies with a coefficient of mutual overlap K_{vz} equal to one during stationary friction. This analysis yielded a criterion, h, that functions as an integral friction characteristic for the type of friction system described and that takes into account its geometric dimensions, contact gap height, the chemical activity of the contacting materials, and the temperature and dynamics of the gaseous medium surrounding the system. The theoretical equations derived from this analysis were compared with the data from experimental studies performed with steel 45 contacting bodies 28 by 20 mm in size. The disparity between the experimental and theoretical values did not exceed 15 percent at negative pressures that did not exceed 5×10^2 Pa. With further increases in the degree of negative oxygen pressure, the experimental and theoretical data did not coincide. At these pressures, the wear rate for the contacting bodies and the coefficient of friction both sharply increased. On the basis of these findings, it was concluded that, under the friction conditions described, oxidative wear prevails only at negative pressures up to the order of 5×10^2 Pa. Figures 4; references 15: 12 Russian, 3 Western.

Specific Behavior of the Structural, Mechanical, and Frictional Properties of Tool Steels Exposed to Powerful Ion Beams

937D0052E Minsk TRENIYE I IZNOS in Russian Vol 13 No 5, Sep-Oct 92 pp 865-873

[Article by I. G. Romanov, I. N. Tsareva, A. D. Pogrebnyak, G. M. Romanova, G. Ye. Remnev, Nizhegorod Branch of the Institute of Machine Design imeni Academic A. A. Blagonravov; UDC 691.793]

[Abstract] Structural and phase transformations were studied in tool steels exposed to powerful ion beams to determine how they affect the mechanical and friction properties of the steels. Specimens of U-10, R6M5, and 6Kh4M2FS steel of varying degrees of roughness were irradiated from three to 10 times each by 300-keV C+ ion beams produced by a "Temp" accelerator with an ion current density of 120 A/sq cm and a pulse length of 10^{-7} s. Metallography and X-ray diffraction analysis performed on a DRON-3 diffractometer using MoK-radiation revealed that ion irradiation induced the formation of an austenitic layer up to 2 μm thick on the R6M5 and 6Kh4M2FS specimen surfaces and up to 4 μm thick on the U-10 specimen surfaces. The different layer thicknesses were attributed to the steels' different thermal conductivities and extent of surface preparation. Microhardness measurements obtained with a PMT-3 hardness tester showed that the formation of the austenitic layer caused specimen near-surface microhardness to decrease, but increased the microhardness of the zone immediately beneath the austenitic layer. Two different explanations were offered for this finding. Conventional dry friction tests using a round ShK15 steel indentor showed that the coefficient of friction of the U-10 steel decreased after irradiation, while it increased for the other two steels. This finding was explained in terms of the adhesion theory of friction. It was concluded that ion-beam irradiation parameters could be controlled well enough to induce specific changes in the mechanical and tribological properties of tool steels. Figures 5, tables 3; references 14: 12 Russian, 2 Western.

Effect of Filler Nature on Structure Formation and Properties of Low-Friction Coatings Based on Polyaminoimide

937D0052F Minsk TRENIYE I IZNOS in Russian Vol 13, No 5, Sep-Oct 92 pp 887-891

[Article by A. P. Krasnov, L. S. Fedorova, G. Ye. Morozova, V. V. Stepochkina, V. M. Yarosh, L. I. Komarova, D. V. Zagorevskiy, and I. A. Gribova, Institute of Elemental Organic Compounds imeni A. N. Nesmeyanov, Moscow; UDC 621.891.893]

[Abstract] Molybdenum disulfide and graphite fillers were studied to determine how their nature affects the process of cross-linked structure formation in low-friction coatings based on polyaminoimide and the friction properties of these coatings. Thermal friction tests showed that the graphite-filled coatings had superior friction properties and wear resistance than the MoS_2-filled coatings throughout the range of temperatures tested (273-673 K). To clarify the relationship between coating structure and friction properties, sol-gel, IR spectroscopic, and mass-spectrometric analyses were performed during thermal processing of the filled coatings at temperatures up to 523 K. It was found that, depending on the nature of the filler, the coatings formed had quite different structures than the original polymer, even if the curing temperatures were the same. MoS_2 filler had a catalytic effect that intensified the process of double-bond polymerization in the imide cycle, thus promoting the formation of a partially cross-linked structure as the polymer formed and, at higher temperatures, a significantly greater gel-fraction output (73 percent). Mass spectrometry was also used to study the thermal and tribochemical resistance of the coatings. An MS-30 mass spectrometer equipped with a DS-50 data-collection system was used for this purpose. The mass spectra showed that virtually all of the volatile product fragments released during thermal breakdown of the coating were identical in mass. Volatilization was less intense for the graphite-filled coatings than for the MoS_2-filled coatings, which probably explains why the former had greater wear resistance. Figures 3, tables 3; references 12: 9 Russian, 3 Western.

A Study of Friction Interaction Between Material Surfaces During Selective Transfer in an Epoxy Composite-Metal Mated Surface

937D0052G Minsk TRENIYE I IZNOS in Russian Vol 13, No 5, Sep-Oct 1992 pp 918-924

[Article by A. T. Kozakov, D. N. Lyubimov, A. Ye. Ivanov, A. V. Nikolskiy, M. M. Panasyuk, and P. N. Kozachenko, the Kredo-Invek Scientific Promotional Enterprise, Novoshakhtinsk; UDC 621.891:621.893]

[Abstract] Friction interaction between an epoxy composite and a number of different metals was studied to determine its effect on "third body" formation. The epoxy composite was made from PEPA-cured ED-6 epoxy resin modified with tetraethyl thiuram disulfide (Merkupral). The metals tested were steel 45, copper, zinc, galvanized

steel, nickel, and silver. Friction tests were carried out on a friction tester set up in a pin (epoxy composite) and disk (metal) configuration with a load of 0.1 MPa and a sliding speed of 0.8 m/s. Disk roughness was 1.8 μm. Friction time was six hours. The disks had the following coefficients of friction: silver—0.21; nickel—0.17; copper—0.15; steel 45—0.14; galvanized steel—0.12; and zinc—0.09. Friction interaction between the contacting bodies was studied using electron spectroscopy of X-ray-excited $ZnL_3M_{4.5}M_{4.5}$ auger electron spectra. The data showed that frictional interaction between the epoxy resin and the galvanized disk causes the latter to experience continuous intermediate oxidation that is easily reduced during interaction with the sulfur in the Merkupral, thereby allowing a clean metal surface to take part in the tribochemical reactions. Figures 4, tables 1; references 14: 13 Russian, 1 Western.

Wear Resistance of Porous Iron During Dry Friction

937D0045H Minsk TRENIYE I IZNOS in Russian, Vol 13 No 5, Sep-Oct 92 pp 939-942

[Article by V. N. Antsiferov, N. N. Masslennikov, and A. A. Shatsov, Perm Polytechnic Institute; UDC 621.785: 669.14]

[Abstract] The wear resistance of specimens of sintered h.p. 6-2 iron, Specification No. 6-09-3000-78, was studied on an SMTs-2 wear tester per State Standard 26614-85. The other component of the friction system was quench-hardened steel 45. No lubricants, lapping materials, or diamond disks were used. The iron contained no more than 0.02 percent carbon and no more than 0.001 percent residual impurities. The specimens had an average particle size of 5 μm, porosity of 2, 4, 8.6, 13.6, and 20 percent, and Brinell hardness values of 1010, 950, 763, 750, and 483. Friction test pressure varied from 0.35 to 4.2 MPa. Friction surface topography was examined on an REM-200 scanning electron microscope, which yielded photomicrographs showing that dry friction results in a fatigue-induced type of wear. For this reason, the experimental results were checked against the basic tenets of fatigue wear theory. Mathematical calculations based on the experimental data and fatigue-wear expressions yielded an equation that correlates the fatigue wear rate to surface properties, defect size, the crack resistance, strength, and deformational properties of the material, and the Parise equation coefficients. It was shown that the fatigue wear rate generally tended to generally increase at the higher pressures and porosities. Figures 2, tables 1; references 11: Russian.

Thermodynamic Properties of the Gadolinium Silicides GdSi and $GdSi_{1.5}$

937D0056B Kiev POROSHKOVAYA METALLURGIYA in Russian No 9, Sep 92 (manuscript received 20 Feb 91) pp 75-78

[Article by G.M. Lukashenko (deceased) and R.I. Polotskaya, Materials Science Problems Institute, Ukraine Academy of Sciences, Kiev; UDC 541.11]

[Abstract] The thermodynamic properties of the gadolinium silicides GdSi and $GdSi_{1.5}$ were studied by the method of measuring the electromotive force of galvanic elements within the temperature range 600 to 960 K. By using an auxiliary normal electrode made of a gadolinium-tin alloy with a phase composition whose thermodynamic properties had been determined by the method of electromotive force measurement, the researchers were able to reduce the reaction of the gadolinium with the chloride melt, thereby making the operation of the galvanic elements reversible. The alloys were smelted from semiconductor silicon (99.99 percent pure) and GM-1 gadolinium (99.81 percent Gd) in an electric arc furnace on a copper water-cooled hearth in an argon medium. All of the specimens were subjected to homogenizing annealing. Mixtures of chlorides that had been remelted in a vacuum (10^{-2} Pa) was used for the electrolytes. Mixtures of KCl-NaCl-$BaCl_2$, KCl-LiCl-$BaCl_2$, and $BaCl_2$-CsCl-NaCl with an additive of 0.5 percent anhydrous gadolinium chloride were used. The Gibbs energy and formation enthalpy and entropy of $Gd_{0.5}Si_{0.5}$ ($\Delta_f H^0$ 800 K = -84.07 +/- 0.43 kJ; $\Delta_f H^0$ = -109.8 +/- 5.3 kJ; $\Delta_f S^0$ = -32.1 +/- 7.0 J/k) and $Gd_{0.4}Si_{0.6}$ ($\Delta_f H^0$ 800 K = -73.60 +/- 0.42 kJ; $\Delta_f H^0$ = -943 +/- 4.2 kJ; $\Delta_f S^0$ = -23.0 +/- 3.8 J/k) from the mixture components were determined. The previously obtained thermodynamic functions of gadolinium disilicide formation were recalculated to allow for the imperfect phase $GdSi_{1.89}$ ($\Delta_f H^0$ 800 K = -63.86 +/- 0.34 kJ; $\Delta_f H^0$ = -82.3 +/- 3.4 kJ; $\Delta_f S^0$ = -23.0 +/- 3.8 J/k). The calculations established that the absolute values of the Gibbs energy and formation enthalpies and entropies increase as the amount of gadolinium in the silicides increases. Gadolinium germanides have been shown to be characterized by an analogous dependence of thermodynamic functions. Tables 2; references 13: 12 Russian, 1 Western.

Brittle-Plastic Transition in Silicides of Refractory Metals

937D0056C Kiev POROSHKOVAYA METALLURGIYA in Russian No 9, Sep 92 (manuscript received 6 Aug 90) pp 88-91

[Article by A.D. Osipov; UDC 539.56/52:661.685; 669.018.48]

[Abstract] Specimens of $MoSi_2$, WSi_2, and VSi_2 that had been produced by the method of vacuum siliconization were studied to determine the temperature dependences of their plastic deformation and to gain information about the factors determining the brittle-plastic transition in silicides and other metals whose interatomic bonds have a significant covalent component. Specimens of the study disilicides measuring 0.2 x 10 x 20 mm were produced by diffusion silicon saturation of metal plates throughout their entire thickness in a vacuum of about 10^{-3} Pa. The impurity content of the study disilicides did not exceed 0.05 percent, and their density and stoichiometric composition were close to theoretical. The specimens had a partially columnar structure with a weakly pronounced texture. The temperature dependences of the specimens' plastic deformation and their yield points were studied as they were bent while being heated in an air medium and in a vacuum. The plastic deformation rates of the $MoSi_2$ and WSi_2 changed dramatically in a relatively narrow temperature interval (about 1,300 to 1,400°C). Above these temperatures, plastic deformation before fracture reached a significant level (with a bend angle of about 90°) with low

deformation rates (about 10^{-3}/s). The strength properties of these two silicides also changed at temperatures close to those of a strong change in plastic deformation. Yield point changed sharply in the interval from 0.6 to $0.7T_{melt}$. The $MoSi_2$ and WSi_2 specimens studied were found to have a plastic deformation activation energy of about 2 eV; VSi_2 had a lower activation energy (1.7 eV). A correlation was found between the experimental and theoretical temperatures of intensive change of the flow stresses of the study compounds and their temperatures of polymorphous transformation and atomic characteristics. Figures 2, table 1; references 14: Russian.

Dynamic Strength and Fracture Toughness of Metals Within 293-77K Temperature Rate

937D0057B Lviv FIZIKO-KHIMICHESKAYA MEKHANIKA MATERIALOV in Russian Vol 28 No 1, Jan-Feb 92 pp 14-18

[Article by A.V. Vashchenko, V.A. Makovey, Strength Problems Institute at the Ukrainian Academy of Sciences, Kiev; UDC 620.172.2]

[Abstract] The need to analyze the taut strained state and strength of structures operating under intense dynamic loads prompted the Strength Problems Institute to develop special testing equipment and procedures for studying the mechanical properties and crack resistance of metals under dynamic loading whereby straining rates of up to 10 m/s are ensured in vertical impact testing machines with a free falling striker and up to 500 m/s or more—in air and powder charge-driven impact testers. The testing method is outlined and the dependence of the strength and ductility characteristics or armco iron on the straining rate and temperature, the dependence of dynamic fracture toughness of steel on the straining rate, and correlation between the temperature and straining rate for steel with a static ultimate strength of 1,100 MPa at a constant fracture toughness and at a constant reduction in area are plotted. Uniaxial tension tests of steels and titanium and aluminum alloys reveal a considerable increase in both strength and ductility with an increase in the straining rate, especially over 10^3 s^{-1}. The results of fracture toughness tests within a notch sensitivity index range of 10^6-8 x 10^7 MPa x $m^{1/2}$ per second and tensile tests within a 10^{-4}-10^5 s^{-1} rate show that an increase in the straining rate at low temperatures is not the factor which leads to embrittlement since the crack resistance increases sharply at high straining rates regardless of temperature. High-speed loading tests do not confirm the hypothesis of the equivalent effect of a decrease in temperature and increase in straining rate on the mechanical properties. Both the strength and crack resistance characteristics of metals within the temperature range under study improve with an increase in the loading rate. Figures 5; references 12.

Experimental Methods and Devices for Studying Metal Fracture Toughness

937D0057C Lviv FIZIKO-KHIMICHESKAYA MEKHANIKA MATERIALOV in Russian Vol 28 No 1, Jan-Feb 92 pp 18-22

[Article by S. Vodenicharov, IMTM at the Bulgarian Academy of Sciences, Sofia; UDC 620.1]

[Abstract] Increasingly stringent requirements imposed on the quality of materials used in crucial structures call for improving the crack resistance assessment methods which make it possible to simulate actual operating conditions. Attention is focused on the use of acoustic emission testing for studying crack nucleation and propagation processes, particularly acoustic emission signals under alternating loading. The development of a new wedge indentor for determining the fracture toughness and a neutron generator for studying the behavior of nuclear industry devices under neutron irradiation is reported. The methods of three-point bending for measuring the dynamic crack resistance and gas-propelled gun for impact tests are discussed. Experimental procedures are outlined. Figures 10; references 12.

Structural Fracture Toughness Criterion of Steels With Weakened Grain Boundaries

937D0057D Lviv FIZIKO-KHIMICHESKAYA MEKHANIKA MATERIALOV in Russian Vol 28 No 1, Jan-Feb 92 pp 22-26

[Article by V.M. Goritskiy, Central Scientific Research Institute of Steelwork Design imeni N.P. Melnikov, Moscow; UDC 669.018.95:539.56]

[Abstract] A structural criterion of crack resistance which takes into account the possibility of realizing the mixed fracture mechanism at the apex of the macrocrack is proposed on the basis of known concepts and approaches which identify the correlation between the fracture toughness and the growth direction distribution of the leading microcracks in transgranular spalling (TS) at the macrocrack apex. The fracture toughness formula is derived, and the systematic representation of mixed fracture at the macrocrack apex and the behavior of the stress corrosion cracking (KRN) resistance of bolt steel and improved steel 10Kh2GNM are plotted. The conclusion is drawn that the proposed criterion is suitable not only under brittle but also quasibrittle failure within the stable range of crack growth and is applicable in the case of weakened grain boundaries. A close relationship between the stress corrosion cracking and dimple and intergranular fracture under brittle and quasibrittle failure conditions of bolt steel is established. Figures 3; references 6.

Effect of Structural State on Fatigue Crack Nucleation Mechanism and Growth Kinetics in Aluminum and Magnesium Alloys

937D0057E Lviv FIZIKO-KHIMICHESKAYA MEKHANIKA MATERIALOV in Russian Vol 28 No 1, Jan-Feb 92 pp 26-33

[Article by N.M. Grinberg, V.A. Serdyuk, Engineering Physics Institute of Low Temperatures at the Ukrainian Academy of Sciences, Kharkov; UDC 539.385:620.187.5]

[Abstract] The trends observed in studies of the physical aspects of fatigue failure and fatigue failure mechanisms and their relationship with the dislocation structure and slip are outlined, and some characteristics of fatigue failure of medium-strength aluminum alloys with a yield point of 200-470 MPa and magnesium alloys with a yield point of 140-300 MPa are considered. The study is aimed at

determining the following fatigue mechanisms: macroscopic hardening, microscopic near-surface layer hardening, dislocation structure, formation or lack of slip strips or stable slip strips, and crack nucleation and growth peculiarities. The specific Al and Mg alloys and testing procedure are outlined in detail. The findings show that the fatigue failure mechanisms depend on the initial structural state: in the annealed state, the A-fatigue mechanism is realized and in the thermally hardened state—the F-fatigue mechanism is realized. The characteristic features of these as well as H- and B-mechanisms are described. It is noted that the through fatigue crack growth mechanisms are the same in annealed and hardened alloys while the growth kinetics patterns of small cracks depend on the fatigue mechanism, yet their rate exceeds that of through cracks under either the F- or A-mechanism. Figures 5; tables 1; references 20: 9 Russian, 11 Western.

Effect of Structure on Crack Resistance of Nitrogen-Alloyed High-Strength Steel 30Kh2N2MAF

937D0057F Lviv FIZIKO-KHIMICHESKAYA MEKHANIKA MATERIALOV in Russian Vol 28 No 1, Jan-Feb 92 pp 46-49

[Article by Yu.I. Zvezdin, Z.N. Petropavlovskaya, A.V. Rabinovich, S.N. Yegorov, Ts. Rashev, I. Rasheva, Kh. Argirov, Scientific Production Association of the Central Scientific Research Institute of Mechanical Engineering, Moscow; UDC 620.193.29]

[Abstract] The need to increase the reliability and extend the service life of the thermal and nuclear power plant generating equipment prompted the development of new structural materials with an elevated strength and brittle failure resistance for highly stressed parts, especially fasteners. The new nitrogen alloyed (0.02-0.16 percent) high-strength steel 30Kh2N2MAF developed jointly by the Scientific Production Association of the Central Scientific Research Institute of Mechanical Engineering and Bulgarian metallurgical research institutes is characterized by an elevated fracture toughness. The chemical and phase composition of several steel batches oil-hardened at 900°C and tempered at 580 and 600°C for six hours is summarized, and the short-term yield point, ultimate strength, elongation, reduction in area, toughness, and crack resistance of several meltings are measured and compared to similar indicators of steel 38KhN3MF. The dependence of mechanical properties on the nitrogen concentration and the temperature dependence of toughness of steel 30Kh2N2MAF are plotted. An analysis demonstrates that nitrogen-alloyed steel 30Kh2N2MAF is characterized by a higher crack resistance than steel 38KhN3MF which has no nitrogen. The new high-strength steel is promising for making bolts, studs, and other parts operating under static and dynamic loads at elevated (up to 350°C) temperatures. Figures 4; tables 2.

Influence of Iron Quantity on Fatigue Behavior of Cast Aluminum Alloy

937D0057G Lviv FIZIKO-KHIMICHESKAYA MEKHANIKA MATERIALOV in English Vol 28 No 1, Jan-Feb 92 pp 73-78

[Article by Yu. Davydov, Institute of Metal Science and Technology at the Bulgarian Academy of Sciences, Sofia; UDC 620.1]

[Abstract] The results of a study of the low cycle fatigue behavior and fatigue crack growth resistance of five modifications of the AlSi7Mg alloy with 0.12-0.28 percent Fe are presented and discussed, and the chemical composition of the samples is summarized. The study is aimed at determining the effect of the concentration iron—an impurity in AlSi7Mg—on the low cycle fatigue behavior and fatigue crack growth resistance of an alloy used to make cast automotive wheels. For this purpose, samples were cut from wheel areas (determined by the photoelasticity method) where cyclical stress is the highest under the operating conditions. Additional measurements were taken by strain gauges to determine the precise stress values in these areas. Low cycle fatigue tests were carried in an MTS 810 closed loop servohydraulic tester under controlled strain conditions according to the ASTM Standard E 606. The total stress and its elastic and plastic components, the behavior of the maximum stress value as a function of loading cycles, and cyclical and monotonic ductility vs. strength curves are plotted. The fracture mechanism during crack propagation is examined in samples cut from the wheels by scanning electron microscopy. The findings indicate that alloys with 0.29 percent Fe are characterized by the lowest decrease in cyclic ductility and are thus the most suitable for making car wheels by die casting with counterpressure. Figures 11; tables 2; references: 8 Western.

Methodological Principles of Experimental Investigation Into Effect of Circumterrestrial Space on Cyclic Strength of Structural Materials

937D0088B Kiev PROBLEMY PROCHNOSTI in Russian No 10 (280), Oct 92 pp 53-61

[Article by Yu.D. Skripnik, V.A. Strizhalo, Kiev; UDC 539.4]

[Abstract] The emerging trend of building large long-term open space structures without a protective coating (in order to simplify their production and lower their mass and cost) prompted an increased interest in the effect of a number of damaging environmental factors (FOS) on the long-term strength of structural materials, *viz.*, vacuum, alternating temperatures, solar wind, solar cosmic radiation, galactic cosmic radiation, radiation from the earth's Van Allen radiation belt, meteors, space dust, etc. An extended exposure to these factors combined with operational loads may lower the structure's reliability or even result in its breakdown. The environmental factors in the circumterrestrial space usually affecting spacecraft (KA) orbits with a mean distance of 350 km from the earth (such as the Mir space station) are briefly summarized, and an experiment with a uniform-strength beam carried out to simulate the space conditions is described. The sample strain diagram and timing chart and a typical low-cycle fatigue curve are plotted, and a schematic diagram of the experimental testing unit is cited. The outcome of alternating-sign bending tests of flat samples demonstrates that the proposed low-cycle fatigue testing procedure is simple and reliable and meets the weight and dimensional requirements for experimental equipment, making it possible to recommend it for implementation. Figures 5; references 5.

Effect of Loading Frequency on Physical-Mechanical Properties of Aluminum Alloys Under Fatigue

937D0088C Kiev PROBLEMY PROCHNOSTI in Russian No 10 (280), Oct 92 pp 61-64

[Article by N.A. Dolbin, I.G. Dovgyallo, F.F. Tsaruk, B.N. Redkin, G.G. Zavirukho, Minsk and Zhukovskiy; UDC 534.9:620.178]

[Abstract] The difficulty of simulating the actual operating conditions under which aluminum alloy parts are exposed to loading at a frequency of up to 10^{12} and the need to find a scientifically sound correlation between the data obtained at high and classical (low) frequencies on the basis of a comprehensive examination of the behavior of the physical and mechanical properties of materials (FMSM) under various amplitude-frequency conditions prompted a study of the effect of the loading frequency on these properties of aircraft aluminum alloys under fatigue. The bending tests of samples made from hardened and naturally aged aluminum alloys D1604AT15 and 14200STT1 carried out at frequencies of 180 Hz and 2.8, 8.8, and 17.6 kHz are described in detail. The fatigue curves of the D1604AT15 alloy at various frequencies and the behavior in the microhardness and dislocation density of the D1604AT15 alloy as a function of the loading frequency and the number of loading cycles are plotted. The tests indicate that as the loading frequency increases, the cyclic strength of the materials increases too. It is noted that although the character of the microhardness and dislocation density curve behavior is virtually the same within the frequency range under study, the magnitude of the changes and the position of their extrema along the number-of-cycles axis depends on the frequency. The findings point toward a monotonic character of the fatigue process. Figures 2; references 5.

Patterns of Thermal Chain Explosion of Carbon Monoxide With Oxygen in Presence of Hydrogen

937D0092A Moscow KHIMICHESKAYA FIZIKA in Russian Vol 11 No 11, Nov 92 pp 1560-1567

[Article by V.T. Gontkovskaya, T.S. Lukyanova, V.V. Azatyan, Structural Macrokinetics Institute at Russia's Academy of Sciences, Moscow; UDC 541.126.4]

[Abstract] Interest in branching chain combustion and its nonisothermal patterns is noted and the characteristics of nonisothermal oxidation of carbon monoxide in the presence of hydrogen are investigated in order to identify the patterns of the nonisothermal combustion's transition to the process of chain thermal ignition. This branching chain process is selected because its rate constants and mechanism of the elementary stages are known and are important from the application viewpoint. The study is carried out by solving a system of rate and thermal balance equations under the conditions where there are no concentration and temperature gradients in the reaction volume and the process is described by a system of ordinary differential equations. The 31 stages of the reaction and reaction constants are summarized; the maximum concentration of the intermediate products and water are calculated. The dependence of the ignition time (at which 10 percent of the final product, i.e., CO_2, has formed) on the hydrogen concentration in the initial mixture at a 150 torr pressure and on pressure at a 6 percent hydrogen concentration, the behavior of the water concentration with various hydrogen additions, the dependence of the maximum OH radical, CO_2, and water concentration on the hydrogen addition at the OH concentration peak, the behavior of the rate of certain elementary process stages and the behavior of the full process, the dependence of the peak temperature and peaking time on the critical parameter, the dependence of critical thermal explosion parameters on the hydrogen addition, and the relationship between the pressure and critical vessel diameter are plotted. The findings confirm that the thermal bounds of the chain ignition are not unique, i.e., different hydrogen additions or pressures may correspond to the same critical reaction vessel diameter due to a change in the mixture composition or the reaction mechanism; this may sharply retard the process under isothermal conditions and upset the monotonic dependence of the critical conditions on the experimental conditions under nonisothermal combustion. Figures 8; tables 3; references 12: 10 Russian, 2 Western.

Orifice Plate-Free Shock Tube for Pulse Infrared Spectroscopy of Heated Gases

937D0092B Moscow KHIMICHESKAYA FIZIKA in Russian Vol 11 No 11, Nov 92 pp 1568-1574

[Article by A.B. Britan, V.V. Krasnikov, V.A. Levin, S.Yu. Mitichkin, M.S. Pshenichnikov, V.S. Solomatin, V.G. Testov, Moscow State University imeni M.V. Lomonosov; UDC 533.6.07:543.422:547.211]

[Abstract] The requirements imposed on the experimental measurements of the kinetic processes behind shock waves are discussed, and the outcome of calibration of a shock tube whose design was specially modified for examining the infrared absorption spectra of hydrocarbons behind the trailing edge of the shock waves is described. Wave flow diagrams of shock tubes, experimental and analytical pressure oscillograms of shock tube channels, and segments of the methane absorption spectra in the neighborhood of the *Q*-band of the ν_3 oscillatory-rotational mode are plotted. A block diagram of a YAG pulsed laser spectrograph is cited. The use of the high-speed air operated valve instead of the orifice plate for calibrating the shock tube ensures an experimental rate data spread of less than 1 percent. The application software package developed for computer simulation of the wave processes in the shock tube with a variable cross section demonstrates the applicability of the analytical model developed for this purpose for describing the wave processes in the shock tube. The air operated valve greatly increases the reproducibility of the operating conditions necessary for pulsed infrared spectroscopy. The spectrometer resolution estimated by comparing the experimental spectra to analytical data demonstrates the consistency of the experimental findings and theoretical calculations. Figures 4; references 10: 7 Russian, 3 Western.

C_1-C_3 Hydrocarbons in Internal Combustion Engine Exhaust

937D0092C Moscow KHIMICHESKAYA FIZIKA in Russian Vol 11 No 11, Nov 92 pp 1575-1579

[Article by V.Ya. Basevich, V.S. Isamukhamedov, V.P. Karpov, Chemical Physics Institute imeni N.N. Semenov at Russia's Academy of Sciences, Moscow; UDC 541.126.]

[Abstract] The effect of carburation and injection on the one hand and of the liquid phase on the other on the internal combustion engine performance is discussed, and an attempt is made to improve the fuel carburation and injection and analyze the exhaust products using both gaseous and liquid fuel in a Waukesha single-cylinder engine with different types of carburetors. To this end, the concentration of C_1-C_3 hydrocarbons, including the unsaturated ones which precede the development of polycyclic aromatic hydrocarbons (PAU), are compared. Methane and *n*-butane are used as the gaseous fuel and isooctane, benzene, A-76 and AI-93 gasoline, and gas condensate—as the liquid fuel. The dependence of the hydrocarbon concentration on the excess air coefficient for various fuels under different conditions is plotted, and the concentration of various hydrocarbons in all types of fuel is summarized. Despite the uniformity of the general exhaust gas pattern, the hydrocarbon concentration largely depends on the fuel's chemical structure. The principal exhaust component in all cases is the initial fuel. Figures 5; tables 1; references: 6 Western.

Effect of Structural State of TiN Coats on Their Strength

937D0042E Kiev SVERKHTVERDYYE MATERIALY in Russian No 5 (80), Sep-Oct 92 pp 30-37

[Article by A.V. Byakova, Kiev Polytechnic Institute; UDC 62-761]

[Abstract] The limitations imposed on the use of ion plasma sprayed TiN coats by the instability of their operating characteristics and low accuracy and wide spread of published data on the microhardness of TiN coats as well as the futility of past attempts to make corrections for the layer thickness prompted a study of the effect of the TiN coat composition and structure on the microhardness and fracture toughness. The coat deposition and examination procedure is outlined in detail: the coats are applied onto a Ti alloy and stainless steel by condensation with ion bombardment (KIB) in a NNB-6.6-I1 unit in a nitrogen atmosphere and the phase composition and crystallographic structure are studied by a DRON-3.0 diffractometer in monochromated radioation of the Cu-anode. The coat composition is examined by electron Auger spectroscopy in an ASTs-2000 unit. The dependence of microhardness and fracture toughness on the nitrogen concentration and the dependence of the fracture toughness on the relative contribution of the [111] axial structure are plotted. An analysis demonstrates that in coats deposited by the KIB method in a chamber where the partial nitrogen pressure increases from 0.010 to 10,000 Pa, its concentration rises from 32 to 44 percent while the coat structure changes from heterophase with a ε-Ti_2N lattice to homophase with a δ-TiN lattice. The nitride layer composition and structure selectively affect the coats' microhardness and brittle strength; there is no functional link between the microhardness and fracture toughness for brittle coats. The author is grateful to Prof. V.G. Gorbach for discussing the findings and A.A. Smekhnov for analyzing the coats. Figures 3; tables 1; references 20: 13 Russian, 7 Western.

Stressed State of the Protective Coatings and Surface Layers of Machinery During Erosive and Cavitational Wear

937D0052B Minsk TRENIYE I IZNOS in Russian, Vol 13 No 5, Sep-Oct 92 pp 837-847

[Article by A. V. Lagerev, Bryan Institute of Transport Machinery Manufacturing; UDC 621.165]

[Abstract] A wave-theory model was constructed to describe the formation of stressed states in the protective coatings and surface layers of machinery exposed to erosive wear from water droplets, such as aircraft and steam turbines, and/or cavitational wear from gas bubbles, such as hydraulic turbines and pumps. Beam theory was used to verbally and mathematically describe the propagation, interference, diffraction, and refraction of elastic stress waves and to develop two idealized expressions, one for the stressed state of coatings and one for the stressed state of surface layers. Since minute differences in the roughness of coating/surface layer interfaces and in microhardness, which varies throughout a coating and the surface layers it protects, quantitatively affect the input of individual secondary waves, the idealized expressions were further refined by simultaneously factoring in coefficients that account for these two characteristics. The values for these coefficients generally fell within a range of 2 to 8. The calculations showed that, in a heterogeneous material, the qualitative nature of the stress field in a coating and a protected surface remains unchanged; only quantitative differences are of consequence. Depending on the law according to which microhardness changes, stress in homogeneous and heterogenous materials may differ by 10 to 20 percent. This model was successfully used to estimate the stressed state of an electron discharge coating of T15K6 alloy 200 μm thick applied to a steam turbine rotor blade made of 20Kh13 steel. The blade was exposed to erosive wear from moisture droplets 75 μm in radius, which impinged it perpendicularly at 260 m/s. Figures 5, tables 1; references 8: Russian.

Applying Aluminum-Zinc Coatings to Water and Gas Linepipe

937D0054I Moscow STAL in Russian No 9, Sep 1992 pp 49-54

[Article by N. P. Karpenko, Yu. A. Mednikov, I. I. Sergeyev, V. P. Baykov, Yu. I. Blinov, and I. S. Nevyanstev, Chelyabinsk Tube-Rolling Plant and the Ural Scientific Research Institute of Technology; UDC 621.774.2:621.793.4:669.58]

[Abstract] The Chelyabinsk Tube-Rolling Plant, the Ural Scientific Research Institute of Technology, et al. have worked together to develop an experimental technology for applying aluminum-zinc coatings to water and gas linepipe 15-20 mm in diameter and up to two meters in length. They have also completed the specifications for an experimental production line capable of coating pipe up to eight meters in length. The equipment and process parameters used to coat water and gas pipe with these types of coatings was described and illustrated. It was shown that it is possible to apply coatings containing up to 15 to 20 percent aluminum to conventionally prepared surfaces, thus avoiding the costs of having to master the application of fundamentally new types of coatings. The process includes the following operations: wetting, pickling, rinsing, brightening, and rinsing the pipe in cold and hot water, fluxing and drying the pipe, applying the coating, blast cleaning, cooling, and controlling coating quality, solution composition, and process parameters. Metallographic and X-ray spectrometric analyses of the structure and corrosion resistance of the pipe treated with the experimental coatings showed that it has obvious advantages over conventionally coated pipe. The intermetallic layer between the coating and the basis metal was similar in composition to Al_5Fe_2, with its thickness increasing as aluminum concentration was increased. Coatings with up to 5 percent aluminum experienced only 18 percent corrosion after 20 testing cycles in a humid atmosphere containing SO_2. Similar results were obtained when testing the experimental coatings in a 0.01- percent solution of H_2SO_4. Figures 7, tables 1; references 16: 13 Russian, 3 Western.

Theoretical Analysis of the Conditions of the Amorphization of Metal Alloys During Gas-Thermal Spraying. 1. Determination of the Cooling Rates of Disperse Sprayed Material

937D0056A Kiev POROSHKOVAYA METALLURGIYA in Russian No 9, Sep 92 (manuscript received 21 Mar 91) pp 56-61

[Article by V.N. Korzhik, Electric Welding Institute, Ukraine Academy of Sciences, Kiev; UDC 621.793]

[Abstract] A theoretical study was performed to determine the factors facilitating the formation of amorphous phases when the method of gas-thermal spraying is used to apply coatings of amorphized alloys. Equations are derived to describe the cooling of a sprayed deformed particle on a semi-infinite base through a layer of coating. The coating formation process is examined from the second cycle of particle build-up onward. The mathematical relationships derived make it possible to study the heat conditions developing as particles solidify as a function of the following parameters: coefficient of heat release at the coating-substrate interface, particle temperature, substrate temperature, particle thickness, coating thickness, and coating heat conduction. These relationships were taken together with available published data regarding the effect that various spraying process parameters have on the aforesaid coating and substrate parameters and were used to model the process of the cooling of particles of the alloy $Fe_{83}B_{17}$ under conditions of gas-thermal spraying. The rate at which the sprayed material cooled was found to depend primarily on the thickness of the solidifying metal particles. The composition of the metal substrate and thickness and heat conduction of the previously formed coating proved to be less important. Efforts should thus be made to use the thinnest particles possible when applying gas-thermal coatings. The calculated data were qualitatively confirmed by a series of experiments. X-ray phase analysis of study specimens established that coatings of the alloy $Fe_{83}B_{17}$ applied onto a copper substrate with a temperature not exceeding 350 K have an amorphous-crystalline structure. As the size of the powder particles increases and the thickness of the deformed particles on the substrate increases, the volume content of amorphous phase decreases. X-ray crystallographic studies also demonstrated a slight increase in the fraction of crystalline phases as the thickness of amorphous-crystal coatings is increased and when a steel base is used instead of a copper base. Figures 4; references 15: 11 Russian, 4 Western.

Investigation of Phase and Chemical Composition of Ion Plasma Coat on High-Speed Steel R18 After Brief Heating

937D0057J Lviv FIZIKO-KHIMICHESKAYA MEKHANIKA MATERIALOV in Russian Vol 28 No 1, Jan-Feb 92 pp 123-125

[Article by A.K. Verner, V.D. Dalner, M.G. Karpman, Moscow Automotive Plant imeni I.A. Likhachev; UDC 621.793.18]

[Abstract] The efficacy of ion plasma coat spraying (the KIB method) for making wear resistant TiN-based coats and the wide spread of serviceability indicators of the coated tools as well as their limited operating temperature are discussed and an attempt is made to examine the behavior of the phase and chemical composition of the coat/base surface layer after a brief high-frequency heating of high-speed steel samples with a TiN coat. To this end, 200x22x2 mm samples are cut from steel R18 heat treated to an HRC 62-64 hardness by a standard technique and polished to an arithmetic mean deviation of the profile of R_a=0.63 μm. A 15 μm thick coat with a hardness of 18,000-22,000 MPa is deposited in an NNV 6.6-I1 unit, and the samples are heated to 800°C for 10 s using an 8 kHz generator. The diffusivity of oxygen and nitrogen in various systems is summarized, and the relative carbon line strength in the coat/base system, Auger spectra of the TiN coat and steel R18 base after brief heating, and the Auger line strength behavior with an electron beam scanning along the direction intersecting various structural components of the metallographic section are plotted. Thermodynamic theoretical studies with a subsequent check by X-ray diffraction and Auger spectral analyses demonstrate the possibility of controlling the oxygen, nitrogen, and carbon concentration under a brief thermal shock in an air medium and show that other titanium compounds with oxygen and carbon in addition to TiN are formed in the coat and Cr_2N—in the base. This makes it possible to manipulate the coat properties within a broad range and control their friction coefficient, hardness, and corrosion resistance. Figures 3; tables 1; references 5.

Composition, Structure, and Properties of Electrolytic Coats From Aluminum Alloyed With Transition Metals

937D0064F Moscow ZASHCHITA METALLOV in Russian Vol 28 No 6, Nov-Dec 92 pp 967-971

[Article by V.N. Titova, R.Kh. Zalavutdinov, N.V. Petrova, A.Ye. Gorodetskiy, V.A. Kazakova, Physical Chemistry Institute at Russia's Academy of Sciences; UDC 620.197.5]

[Abstract] The use of transition metals, e.g., Mo or Zr, as grain fining additions in aluminum alloy casting which may also result in new physical and chemical properties of Al coats and expand their applications is discussed, and the effect of the electrodeposition conditions of Al with Mo and Zr on the composition, structure, and physical and chemical properties of aluminum coats on copper or glass carbon is examined in ethyl benzene electrolytes (ETB) with anhydrous Mo and Zr chlorides. The corrosion resistance of aluminum alloys is determined by the difference of the corrosion and pitting potentials on the potentiodynamic curves in a 0.1 *M* NaCl solution. The effect of the current density on the current efficiency of Al, Mo, and Zr and on the transition metal (PM) concentration, the Zr distribution on the coat surface and cross section, and anodic polarization curves of Al, Al-Zr, and Al-Mo are plotted. X-ray and electron diffraction analyses did not detect metallic Mo or Zr or their intermetallic compounds in the precipitates. The findings show that an addition of transition metals to the coats is accompanied by fining of the growing crystals, the appearance of a (200) axial structure, and formation of local microdistortions and tensile macrodeformations. These structural and phase coat features affect the physical and chemical properties, particularly hardness and corrosion resistance. When alkyl

benzene-based electrolytes are used, the coats are deposited in the form of large crystals with dendrites and whiskers. Figures 3; tables 1; references 5: 4 Russian, 1 Western.

Oriented Modification of Anticorrosion Epoxy Compositions

937D0064G Moscow ZASHCHITA METALLOV in Russian Vol 28 No 6, Nov-Dec 92 pp 976-980

[Article by V.G. Shigorin, N.I. Fomina, T.G. Lapushkina; UDC 620.197.6]

[Abstract] Expanding uses of epoxy oligomers for corrosion protection are discussed and it is noted that without special modification, they produce coats with poor anticorrosion properties, primarily due to their insufficient adhesion to metal. Thus, amines, including aromatic ethoxyamine and phenols (shale) are used as modifiers. The effect of the aromatic amine containing an ethoxy group and a secondary amine in the heterocycle on the protective action mechanism of the epoxy coat is examined. The modifier efficiency is assessed by anodic potentiodynamic curves of armco iron with the adsorption layer under study. The potentiodynamic curves of armco iron in a 3 percent NaCl solution and the infrared spectra of shale oil (SM), aromatic ethoxyamine (AEA), and their mixtures are plotted. The effect of the modifiers on corrosion inhibition is compared. The study made it possible to develop a modified composition containing SM and AEA which is cheaper and does not require scarce epoxy oligomers. A stable chemisorption layer spontaneously forms under the coat, helping attain coats with a good adhesion and protective properties. Its potentiodynamic curves attest to a decrease in the anodic Fe dissolution rate under the coat within a broad range of potential. Lab and full-scale tests confirm the high protective properties of the coats. Figures 5; tables 1; references 7.

Coat Classification by Protective Properties Under H_2S-Cracking of Steel

937D0064L Moscow ZASHCHITA METALLOV in Russian Vol 28 No 6, Nov-Dec 92 pp 1032-1035

[Article by V.M. Kushnarenko, Orenburg Polytechnic Institute; UDC 620.198]

[Abstract] A procedure for qualitative and quantitative assessment of the protective properties of coats recommended for preventing steel products from H_2S-cracking is outlined. Ion plasma coats are sprayed in a Bulat 3T unit in an inert medium and an atmosphere of especially pure gaseous nitrogen at a 5 x 10^{-3} Pa pressure. The VT-1-00 Ti alloy, Al, Mo, or Cr are used as the evaporated material, depending on the coat type. The coat deposition method and the coat and electrolyte components are described in detail. The coats are classified by their protective action based on experimental research optimization techniques using Harrington's desirability function as the optimization criterion. The coats are thus classified as diffusion, galvanic, ion-plasma, and chemical. An analysis shows that Cr diffusion coats produced under certain conditions have high protective properties; the shortcoming of the coats produced at a 1,273K temperature or higher is the need for additional heat treatment in order to refine the base metal grain and restore its mechanical properties. It is noted that the proposed procedure makes it possible soundly to classify both existing and prospective coats. Tables 4; references 3: 2 Russian, 1 Western.

Wear-Resistant Diffusion Coatings on Steels for Blanking and Coining Tools

937D0072C Moscow METALLOVEDENIYE I TERMICHESKAYA OBRABOTKA METALLOV in Russian No 10, Oct 92 pp 7-8

[Article by M.G. Karpman, N.Kh. Sokolova, Ye.M. Dmitriyeva, S.Ye. Andryushechkin, and S.S. Savkov, Moscow Institute of Aviation; UDC 621.785.532: 621.7.073]

[Abstract] Three steels for blanking and coining tools (9CrSi, CrWMn, Cr12Mo) were selected for an experimental study of diffusion coating by a thermochemical process, followed by heat treatment, to ensure a high wear resistance. Specimens of each steel were impregnated with chromium (48 percent Cr, 50 percent Al_2O_3, 2 percent NH_4Cl), with boron (39 percent B_4C 68 percent Al_2O_3, 2 percent NaF), with boron + chromium (30 percent B_4C, 20 percent Cr, 48 percent Al_2O_3, 2 percent NaF), and with chromium+vanadium (43 percent Cr, 5 percent V, 50 percent Al_2O_3, 2 percent NH_4 Cl) respectively. Specimens of 9CrSi and CrWMn steels were processed in two ways: 1) thermochemical treatment at 1000°C in a container with fusible gate for five hours followed by furnace cooling, then heat treatment at 850° (quenching temperature) in the same but hermetically sealed container for two hours followed by water cooling; 2) thermochemical treatment at 850°C in a container with fusible gate for five hours followed by water cooling in the same but hermetically sealed container. Specimens of Cr12Mo steel were processed by combining thermochemical treatment at 1050°C for five hours in a container with fusible gate and water cooling in the same but hermetically sealed container. Subsequent tests revealed that the hardness of 9CrSi steel had not exceeded 40-43 HRC, inadequate for blanking tools, but the hardness of CrWMn steel and Cr12Mo steel had become 58-60 HRC and 60-62 HRC respectively. Chromium and chromium+vanadium impregnation has produced two hardening carbide phases $M_{23}C_6$ and M_7C_3. Boron impregnation has produced two hardening boride phases FeB and Fe_2, while boron+chromium impregnation has produced hardening boride phases MB and M_2B (M = V,CrMn,Mo). Tables 2. references 2.

Formation of Structure Properties of Cast Macroheterogeneous Composites

937D0067C Moscow LITEYNOYE PROIZVODSTVO in Russian No 9, Sep 92 pp 10-13

[Article by S.S. Zalutovskiy, R.K. Ivanova, A.S. Zalutovskiy, I.O. Shinskiy; UDC 621.74.046]

[Abstract] A new cast macroheterogeneous composite (LMKM) developed at the Ukrainian Academy of Sciences is capable of extending the service life of bearings in high-stress friction assemblies by three- to tenfold. The LMKM are cast or bulk composites in which the reinforcing phase is bound to the cast metal matrix while single structure elements periodically recur within the macrovolumes. LMKM items are produced by casting heterogeneous melts and by isothermal and nonisothermal impregnation of the reinforcement, placed in the mold cavity beforehand, with the matrix melt. The advantages of the liquid phase casting technologies over solid phase methods are summarized. The element distribution in the contact zone on the reinforcing granule/matrix interface, the microhardness behavior of LMKM phases as a function of temperature, and the formation diagram of LMKM structure zones are plotted. The new composite production technology is characterized by a shortened production cycle, simple equipment, use of available components, and high technical and economic efficiency, making it possible to recommend it for extensive implementation in various mechanical engineering fields for making high-resistance bearings for stressed friction units. Figures 4; tables 1; references 1.

Aluminum-Based Composite Alloys

937D0067D Moscow LITEYNOYE PROIZVODSTVO in Russian No 9, Sep 92 pp 13-14

[Article by V.S. Shumikhin, A.K. Biletskiy, A.A. Shcheretskiy; UDC 621.763:669.71]

[Abstract] The main condition for producing quality composites (KM), i.e., ensuring the filler wetting with the liquid metal without a chemical interaction of the components, and various methods of adding the filler to the metal and their shortcomings are outlined. Attention is focused on the method of blowing filler particles by neutral or plasma flows which is accompanied by a melt stirring, thus facilitating a more uniform distribution. Mechanical mixing in of the filler particles is also considered. The microstructure of Al- and Cu-based composites is shown, and the effect of the disperse graphite particle concentration on the wear rate and thermal expansion coefficient is plotted. A comparison of various filler addition methods demonstrates the advantages of the alloying addition-type introduction of disperse particles whereby an alloying composition with a relatively high concentration of refractory particles is prepared first, then added to aluminum. The two-stage method of making cast composites with metallized graphite articles makes it possible to produce alloys with a uniquely high $\leq$ 15 percent graphite concentration and optimize the impregnation technology. Silicon carbide can also be used as the reinforcing phase. The properties of the new composites greatly exceed those of known alloys. Figures 2.

Analytical Techniques for Predicting Elastic Properties of Three-Dimensional Reinforced Composites

937D0074A Riga MEKHANIKA KOMPOZITNYKH MATERIALOV in English No 5, Sep-Oct 92 pp 579-596

[Article by Y.A. Gowayed, C.M. Pastore, North Carolina State University; UDC 539.37:678.5.06]

[Abstract] The specific data necessary for adopting a new engineering material—a sound and reproducible analytical procedure and sufficient data to support it—are mentioned and the lack of such data for textile composites is addressed. To this end, two approaches to developing an analytical prediction method are outlined—averaging and detailed models—and several specific techniques are studied in detail: the modified matrix, curved fiber, stiffness averaging, fiber inclination, bridging, finite cell, finite discrete element, and unit cell continuum methods. These methods are divided into elasticity techniques and finite elements methods and the relative advantages and shortcoming of each method and groups of methods are examined in detail. The need to unify the above techniques and integrate them with the composite production process, including processing simulation, matrix and fiber architecture variations, macro- and microcrimp analysis, twisting effects, and interface bonding, is stressed. Analytical procedures are illustrated by specific examples on the basis of published data. Figures 17; tables 2; references 22: 10 Russian, 12 Western.

Stability of Composite Materials With Interlaminar Cracks

937D0074B Riga MEKHANIKA KOMPOZITNYKH MATERIALOV in Russian No 5, Sep-Oct 92 pp 603-608

[Article by I.A. Guz, Mechanics Institute at the Ukrainian Academy of Sciences, Kiev; UDC 539.3]

[Abstract] The advantages of the three-dimensional linearized theory of stability of deformable bodies (TLTUDT) and a model of piecewise-uniform media which yield the most accurate results in solving the task of layered composite material (SKM) stability, and the limited utility of the assumptions made for this purpose prompted a study of the stability of laminated composites under compression along interlaminar cracks. The problem is considered in the most precise formulation known—a model of a piecewise-homogeneous medium with the principal formulae of the three-dimensional linearized theory of stability of deformable bodies as they apply to the simplest type of laminated composite consisting of two alternating layers of filler and binder. The composite's layers are simulated by compressible/incompressible and elastic/elastoplastic bodies and the interlaminar cracks are classified depending on the ratios of their lengths to characteristic dimensions of the laminated composite material structure, i.e., the layer thickness. In particular, macro- and microcracks and structural cracks are considered and the problem of stability is solved numerically in three stages. In so doing, orthotropic layer materials with elastoequivalent directions parallel and perpendicular to the interfaces compressed by dead loads are considered. It is noted that the calculated critical load parameters (KPN)

are smaller than the shear modulus for a less rigid half-plane and are closer to the values for this half-plane's surface instability. More complex structures will be examined in subsequent publications. Figures 1; tables 1; references 9.

Formation of Composite Material Structure and Effective Properties During Production of Bias Ply Reinforced Shells

937D0074C Riga MEKHANIKA KOMPOZITNYKH MATERIALOV in Russian No 5, Sep-Oct 92 pp 609-617

[Article by N.V. Kireyev, G.I. Starostin, Computer Center at the Siberian Department of Russia's Academy of Sciences, Krasnoyarsk; UDC 678.027.942:539.216.1]

[Abstract] The urgency of the task of predicting the thickness and effective physical and mechanical characteristics of composite layers during production of multilayer shells is stressed, and the problems which must be solved for this purpose are identified. A method of approximate analysis of the geometrical structure parameters of the frame in axisymmetric shells made by the method of oblique cross-ply winding (KPPN) is proposed, and the concepts of oblique cross-ply winding and transition forming in the circumferential braid ply are depicted graphically. It is assumed *inter alia* that the semifinished product has a laminated structure, that each longitudinal reinforcing fiber passes through all circumferential reinforcement layers and the fiber projections upon the mandrel surface are the latter's geodesic lines while the fibers are slightly twisted. A system of nonlinear equations is derived on the basis of these assumptions for determining the characteristics of the composite shell as a function of process parameters, and an algorithm is proposed for numerically solving this system of equations. The algorithm is illustrated by determining the geometrical parameters of the reinforcing frame and the efficacy of the composite's rigidity characteristics in the shell made by the oblique cross-ply winding method on a mandrel. The fiber content and reinforcement angle variations in unidirectional plies near the shell's inner and outer surface, the shell thickness variation, the behavior of the effective rigidity characteristics, and the dependence of the shell strain on pressure are plotted. The findings show that the layer thickness and the fiber content and reinforcement angles, i.e., the effective composite rigidity characteristics, vary substantially both in the meridional direction and through the shell thickness. The authors are grateful to V.A. Frolov for providing experimental data. Figures 8; references 14.

Winding Mechanics Problems of Thick-Walled Composite Structures

937D0074D Riga MEKHANIKA KOMPOZITNYKH MATERIALOV in Russian No 5, Sep-Oct 92 pp 618-626

[Article by Yu.M. Tarnopolskiy, Polymer Mechanics Institute at the Latvian Academy of Sciences, Riga; UDC 669.018]

[Abstract] The principal concepts of winding—the main method of making such crucial structural members as axisymmetric bodies from fiber composites with a polymer matrix—and semifinished products, i.e., impregnated fibers and braids used for windings, are considered in detail and the history of winding practices since production of the first item by J. Lubin in 1944 is reviewed. The products made by winding are divided into three categories—thin-walled, sectional, and thick-walled items—and attention is focused on the latter category. The stages involved in making thick-walled composite structures and recent developments in thick-walled product winding practices are examined. The pressure on the mandrel during winding and the pressure behavior during various winding stages are plotted and models for analyzing the taut strained state of thick-walled product, thick-walled composite rods in torsion, torsion performance of a spatially reinforced thick-walled composite, and a model of a rod reinforced along the single-sheet hyperboloid generator line are presented graphically. The winding process is divided into individual phases and the interlaminar compliance is taken into account; together with the circular models, these factors make it possible to predict the effect of the winding process parameters and the tension force on the ready product properties and performance and develop engineering models for designing would thick-walled composite products. It is noted that the above analysis serves as a starting point for subsequent research in this field. Figures 7; tables 1; references 19: 10 Russian, 9 Western.

Experimental Investigation of Natural Frequencies and Vibration Decrements of Composite Rim Flywheels

937D0074E Riga MEKHANIKA KOMPOZITNYKH MATERIALOV in Russian No 5, Sep-Oct 92 pp 639-649

[Article by G.G. Portnov, I.N. Barinov, Polymer Mechanics Institute at the Latvian Academy of Sciences and Riga Experimental Center of the State Scientific Research Institute of Civil Aviation; UDC 62.562+621.8-0.3:678.067]

[Abstract] The advantages of composite rim flywheels with radial and chord spokes which reach an energy capacity of up to 230 kJ/kg in overspeed tests and their design are discussed, and it is noted that the energy capacity can be increased further by concentrating most of the mass in the rim while making the spokes and hub as light as possible. Five rim flywheels differing by the number and slope of the spokes relative to the rim plane and the rim and hub mass are studied in order to establish the principal patterns of their dynamic properties (allowing for the limited number of specimens) and assess the possibility of controlling them and using streamlined hypotheses for theoretical descriptions of the flywheel energy storage systems. The experiment design and experimental procedure are discussed, and the flywheel characteristics are summarized. Hysteresis loops (the dependence of displacement on the load applied periodically by a saw-tooth law at a 40 s period) are plotted under axial, radial, and angular loading. A hysteresis loop linearization is considered, and the dependence of the resonant vibration frequency on the excitation level characterized by the relative resonant amplitude in both types of flywheels is examined graphically. Natural frequencies and decrements and the second and third natural vibration frequencies are calculated for axial, radial, and

angular vibrations and compared to test data. Dynamic tests of the flywheels do not reveal any significant nonlinear effects, so vibration analysis in engineering systems with these flywheels can be safely made in a linear formulation with sufficient accuracy. The vibration decrement under radial and angular oscillations is considerable and may lead to a rotational instability in the postcritical area. Figures 7; tables 5; references 11.

Characteristics of Strain Gauge Measurements on Composites

937D0074F Riga MEKHANIKA KOMPOZITNYKH MATERIALOV in Russian No 5, Sep-Oct 92 pp 692-697

[Article by L.P. Tairova, S.V. Tsvetkov, Moscow State Engineering University imeni N.E. Bauman; UDC 539.376]

[Abstract] The differences between strain gauge measurements taken on metal structures and composites (KM) due to such KM properties as the surface irregularity of wound products, high anisotropy of mechanical properties and thermal expansion coefficients, and low thermal conductivity prompted a study of the effect of these properties on the method of strain gauge measurements on composites and ways for taking them into account. To this end, five flat samples from the KMU-3l carbon plastic made by compaction are examined; three KF5P1 strain gauges are glued to each sample. The experimental procedure is outlined in detail, and the experimental data on the effect of the glue layer on the strain gauge readings are summarized. In addition, the effect of the glue layer thickness on the measurement results and the strain measurement errors of strain gauges as a function of the ratio of longitudinal and transverse strain are plotted. An analysis shows that in order to increase the confidence of results in strain gauge measurements on composites, the longitudinal and transverse strain gauge sensitivity must be determined experimentally for each gauge batch; other recommendations are given for greatly lowering the systematic error probability, e.g., using a strain gauge with a base greater than the characteristic irregularity size on the surface by tenfold and using systems with a short strain gauge sampling time, etc. Figures 4; tables 1; references 7: 4 Russian, 3 Western.

Mass Spectrometric Thermal Analysis of γ-Ray Irradiated Polyethylene-Aluminum Composite

937D0074G Riga MEKHANIKA KOMPOZITNYKH MATERIALOV in Russian No 5, Sep-Oct 92 pp 698-703

[Article by T.M. Muinov, L.I. Gabaydulina, Engineering Physics Institute imeni S.U. Umarov at the Tadzhik Academy of Sciences, Dushanbe; UDC 539.196.3: 678.01.543.51]

[Abstract] A laminated polyethylene-aluminum (PE-Al) composite, both irradiated with γ-rays and not, is examined by pyrolytic mass spectrometry in order to establish the possibility of using radiation treatment to improve the PE adhesion to aluminum foil and thus increase the composite's thermal stability. An MI-1201 mass spectrometer adapted for studying thermal decomposition of polymers and composites on their basis is used at a 5 kV accelerating voltage and a 50 eV ionizing electron energy. Mass spectra of molecular volatile products liberated during the diffusion heating of PE and PE-Al composite with and without γ-irradiation and the kinetics of volatile product liberation from various hydrocarbons during thermal decomposition are plotted. The kinetic parameters of the thermal decomposition process in PE peeled from the PE-Al composite and intact PE-Al composite are summarized. An analysis of the findings obtained in irradiated and nonirradiated samples of PE-Al composite shows that thermal decomposition of the PE-Al composites occurs in three stages and indicate that the effect of γ-irradiation is manifested in that the PE structure defects which decompose during the first stage are cured, the polymer becomes cross-linked, and oxygen-bearing groups form. The latter factor increases the number of contact centers between polyethylene and aluminum foil. The authors are grateful to Prof. V.R. Regel for constructive discussions. Figures 5; tables 1; references 6: 5 Russian, 1 Western.

Elasticity Modulus Defect of Composites Under Ultrasonic Loading

937D0088A Kiev PROBLEMY PROCHNOSTI in Russian No 10 (280), Oct 92 pp 32-36

[Article by S.A. Golovin, V.V. Naumov, Tula; UDC 539.4]

[Abstract] The importance of determining the elastic constants of composites and pseudoalloys for assessing the unit strength of these materials is stressed, and the effect of cyclical thermal and force factors on these constants is discussed. In particular, the effect of an amplitude-cyclical and temperature factors on the behavior of the modulus of elasticity defect of the D30 Fe alloy with 30 percent Cu produced by liquid phase sintering and of the pure components of this composite system is investigated. The experimental and design values of the Young modulus are summarized, and the procedure for measuring the Young modulus in a resonance ultrasonic unit under compression and tension operating in a self-excited mode at a 21,500 Hz loading frequency is outlined. An expression is derived for calculating the defect of the elasticity modulus. The effect of the pace of ultrasonic loading of the Fe and Cu pseudoalloy components on their amplitude dependence of the Young modulus, the amplitude and cyclical dependence of the Young modulus of the D30 pseudoalloy and its components, and the amplitude dependence of the Young modulus defect of the D30 pseudoalloy at various testing temperatures are plotted. The findings show that the defect of the Young modulus under ultrasonic loading substantially affects the plastic deformation resistance of the composite whereby the Young modulus defect (DM) magnitude depends on the composite structure, component properties, and external load conditions. It is stressed that the loading conditions must be taken into account in strength analyses as well as in determining the service life of the parts and products from this material. Figures 3; tables 1; references 7.

Amine Rate Optimization and Corrosion Prevention in Gas Processing Plant Equipment

937D0057A Lviv FIZIKO-KHIMICHESKAYA MEKHANIKA MATERIALOV in Russian Vol 28 No 1, Jan-Feb 92 pp 11-13

[Article by E.B. Bukhgalter, V.N. Polyakov, All-Union Scientific Research Institute of Gas Industry Economics, Moscow; UDC 658.511.2:66.074]

[Abstract] The increasing production volume of natural gas containing various types of sulfur compounds calls for extensive uses of amine refining processes for removing acid components at oil and gas processing plants using mostly aqueous solutions of diethanolamine (DEA) and methyldiethanolamine (MDEA). The high cost of amines prompted the development of sound procedures for standardizing their consumption rates and finding new ways of protecting the equipment from attendant corrosion. A formula for optimizing the amine rate is derived, and the protective properties of paint and varnish, plastic, rubber, and metal coats and inhibited lubricants on the metal surface of certain units operating under gas corrosion conditions typical of gas processing plants (GPZ) are analyzed. The performance of thermosetting plastic coats—layers of epoxy phenol and polyester resin—measured on actual equipment over three years is summarized and data on the protective properties of lubricants modified with the I-25-D and PKU-K inhibitors on fasteners used at the gas processing plants are presented. The findings indicate that the gas processing plant equipment operation can be improved by optimizing the amine rate during desulfuration and by using protective coats. Figures 2; references 7.

Determining Corrosion Cracking Resistance of Cast Ferritic-Austenitic Steels

937D0057H Lviv FIZIKO-KHIMICHESKAYA MEKHANIKA MATERIALOV in Russian Vol 28 No 1, Jan-Feb 92 pp 99-105

[Article by Yu.I. Romatovskiy, B.I. Voronenko, G.V. Chumalo, R.K. Melekhov, Nizhniy Novgorod Branch of the Prometey Central Scientific Research Institute and Physical Mechanics Institute imeni G.V. Karpenko at the Ukrainian Academy of Sciences, Lvov; UDC 620.194]

[Abstract] The tendency of ferritic and duplex steels toward corrosion cracking, intergranular corrosion, and pitting prompted a study aimed at finding new applications of such corrosion-resistant steels; the scarcity of published data on the corrosion resistance and corrosion cracking resistance of these steels is noted. Four batches of cast duplex steels are examined in the following testing media which are the most common in industry and nature: tap water at 100°C, standard NACE sulfide cracking solution, a 3 percent NaCl solution at 100°C, 42 percent and 30 percent $MgCl_2$ solutions at 154 and 132°C, and a 30 percent NaOH solution at 105°C. The corrosion cracking tendency is estimated by the threshold stress method under static tension for 2,880 hours by a change in the ductility characteristics in the corrosion medium and by a time to fracture at a low straining rate. The polarization curves of steels in some of the above media and the long-term corrosion strength of steel 04Kh25N7AM3 in various media are plotted. The tendency of this steel to hydrogen embrittlement is noted, making it unsuitable for use in the petroleum and gas industry. Otherwise, steel 04Kh25N7AM3 can be recommended for use for structural members operating in a corrosive environment. It can be used without limitations in cold and hot tap water and seawater and in alkaline solutions. Figures 5; tables 4; references 7: 3 Russian, 4 Western.

Quantitative Estimate of Local Corrosion Damage Volume

937D0057K Lviv FIZIKO-KHIMICHESKAYA MEKHANIKA MATERIALOV in Russian Vol 28 No 1, Jan-Feb 92 p 126

[Article by V.N. Polyakov, V.N. Geminov, A.P. Makarov, Orenburg Gas Industry Association, Moscow Instrument Engineering Institute, and Metallurgy Institute imeni A.A. Baykov at Russia's Academy of Sciences; UDC 620.199]

[Abstract] The difficulty of finding the amount of metal that passed to corrosion products in the case where corrosion damage is highly localized and the area, depth and shape of affected areas cannot be easily determined prompted the development of method of quantitatively assessing the local corrosion damage volume whereby a rectangular coordinate grid which is superimposed on the surface under study and the number of squares fully covering the local damage area is calculated and added to one-half of partial squares. An integral formula for computing the corrosion pit volume is derived, and a formula for determining the total volume of all pits is cited. One can see that in order to determine the total volume of all pits, it is necessary to measure either the principal axes or the areas of all pits on the surface as well as the depth of a single corrosion pit.

On Corrosion Cracking of High-Strength Steels in Neutral Media

937D0064A Moscow ZASHCHITA METALLOV in Russian Vol 28 No 6, Nov-Dec 92 pp 894-901

[Article by I.I. Dikiy, I.M. Protsiv, Mechanical Physics Institute imeni G.V. Karpenko at the Ukrainian Academy of Sciences; UDC 620.194]

[Abstract] Conflicting data on the mechanism of corrosion cracking (KR) of steels, the role of hydrogen in the crack nucleation-propagation process, and the effect of primary metal surface processes and secondary reactions in the solution on the thermodynamic and kinetic patterns of its liberation which attest to the diversity of the metal-medium system properties prompted an attempt to assess the dynamics of hydrogen redistribution on the interfaces and within the phases with the help of mass spectrometry, thermal desorption, and atomic absorption spectrometry. The ionic equilibrium at the crack apex and hydrogen liberation on the metal are examined in detail. The pH behavior of a 3 percent NaCl solution in contact with various Fe-based powders, at the crack apex on OSCh especially pure-grade copper in various media, in contact with Cu-based powders, and in contact with Pd-based powder is plotted. A solution alkalization is noted in all cases; it is mainly caused by hydrogen liberation on the metal surface. An analysis of the findings leads to the

conclusion that the primary event which determines the energy relations of the entire liquid media interaction process with the metal surface is the dissociative chemisorption of the solvent molecules on active surface sections with hydrogen occlusion by the metal. Figures 4; references 33: 28 Russian, 5 Western.

Effect of Oxygen-Bearing Oxidizers on Corrosion-Electrochemical Behavior of Tin in Acid Media

937D0064B Moscow ZASHCHITA METALLOV in Russian Vol 28 No 6, Nov-Dec 92 pp 902-908

[Article by A.I. Marshakov, N.P. Chebotareva, Physical Chemistry Institute at Russia's Academy of Sciences; UDC 620.193.3:546.811]

[Abstract] The role of oxygen-bearing oxidizers in accelerating the metal dissolution during iron and zinc corrosion in acid media is discussed, and the need to examine the dissolution patterns of metals with different electrochemical properties in acid media is stressed. The behavior of tin in acid sulfate solutions with H_2O_2, NO_3, HNO_2, and SO_3^{2-} oxidizers is studied within a broad range of potential. The electrochemical behavior of Sn is analyzed in a tin disc electrode spinning at a 710 rpm rate in a deaerated solution of sodium sulfate and sulfuric acid. The mass loss is adjusted for the corrosion current density on Sn^{2+}; the quantitative analysis is performed in a colorimeter with a Nessler reagent at $\lambda = 410$ nm is a Specol spectrophotometer. The dependence of the Sn corrosion current on potential, the potentiostatic dependence of the Sn corrosion current on the $NaNO_2$ concentration and pH of the background electrolyte, cathode potentiodynamic Sn curves, and the dependence of the Sn corrosion rate on potential and $NaNO_2$ concentration are plotted. The curves show that as in the case with Fe and Zn, the oxidizers enhance the Sn dissolution at a constant potential. In acid media in the presence of oxygen-bearing oxidizers, the Sn mass loss is observed at a potential which is 1 V below the free corrosion potential under such conditions. It is speculated that the process occurs through tin hydride formation as an intermediate compound with oxidizer reduction products participating as a proton donor. In the anodic potential area, the oxidizers activate the anodic dissolution due to an increase in the surface concentration of adsorbed OH-ions forming during the oxidizer reduction. Figures 5; references 19: 17 Russian, 2 Western.

On Anodic Formation of Adhesion-Strong Priming Layers on Carbon Steels

937D0064C Moscow ZASHCHITA METALLOV in Russian Vol 28 No 6, Nov-Dec 92 pp 909-915

[Article by A.I. Sverdlov, M.N. Fokin, Kazan Civil Engineering Institute and Physical Chemistry Institute at Russia's Academy of Sciences; UDC 621.357.7]

[Abstract] The use of firm oxide and conversion films for increasing the metals' adhesion to various varnishes and paints, increasing their corrosion resistance, and making metal-polymer composites is discussed, and a principally new method of applying firm adhesion priming to the surface of carbon steels by anodic treatment which results in a layer strongly bonded to the metal matrix is noted. The galvanostatic and potentiostatic polarization curves, thickness, defective layer porosity, and its structure and phase composition on pearlitic-ferritic steels 10, 20, 45, and 65G are investigated. To this end, the adhesive properties, structure, and composition of anodic priming layers produced in citrate-containing electrolytes prepared from sulfuric, nitric, phosphoric, and other acids are examined under a MIM8 metallographic microscope and TESLA BS 301 scanning electron microscope and TESLA BS 500 transmission electron microscope. The phase compositions are studied with the help of an HP-255 Moessbauer spectrometer. Tests data are processed on an EMC-666 computer using Lorentz's function. The galvanostatic anodic curves of steel 10 in an electrolyte and Moessbauer spectra of the priming layer formed on steel 10 in another electrolyte are plotted. The effect of the electrolyte component origin on the thickness and porosity of this layer is demonstrated. It is speculated that selective corrosion of steels is compounded by secondary precipitation of Fe (II) and Fe (III) oxides and Fe (III) hydroxides. Figures 4; tables 3; references 16: 14 Russian, 2 Western.

Structural Material Resistance in Phospholene Production

937D0064D Moscow ZASHCHITA METALLOV in Russian Vol 28 No 6, Nov-Dec 92 pp 916-923

[Article by N.A. Utkina, T.A. Bocharnikova; UDC 620.193.4]

[Abstract] The reactions and reagents involved in phospholene production (1-oxo-1,3-dimethylphospholene) are summarized, and the corrosion resistance of the structural materials in phospholene production media is examined. It is noted that the corrosive action of the production media is due to HCl which is liberated during the adduct formation and the products of its addition as well as high temperatures. The corrosive action of the isoprene, propylene oxide, methylene chloride, and technical mixture delivery lines and the conditions in the reactor unit are examined. Tests of various materials in labs and in pilot production made it possible to assess the corrosion activity of the media in the initial agent delivery lines, at the end product recovery stage, and at the absorbed gas scrubbing stage. The findings made it possible to determine the corrosion resistance of the structural materials in the liquid and gaseous synthesis phases, in volatile compound collectors, and in volatile compound condensation media. After analyzing the data and examining pilot production units, initial specifications are recommended for feasibility analyses and designs of an enlarged pilot installation with a 250 ton/year output. Figures 1; tables 9; references 3.

Structural Material Resistance in Methyldichlorphosphin Production

937D0064E Moscow ZASHCHITA METALLOV in Russian Vol 28 No 6, Nov-Dec 92 pp 924-930

[Article by N.A. Utkina; UDC 620.193.4]

[Abstract] Methyldichlorphosphin production by gaseous phase interaction of methane and phosphorus trichloride initiated with oxygen at 480-600° is discussed, and the

block diagram of the process is cited. The corrosion activity of the production media is examined in a lab and using a pilot unit whereby various substances are ranked according to their activity. The tests are conducted in a PCl_3 medium at room temperature, at boiling, and in overheated vapors at 300°. The test results made it possible to make a preliminary estimate of the corrosion activity of metallic materials in the PCl_3 delivery and heating line. Similar tests are carried out in the methane delivery unit, reactor unit, hardening chamber, and condensing unit. The corrosion activity of individual production media components, especially the HCl liberated during the reaction, combined with a reaction temperature of up to 600° C complicate the structural material selection. An analysis of the specific types of corrosion at various production stages made it possible to develop recommendations for selecting structural materials for each particular process phase and designing a unit with a 250 ton/year capacity. The use of carbon and low alloyed steels 08Kh21N6M2T or 08Kh22N6T is recommended for the PCl_3 delivery line, but steel 12Kh18N10T is suggested for other devices. The reactor can be made from the KhN65MV alloy; steels and alloys are also suggested for other production line units. Initial feasibility study and design data are formulated on the basis of the above analyses. Figures 1; tables 4; references 6.

Effect of Doping With Y, La, and Ce on Electrochemical Behavior of Titanium

937D0064H Moscow ZASHCHITA METALLOV in Russian Vol 28 No 6, Nov-Dec 92 pp 1001-1005

[Article by N.V. Kuznetsova, A.I. Shcherbakov, Physical Chemistry Institute at Russia's Academy of Sciences; UDC 620.193:546.821:66.046.51]

[Abstract] A new trend toward doping corrosion resistant alloys with rare earth metals (RZM) in order to increase their ductility and practicability is outlined and it is noted that in general, the effect of rare earth metals on titanium's corrosion behavior is virtually unknown. To bridge this gap, the electrochemical behavior of binary titanium alloys smelted from a charge containing 0.2 percent by mass of Y, La, and Ce is investigated. To this end, iodide chips are compacted with or without pieces of the doping addition and melted six times with a nonconsumable W electrode in an Ar atmosphere, then forged, rolled, and annealed at 600° C for one hour. An electrochemical study is conducted in sulfuric aid at 50° C on cylindrical electrodes. A comparative estimate of the cathode and anode alloy characteristics is carried out by relatively fast cyclical volt-amperometry. The cyclical potentiodynamic curves of the doped alloys and pure titanium, cathode potentiodynamic curves of Ti and its alloys, and the dependence of the active→passive transition temperature limit on the acid concentration are plotted. The findings show that even insignificant rare earth metal additions may significantly affect the electrochemical behavior of Ti by decreasing the anodic process efficiency and increasing the hydrogen liberation on the cathode, especially in the case of Ce-doping. The conclusion is drawn that titanium and titanium alloy doping with rare earth metals favorably affects the mechanical properties and even increases, rather than decreases, the alloys' passivation ability and expands the temperature-concentration range suitable for operation. Figures 3; tables 1; references 3.

High-Temperature Oxidation of Certain Metallic Materials in Presence of Atomic Oxygen

937D0064I Moscow ZASHCHITA METALLOV in Russian Vol 28 No 6, Nov-Dec 92 pp 1007-1010

[Article by V.I. Bolobov, K.M. Makarov, Scientific Production Association of the State Applied Chemistry Institute; UDC 620.193]

[Abstract] The effect of atomic oxygen at high temperatures on speeding up the oxidation rate in such metals as Pt and Mo prompted a study of the effect of atomic oxygen on the oxidation rate of materials used in making oxygen equipment. To this end, stainless steel 12Kh18N10T, industrial Ni NP-2 (99.8 percent pure), and technical Fe (99.9 percent pure) are studied in an oxidizing medium created by a N_2O dissociation reaction. Regression lines of the oxidation rate equation of stainless steel, Ni and Fe in active nitrous oxide dissociation products and oxidation rate constants, activation energy, and exponential factor for calculating the parameters of Arrhenius's equation for stainless steel oxidation are plotted. The tests show that the phase composition of the oxide films on the materials is virtually the same in the air and in active dissociation products. The proximity of the film thickness and the curves make it possible to conclude that the presence of O in the oxidizing medium does not significantly affect the rate parameters of high-temperature oxidation of structural materials which is consistent with Kubashewski's and Hopkins's findings. Figures 2; tables 1; references 6.

Aluminum Dissolution Kinetics in HCl Solutions in Ether

937D0064J Moscow ZASHCHITA METALLOV in Russian Vol 28 No 6, Nov-Dec 92 pp 1010-1014

[Article by T.L. Popova, A.I. Bulavchenko, A.D. Afanasyev, T.N. Blokhina, Joint Geology, Geophysics, and Mineralogy Institute at the Siberian Department of Russia's Academy of Sciences; UDC 620.193]

[Abstract] The importance of understanding the patterns of metallic Al behavior in organic media for the theory and practice of corrosion protection, particularly coat application, chemical current sources, and other chemical engineering tasks prompted the development of experimental procedures for examining the kinetics of Al dissolution in HCl solutions in diethyl ether. To this end, studies are carried out in anhydrous solutions of HCl in ether prepared by saturating ether with dry HCl produced from a reaction of NaCl with H_2SO_4. The HCl concentration in the ether solution is determined by dissolving its aliquot in doubly distilled water and potentiometrically titrating it with alkali or measuring the pH. The metallic Al dissolution kinetics in ether solutions of HCl at various concentrations and differential distribution functions of the induction period duration and Al dissolution rate in a linear segment are plotted. A schematic diagram of the experimental test cell is shown. An analysis demonstrates that the rate curves are S-shaped which can be attributed to the surface film dissolution from the sample surface and the autocatalytic character of dissolution. An increase in

the hydrochloric gas concentration in ether shortens the induction period and increases the Al dissolution rate. The study reveals that the differential distribution functions are Gaussian. Figures 3; references 8.

Protective Properties of Some Condensed Imidazole-Bearing Substances in Acid Media

937D0064K Moscow ZASHCHITA METALLOV in Russian Vol 28 No 6, Nov-Dec 92 pp 1020-1023

[Article by S.V. Gruznova, I.N. Kurmakova, A.M. Demchenko, K.G. Nazarenko, Ye.I. Mayboroda, Chernigov State Teachers College imeni T.G. Shevchenko; UDC 620.197.3]

[Abstract] Corrosion inhibition by imidazole or benzimidazole rings with various substituents in acid media is discussed, and substances containing the imidazole ring condensed with isoindole, hydrated pyrrhole, and azepine are synthesized and their protective properties are investigated. The corrosion tests are carried out in sealed eudiometers according to GOST 17322-71. The electrochemical measurements are taken using a P 5848 potentiostat with a cylindrical electrode from steel St45 embedded in teflon. The polarization curves of steel St45 in HCl solutions with and without inhibitors are plotted within a Ph 0.5-2 range at a 0.02 V stationary potential step. The corrosion rate of St45 in various substances at various concentrations is summarized. The inhibiting action of the above organic compounds is confirmed and it is shown that the substituent position in the substance containing the imidazole ring condensed with hydrated pyrrhole affects the parameters of cathodic hydrogen liberation but has virtually no effect on the protective action. Figures 2; tables 3; references 8.

On Corrosion State of Metal-Polymer Interface

937D0064M Moscow ZASHCHITA METALLOV in Russian Vol 28 No 6, Nov-Dec 92 pp 1035-1039

[Article by A.P. Pospelov, M.V. Ved, N.D. Sakhnenko, Kharkov Polytechnic Institute; UDC 620.198]

[Abstract] The origin of the protective action of polymer coats on metals and the effect of the barrier properties of the adhesive-substrate system and the energy state of the interface which is nonuniform and thus determines the high localization and specific rate of metal dissolution are discussed. The effect of competing processes on the anodic surface dynamics at the initial phase of metal-coat system exposure to a corrosive medium is examined in order to assess the protective properties of the coats and the effective value of the corrosion rate. To this end, samples of steel St3 with BEP-0126, BEP-421; VL-02, KhS-413; VL-02, EP-755; and EKZhS-40 protective coat systems are examined; 300 +/- 10 μm thick coats are deposited by a standard method. The measurements are taken in sealed temperature-controlled cells whose media composition is controlled with the help of an inert gas. A 3 percent sodium chloride solution is used as the corrosive medium while the potential of the system is recorded by a VK2-16 high-resistance voltmeter. Chronograms of the specific active surface, moisture absorption, and electrochemically active oxygen molecule fraction and chronograms of the electrode potential shift during the dissolved oxygen delocalization are plotted. A break of adhesive bonds is noted at the initial exposure stage for all types of coats. The alkalization process makes the greatest contribution to the adhesive bond break. The study confirms the assumption that the coats' protective action is due to both their adhesive and barrier properties. The above approach makes it possible to establish the criteria of protective coat properties and determine the degree of active metal dissolution localization zones. The use of these concepts increases the confidence of estimates and service life prediction under operating conditions. Figures 2; references 9: 8 Russian, 1 Western.

Pre-Killing Steel by Silicon Carbide Injection

937D0054A Moscow STAL in Russian No 9, Sep 1992 pp 25-26

[Article by V. N. Perevertin, M. M. Kudrayvstev, and V. N. Domoradskiy, Scientific Research Institute of Metallurgical Technology and the Izhstal Production Association; UDC 669.183.218.55]

[Abstract] The Izhstal PA has adopted a process for pre-killing 38KhS and 20Kh2N4A alloy engineering steels in 45-t open-hearth furnaces by injecting compressed air containing powdered silicon carbide into the melt. A stationary SB-67B-based pneumatic conveyor is used to pump the air-powder stream into the furnace through a stainless-steel pipe. When testing the process, ferroalloy chunks were added to the melt both after and during the injection of the SiC, the consumption of which amounted to 2.5 to 4.0 kg/t. Slag and steel samples were taken both before and after pre-killing, and also before tapping the metal. The ferroalloys dissolved faster when added to the melt during injection rather than before because of the greater degree of agitation achieved and the stable increase in bath temperature by 10°C after injection ceased. As a result, killing time decreased five to six minutes and the conditions for bringing the metal to temperature improved. In comparison with the conventional steelmaking process used for reference, SiC injection greatly intensified the killing process, as the oxygen concentration fell 50 percent to 0.020 percent. It made it possible to increase and stabilize the carbon concentration at 0.02 to 0.04 percent while reducing iron consumption 2.0 to 2.5-fold. Silicon concentration increased to 0.08 to 0.10 percent. Nitrogen and hydrogen content remained unchanged. Chromium and silicon melting loss fell by 17 and 18.5 percent respectively, and ferroalloy consumption by 37.5 tons per year. The editors noted separately that this process requires additional validation from an economic standpoint and that SiC can be used more effectively in other applications, such as refractory production. Tables 1.

Improving Corrosion-Resistant Steelmaking With Oxygen Refining

937D0054B Moscow STAL in Russian No 9, Sep 92 pp 27-30

[Article by S. L. Sergiyenko, G. A. Buryakovskiy, S. S. Kazakov, Yu. V. Sadovnik, and D. V. Zimin, the Dneprospetsstal Plant and the Dnepropetrov Metallurgical Institute; UDC 669.187.25]

[Abstract] An improved oxygen steelmaking process was studied while using the duplex process to make 06-12Kh18N10T, 08- 10Kh17N13M2(3)T, and 10-20Kh23N18 steels. The duplex process entails making a semi-finished batch of steel in an electric furnace and then refining it in an oxygen furnace, in this case a 60-t vessel with three dual tuyeres for submerged injection of the process gasses. FKh800 high-carbon ferrochromium, nickel, and the molybdenum-bearing alloy elements were added to the molten steel before it was transferred to the converter. The steel was first decarbonized with 0.8 to 1.0 cu m/(t-min) of oxygen, using natural gas in the outer tuyere, until the carbon concentration reached 0.20 to 0.22 percent, then with the same quantity of a nitrogen/oxygen mixture (ratio not specified) until the proper carbon concentration was reached. The steel was then reduced with 0.8 cu m/(t-min) of argon for five to six minutes. The improved process yields a clean steel with no more than 0.050 percent nitrogen, which meets the specifications of TU 14-1-790-73, does not affect the steels' properties and characteristics, and reduces argon consumption by five to six cu m/ton of steel. Figures 2, tables 3.

Controlling the Course of the Reducing Period During Corrosion-Resistant Steelmaking

937D0054C Moscow STAL in Russian No 9, Sep 1992 pp 30-32

[Article by D. V. Yermolayev, A. D. Pereverzev, and V. M. Shifrin, Dneprospetsstal Plant and the Dnepropetrov Metallurgical Institute; UDC 669.187.243]

[Abstract] The Dnepropetrov Metallurgical Institute has developed a determinate statistical model for controlling the course of corrosion-resistant steelmaking in electric arc furnaces. The model works in both real and predicted time. The results of previous studies that have made it possible to gain a more precise understanding of the nature of the relationships between the arguments and functions of the reducing processes, given a number of fixed process parameters, were used to develop theoretical equations for constructing an algorithm that could be used to control the course of the killing process after blowing. This algorithm accounts for the particular characteristics of the deoxidation and reducing periods of the steelmaking process and makes it possible to stabilize the killing process and the chemical composition of the metal and to increase the amount of chromium recovered from the slag. A model was also developed to control the course of the thermal conditions in the furnace during corrosion- resistant steelmaking. More precise values were found for the cooling effects of the scrap added to the charge and for the thermal characteristics corresponding to discrete voltage levels of the furnace transformer. When the model was tested against actual production conditions, it yielded values that were reasonably close to real temperatures and made it possible to stabilize the process parameters for the reducing period of the steelmaking process. Tables 2.

Using Ladle Treatment To Improve the Quality of Bearing Steel

937D0054D Moscow STAL in Russian No 9, Sep 1992 pp 33-35

[Article by V. M. Kulik, L. M. Livshits, K. P. Verbitskiy, Ye. I. Kadinov, R. S. Raytmanov, and N. V. Stetsenko, the Dneprospetsstal Plant, the Dnepropetrov Metallurgical Institute, and the Ukrainian Scientific Research Institute of Specialized Steels; UDC 621.746.58]

[Abstract] The Dneprospetsstal Plant has developed a new process for desulfurizing bearing steel. Experimental heats of ShKh15 and ShKh15SG steels were made in 60-t electric furnaces. When the required carbon content and temperature had been reached, the slag was removed, and ferrosilicon, fluorite, fireclay scrap, lime, and ferrochromium were added to the melt while it was being stirred. The quantities of the ferroalloys were calculated to introduce 0.15 to 0.20 percent Si into the melt (not allowing for

melting loss) and to achieve a chromium content at the lower end of the range specified for these grades of steel. Melt composition was adjusted at 1610 to 1630°C (somewhat higher than normal), the slag drawn off, and the metal tapped from the furnace. The ShKh15SG steel was alloyed with manganese both in the furnace and in the ladle. When alloying it in the furnace, the manganese ferroalloys were added to the melt 10 to 15 minutes prior to tapping, after the slag was removed. During ladle alloying of both steels, ferrosilicon, ferromanganese (for the Shkh15SG steel), lime, and fluorite were added to the ladle within 10-15 seconds after tapping had begun. For the ShKh15 steel, powdered aluminum was poured on the bottom of the ladle prior to tapping. The ladle was then transferred to a ladle heating unit, where the metal was simultaneously heated and blown with argon to make the final adjustments in composition. The steel was cast in accordance with existing practices. Use of the experimental technology reduced the sulfur content to 0.0085 to 0.010 percent in the finished steel, lowered the refining temperature for the ShKh15 steel by 26° (furnace) and by 44° (ladle), and decreased processing time by 25 to 30 minutes. Contamination with non-metallic inclusions was greatly reduced, resulting in a substantial improvement in the surface quality of the rolled product. Tables 4.

Making Electroslag Refining of Sheet-Rolling Ingots More Economical

937D0054E Moscow STAL in Russian No 9, Sep 92 pp 35-36

[Article by Yu. G. Gabuyev and L. N. Korol, the Dneprospetsstal Plant; UDC 669.012.7]

[Abstract] The Dneprospetsstal Plant has adopted a more economical electroslag process for refining 09G2SSh and 9Kh2MFSh steel ingots used to roll sheet. Consumable slab electrodes 142 by 1120 mm are remelted into 11.5-ton ingots 650 by 1350 mm. The electrodes are placed back-to-back in the mold to effect a bifilar current-supply circuit for the ES furnace. It was found that a stable electroslag process can be achieved with a minimal slag bath level of 100 mm. The best results were achieved when the addition of the flux brought the level up to 130 to 150 mm and the electrodes were submerged to a depth of 20-60 mm. Two of the fluxes tested, ANF-6 and ANF-32, did not yield satisfactory results, so the slag bath was deoxidized by facing the mold lining with aluminum bars. The new process makes it possible to use slabs as consumable electrodes without first removing the scale and reduces flux consumption by 35 percent in comparison with existing technology. Tables 1.

Electroslag Refinement of 9Kh2MF-Sh High-Carbon Alloy Steel

937D0054F Moscow STAL in Russian No 9, Sep 1992 p 37

[Article by V. G. Knokhin; UDC 669.187.56]

[Abstract] The Dneprospetsstal Plant, in conjunction with specialists from the South Ural Machinery Plant, has proposed using ESR 9Kh2MF steel ingots to manufacture the rollers for hot wide-sheet rolling mills. The semi-finished ingot steel is made in 60-t electric arc furnaces with full oxidation or by remelting and oxygenizing alloy scrap. Final killing is done in the ladle, using 0.48 to 0.52 kg/t of aluminum and 1.8 to 2.0 kg/t of silicocalcium while maintaining a melt temperature of 1650 to 1590°C. After treating it with liquid lime-alumina slag or solid slagging materials while it is being blown with argon, the metal is siphoned into dry ingot molds with an exothermic mixture. The time needed to fill the mold up to the feedhead is 220 to 360 seconds, and an additional 100 to 150 seconds are needed to fill the feeder. The glass of the metal is covered with Lunkerite. The ingots are hot rolled into slabs and sent to the annealing furnaces. ESR was carried out in bifilar circuit furnaces. After removal from the molds, the ESR ingots are slowly cooled under hoods or in thermal wells or soaking pits, and, within five hours after cooling, sent to be annealed. The quality of the ingots, which weigh from nine to 12 tons, is satisfactory, with sulfur content not exceeding 0.20 percent.

Increasing Corrosion-Resistant Steelmaking Efficiency

937D0054G Moscow STAL in Russian No 9, Sep 1992 p 37

[Article by A. F. Startsev, K. P. Verbitskiy, S. S. Kazakov, V. A. Shevchenko, and V. P. Denisenko, the Dneprospetsstal Plant and the Ukrainian Scientific Research Institute of Specialized Steels; UDC 669.187.25]

[Abstract] The Dneprospetsstal Plant and the Ukrainian Scientific Research Institute of Specialized Steels have worked together to develop and test a new process for making Kh18N10T corrosion-resistant steel. The steel is made in electric furnaces using alloy B-26, B-18, and similar scrap, high-carbon ferrochromium, ferronickel, and nickel. The charge is calculated to yield a melt with 12-16 percent Cr, 0.5 to 0.8 percent C, 0.2 to 0.5 percent Si, and 0.2 to 2.0 percent Mn. After blowing with argon at a melt temperature of 1900 to 1950°C, the furnace is turned off, and ferrosilicochromium or ferrosilicon, lime, ferrochromium, nickel, other ferroalloys, and some rolling or forging scraps of the grade of steel being made are added. This process lasts for 15 to 20 minutes, until the melt temperature reaches 1650 to 1670°C. The semi-finished steel is brought to the proper chemical composition while still in the furnace, after which it is tapped into a transfer ladle that already contains 50 to 70 percent electric furnace slag killed with aluminum powder or aluminum alloy scrap. A stand- or pit-mounted casting ladle is charged with lime, fluorite, ferrotitanium or titanium briquettes, aluminum chunks, and steel innoculators. Within 115 seconds, the melt is transferred from the intermediate to the casting ladle through a casting nozzle 150 to 180 mm in diameter, presuming batch weight is 55 to 60 tons. The steel is cast according to existing practice. In comparison with conventional processing, the new process reduces refining time 20 to 25 percent, electrical consumption 15 to 18 percent, and melting loss by 25 to 30 kg/t, while increasing desulfurization to 70 percent and titanium assimilation to 55-65 percent. Hydrogen content is reduced 20 to 25 percent and chromium consumption by 12 to 15 kg/t of steel. Rolled product surface quality is improved, while waste due to cracks and cavities drops 0.15 and 0.12 percent, respectively. Other types of typical are eliminated. Figures 1, tables 2.

Metallurgy, a 'Melted' Market

937D0059A Moscow EKHO DELOVOY ZHIZNI in Russian No 9, Sep 92 p 2

[Article by A. Baliyev: "Metallurgy, a 'Melted' Market"]

[Text] Six months ago, after an attempt to leap into the market, Russia's metallurgical plants are working at only 50-60 percent of capacity, and only 40-50 percent of the demand for iron, steel, and rolled products is being satisfied (as opposed to 25-30 percent in June of last year). The scarcity of metal goods in machine building and, therefore, in branches using machine building products (agriculture, light industry, food processing, wood processing, and others) is becoming acute. The breakdowns in the extraction, delivery, and processing of raw materials and in the sale of finished products not only are disrupting the development of this branch, but also have dealt a painful blow on the entire national economy.

Specialists note that, given the shortages of iron and manganese ores and coking coal, without which the metallurgical complex cannot operate, their export outside Russia and the SNG [Commonwealth of Independent States—CIS] through exchanges and auctions is growing.

According to estimates, more than 60 percent of the ferrous metals sold through exchanges, including 75-80 percent of ferrous allows, is transported from Russia outside the borders of the CIS. The situation in the branch is exacerbated by the acute shortage of cash needed to cover salaries and supplies, to modernize production, and for social and ecological programs. The breakdown in long-standing direct relationships and the elimination of traditional markets complete the picture of the disintegration, the "meltdown," of Russian ferrous metallurgy.

The total volume of exchange transactions involving ferrous metals rose from 381 to 558 million rubles in the first semester, but the volume of actual ferrous metallurgy products sold and kept in Russian increased only from 108 to 182 million rubles. The financial, economic, and technological crises in ferrous metallurgy and industries using its products today makes it impossible to increase the volume of actual sales of ferrous metallurgy products inside Russia. As a result plants in metallurgy, machine building, and related branches are becoming increasingly unprofitable.

An especially adverse situation has developed in ferrous alloy production: more than 60 percent of production capacities are now outside Russia's borders—in the Ukraine, Kazakhstan, and Georgia. Basic resources in chromium, aluminum, and manganese are also concentrated in the Ukraine, Georgia, Azerbaijan, Kazakhstan.... Production and consumption of ferrous alloys is, technologically and economically, inextricably linked to the production and sale of equipment for the extraction industry and metallurgy (i.e., to heavy machine building). But the main heavy machine building capacities in the CIS are located in the Ukraine and Kazakhstan. According to data from June of this year, the shortage of ferrous alloys in Russia was more than 50 percent, while this indicator was no more than 30-35 percent in the Ukraine and Kazakhstan.

The following figures also reflect the crisis in the former USSR's metallurgical complex:

Table 1.

		USSR	United States	Germany	Canada
Oxygen-converter steel as a percentage of the total amount of steel smelted	1988	47.5	65.0	100	100
	1991	45.3	95.3	100	100
Continuously cast steel as a percentage of the total amount of steel smelted	1988	16.6	64.0	88	50
	1991	15.1	63.2	90	53.6

At the end of the first semester of 1992, 138 million tons of slag were left from blast furnace production, 79 million tons from steelmaking. These figures are 5 and 13 times higher than the amount used in six months in the former USSR. That is, Russia and the CIS are falling farther and farther behind industrialized countries in ferrous metallurgy.

According to estimates by the European Coal and Steel Association (July, 1992), the near-term development of ferrous metallurgy in Russia depends on the following factors:

—the way in which the problem of financing is solved at metallurgical enterprises;

—how successful the coordinated economic policy in metallurgy and machine building within the framework of the CIS is;

—whether money will be found to rebuild and modernize most extracting and processing facilities and whether conditions are provided to stimulate an increase in labor productivity in the CIS metallurgical complex;

—the situation in branches consuming metallurgical and machine building products;

—finally, how successfully direct, including interbranch, ties within the framework of the CIS, as well as ties between the CIS members and Eastern European countries formerly members of the CMEA, are restored.

Obviously, no one should count on a quick solution to all these truly complicated problems. A breakthrough in even a few areas, e.g., restoration of ties with former CMEA members, would be encouraging... Some kind of positive movements are needed.

Will There Be Kazakhstan Stainless Steel?

937D0059B Alma-Ata KAZAKHSTANSKAYA PRAVDA in Russian 7 Oct 92 p 2

[Interview with Yan Tampayev, chairman, Aktyubinsk Oblast Economic Committee, assistant chief, Oblast Administration, by Aybas Syzdykov, staff correspondent, place and date not given: "Will There Be Kazakhstan Stainless Steel? There is Much Debate, but Time is Wasting"]

[Text] **The reorientation of Kazakhstan's economy is increasing the demand for corrosion-resistant specialty alloys and stainless steel. But that is not the only reason why the problem of building the electric metallurgical plant ordered by the AO [joint stock company] "KRAMDS-Spetsstal" in Aktyubinsk is critical. Selling finished product rather than raw materials in the form of chromium and ferroalloys to foreign countries will make it possible to make millions—including hard currency.**

But as of today all work has nearly stopped. Why? Yan Tampayev, chairman, Aktyubinsk Oblast Economic Committee and assistant chief, Oblast Administration, answers these and other questions posed by our correspondent.

[Syzdykov] Yan Tampayevich, let's begin our conversation with how the idea of building a stainless steel production plant in Aktyubinsk came about.

[Tampayev] The idea isn't a new one. The question of building a mining and smelting plant using Aktyubinsk chromium ores and ferroalloys came up for the first time in 1975. But the leaders of the Union and the Ministry of Ferrous Metals at that time would have nothing to do with us.

Twelve years later, at the order of the Kazakh SSR Council of Ministers, a special republic Gosplan group worked to prepare material on the feasibility of developing a whole complex with finish processing at the Aktyubinsk Ferroalloy Plant, the Donskoy Mining and Enrichment Combine, and the Aktyubinsk Chromium Compound Plant. But, unfortunately, the CPSU Central Committee and the USSR Council of Ministers left this and a later document untouched.

By 1995, by all technical and economical calculations, the former Union must have the capacity to produce up 2.04 million tons of stainless steel. The increase was supposed to come from expanding the Chelyabinsk, Cherepovets, Oskolsk, and other plants. In essence, nothing that was planned has been done. Moreover, steel output has dropped 20 percent.

[Syzdykov] So all this work in Kazakhstan is now starting from scratch under different, more difficult conditions?

[Tampayev] Yes, we've started from zero. The venture group created a limited liability stock company. Its founders, the KRAMDS Corporation, the Aktyubinsk Oblast Administration, the Donskoy GOK [mining-enrichment combine], the Aktyubinsk Ferroalloy Plant, and the "Yuzhuralnikel" Combine, asked Kazakhstan President N. Nazarbayev for support in creating a branch totally new for the republic. It was to begin with construction of a 200,000-tpy electric stainless steel plant in Aktyubinsk that could be expanded as needed. Products would be sold on both the domestic and foreign markets. We founders were overjoyed at the president's categorical approval.

[Syzdykov] And what happened?

[Tampayev] We started work. After establishing the initial source of funds, we began to prepare the feasibility study. We studied international marketing and investment possibilities, sat down with the general designer. The study was reviewed and approved by an expert commission of the USSR Engineering Academy. The best of seven alternative sites was found, and mining and geological surveying began.

Through competitive bidding we selected two foreign partners who wanted to finance and build a turnkey plant. A cooperation agreement was signed with West Group International of Canada and HECH Associates of Austria. All this happened rather quickly.

[Syzdykov] In the current difficult situation, plant construction is probably costing the founds a pretty penny. How do you intend to solve the financing problem?

[Tampayev] Yes, indeed, the preliminary capital expenditures alone come to 3.047 billion rubles. We are geared for 100 percent financing by foreign investors on a buyback basis. That is, the plant has to be built by the western companies under mutually beneficial conditions guaranteeing production of stainless steel to meet the requirements of the international market. We will return the partners' investment in the form of finished product—30 percent of the annual output sold for hard currency. There's nothing new here. This is a generally accepted form of international cooperation. The main thing is to analyze in detail and cover everything in the contract, to have the appropriate guarantees from both parties.

[Syzdykov] But, as far as I know, construction has again been postponed for an indefinite period. So you still have enemies?

[Tampayev] Absolutely. Enemies appeared, as did alternative proposals, although the president of the republic himself supports principle of building the plant on a buyback basis.

When we emerged from the required analyses, we began drawing up the contract and producing contractor drawings. It became necessary to get the government's official approval of plant construction and of its guarantees to the foreign investor, that is, to insure return on investment. In order for him to assure his own export credit insurance company of guaranteed repayment. That's on the one hand. On the other, completing a major project is impossible without the involvement of republic ministries, departments, concerns.

Because of all this, the Founders' Board turned to the Cabinet of Ministers. Then it started! Representatives of

the Chelyabinsk Metallurgical Combine showed up, agreeing to deliver stainless steel to Kazakhstan on the spot. The republic's Ministry of Industry ordered "ChelyabGIPROMEZ" to immediately develop alternative feasibility studies.

The results of these actions can be presented as follows: after getting US$600 million for our raw materials (they don't have their own chromium, nickel, or titanium ore or scrap metal), Chelyabinsk will buy imported process equipment and rebuild the electric steelmaking shop in order, as promised, to cover Kazakhstan's need for stainless steel once and for all.

Can one believe this promise today, when not even one enterprise in one state can fulfill its obligations to others, despite actions by the government and arbitration courts? Moreover, reconstruction of this shop will cost 3440 billion rubles in 1991 prices; the new shop in Aktyubinsk, 3047 billion. Even with that same ore that we have lying in deposits we can build our own independent stainless steel production. At the very least, if the republic's Ministry of Industry has any doubts on this account, why don't they submit our project for expert review?

Drawing up a contract and conducting expert review take from six to ten months. We've already lost three—that's how long the draft decree has been lying in the Cabinet of Ministers.

[Syzdykov] What will Kazakhstan get with the plant except your stainless steel?

[Tampayev] Quite a lot. First, the prospect of strengthening its economic potential by using modern technologies, improving worker skills, and, most important, a source of hard currency income to the budget. Second, we will actually begin to alter the structure of raw material production toward production of finished product. Just think—we have almost 100 percent of the CIS' chromium ore reserves and most of the world's reserves. And, except for dumps and ecological stress, we have nothing. If you remember the reserves of nickel, copper, and titanium ore, you can understand the kind of pot of gold we're sitting on. We have all the conditions for creating modern, world-class production facilities.

Third, building the plant will create additional jobs, especially for young people. And fourth, this is a boost to the development of the city of Aktyubinsk's industrial and social infrastructure, to the creation of new educational institutions for training specialists.

It is in the interests of the oblast and republic to solve this problem as quickly as possible.

A Model for Injecting Air When Tapping Steel From an Oxygen Furnace

937D0065A Moscow IZVESTIYA VYSSHIKH UCHEBNYKH ZAVEDENIY: CHERNAYA METALLURGIYA in Russian No 9, Sep 92 pp 7-9

[Article by V. B. Okhotskiy and A. A. Dzhusov, Dnepropetrov Metallurgical Institute; UDC 669.184.15]

[Abstract] The effects of having atmospheric air injected into molten steel during the tapping process were studied on a 250-t oxygen furnace at the Dnepropetrov Metallurgical Combine imeni Dzerzhinskiy. The flow rate of the metal was simulated by using a cylinder with a radius equal to the internal diameter of the lined cylindrical portion of the furnace mouth. The cylinder height was equal to that of the cylindrical portion of the opening plus the adjusted height of two cylinders, the volume of which corresponded to the actual working volume of the bottom and domed parts of the furnace. For the purposes of the experiment, it was presumed that the metal was tapped when the furnace was in the horizontal position. The rate at which the metal flowed from the furnace was calculated theoretically and by filming the tapping process at 33 frames/second. The results, which did not differ by more than 7 to 10 percent, showed that the flow rate was 625 to 667 cm/s at the beginning of the tapping process at a distance of 1350 to 1400 mm from the lip of the furnace mouth, and 529 to 551 cm/s as the stream fell into the metal in the ladle. These findings were used as the basis for constructing equations used to calculate the quantity of oxygen injected into the metal by a single circular wave when tapping a known quantity of metal. According to this model, 54.8 cu m of air are injected into a 50-t batch of metal as it falls into the ladle. Of this air, 14.8 kg, or 0.0059 percent of the steel's mass, is made up of oxygen, which is responsible for 14 to 20 percent of the total manganese melting loss. Figures 3; references 7: 6 Russian, 1 Western.

Treating Low-Alloy Steel in the Ladle With a Pulsating Stream of Argon

937D0065B Moscow IZVESTIYA VYSSHIKH UCHEBNYKH ZAVEDENIY: CHERNAYA METALLURGIYA in Russian No 9, Sep 1992 p 10

[Article by O. V. Drobyshevskiy, G. N. Kalyshev, V. P. Meshkov, and V. G. Zalavina, the Orsko-Khalilov Metallurgical Combine; UDC 669.046.554:541.96]

[Abstract] The Orsko-Khalilov Metallurgical Combine has developed a lance for injecting a pulsating stream of argon into steel made in 250-t dual-hearth furnaces. The lances are 3.7 m long and equipped with an easy-to-assemble oscillator made in the form of a blind nipple fit into a rod installed in the lance so as to form a ring-shaped nozzle. Seventy heats of steel treated in the ladle with the new lance (100,000 tons in all) were compared with 70 heats of steel ladle-treated with the conventional lance (212,000 tons in all). In both cases, the pressure of the argon in the gas main supplying the lances was the same—0.3 to 0.4 MPa. Both steels were fully killed in the ladle, which had a capacity of 250 tons, and cast into 13-t ingots that would subsequently be rolled into sheet to make large diameter pipe for high-pressure oil-and-gas pipeline. It was found that, when the new lance was used, the quantity of defective sheet detected by ultrasound or due to non-metallic inclusions was reduced 0.05 percent, from 9.24 to 9.07 percent. For the conventionally blown steel, 0.34 percent of the reject percentage was attributed to ultrasound inspection, and 0.89 percent to non-metallic inclusions. These figures were 0.29 percent and 0.69 percent, respectively, for the test metal. The distribution of the chemical elements in the steel was more uniform, while average deviations from the desired proportions of silicon, manganese, and phosphorus were reduced 10 to 15 percent.

Nitrogen and hydrogen concentrations were also reduced somewhat. Tables 2; references 1: Russian.

Magnetic Structure and Properties of Rapidly Quenched Didymium-Iron-Boron Alloy

937D0065F Moscow IZVESTIYA VYSSHIKH UCHEBNYKH ZAVEDENIY: CHERNAYA METALLURGIYA in Russian No 9, Sep 92 pp 35-38

[Article by A. M. Gabay, A. S. Lileyev, S. A. Melnikov, V. P. Menushenkov, and A. G. Savchenko, Moscow Institute of Steel and Alloys; UDC 621.318.12]

[Abstract] The magnetic structure and properties of rapidly quenched $DD_{14.7}(Fe_{0.88}Co_{0.1}Mo_{0.02})_{78}B_{7.3}$ alloy were studied. The alloy was quenched by pouring it into a drum rotating at 19 m/second. Because it is so brittle, the alloy comes out as individual flakes up to 100 μm, 2 to 5 mm in length, and width. Mesh was used to sort the flakes into four fractions of varying weights. Average flake thickness decreases from 67 μm for the 800 to 5000 μm fraction to 36 μm for the 100 to 300 μm fraction. Hence, fraction size was defined in terms of actual flake width. A vibration magnometer was used to measure the magnetic properties of paraffin-mounted specimens magnetized in a pulse field with an intensity of 5600 kA/m. Thermomagnetic analysis was performed in a field with an intensity of 400 kA/m within a temperature range of 20 to 550°C. X-ray diffraction analysis was performed on a DRON-3M diffractometer using FeK_{α}-radiation. The specimens were heat treated in a 10exp-2-Pa vacuum. After rapid quenching, the alloy consists of an amorphous phase, a $DD_2(Fe, Co)_{14}B$ phase, and α-Fe (or a α-Fe-based solid solution). As fraction size and average flake width decrease, the quantity of both the amorphous phase and the α-FE increase. Full crystallization of the amorphous phase occurs during annealing at 600°C for 15 to 60 minutes. Once this has been done, the magnetic properties of the alloy have virtually nothing to do with flake size, with only the smallest flakes being slightly affected. Remagnetization is presumably controlled by the inception of reversed polarity domains in the grains of the base phase. Figures 5, tables 1; references 10: 1 Russian, 9 Western.

Hydrogen Brittleness of Dispersion-Strengthened 10Kh11N23T3MR Austenitic Steel

937D0065G Moscow IZVESTIYA VYSSHIKH UCHEBNYKH ZAVEDENIY: CHERNAYA METALLURGIYA in Russian No 9, Sep 92 pp 39-41

[Article by A. V. Mikhaylov and V. B. Shepilov, Voronezh Polytechnic Institute; UDC 669.15'24'26'28'-194: 669.788]

[Abstract] Dispersion-strengthened 10Kh11N23T3MR austenitic EP-33 or EI696M steel was heat-treated in a hydrogen atmosphere to determine how hydrogen affects its mechanical properties, its susceptibility to hydrogen embrittlement, and the embrittlement mechanism. After conventional heat treatment, the steel was hydrogen heat-treated in special autoclaves at 450 and 650°C and pressures from 0.05 to 15 MPa for 0.5 to 24 hours. Hydrogen concentration in the steel was determined by using a LECO RH-3 to melt samples in an inert gas atmosphere. Cylindrical specimens 5 mm in diameter with a gauge length of 5 were tested per GOST 1497-84 at temperatures from -196 to +20°C and a strain rate of 1×10^{-4} to 2×10^{-1} seconds^{-1}. It was found that the high-temperature hydrogen treatment led to a substantial reduction in ductility and had virtually no effect on the strength characteristics of the steel in question. Hydrogen (acid) brittleness was observed at temperatures near 20°C, and hydrogen concentrations exceeding 0.04 to 0.05 percent (at.) were also characterized by an increase in the brittle fracture component. It was concluded that embrittlement is caused by a hydrogen-induced reduction in the forces of atomic interaction at the grain boundaries, primarily close to the grain-boundary precipitations of the γ'-phase. Figures 2; references 7: 6 Russian, 1 Western.

Ultrasonic Sensor of Metal Level in a Mold

937D0065H Moscow IZVESTIYA VYSSHIKH UCHEBNYKH ZAVEDENIY: CHERNAYA METALLURGIYA in Russian No 9, Sep 92 p 82

[Article by N. I. Shesnakov, Yu. P. Kostin, and A. P. Shchegolev, Cherepovets Technical Institute; UDC 669.18:621.746]

[Abstract] A sensor that works on the principle of ultrasound location was developed for measuring the level of metal in molds. The sensor consists of a search unit, a mechanism to move the sensor up and down, a display unit, and a signal processor. The search unit incorporates a piezoelectric transducer that directly contacts the outer surface of the mold wall. The mechanism that moves the search unit up and down consists of a screw-type gear, a reduction gear, and a stepper motor. The search unit and the screw gear are housed in an airtight steel container mounted on the external surface of the mold wall. The housing is filled with transmission fluid that enables the search unit to make acoustical contact with the mold wall. The motor and reduction gear are mounted on the external surface of the housing. The display unit consists of a device that counts the turns of the gear screw and a device for displaying the metal level. A UD-11PU flaw detector is used as the signal processor. The device was first tested on a laboratory mock-up simulating an actual mold, then on an actual mold at the Cherepovets Metallurgical Combine. The results of these tests showed that the level of metal in a mold fluctuates with a frequency between 0.8 and 1.3 Hz, a frequency that matches the fluctuations of the output signal, the amplitude of which falls between 25 and 30 percent. The sensor is capable of measuring the level of metal in mold to within 0.15 m. The position of the search unit relative to the mold wall can be measured to within 1 mm. Figures 1; references 1: Russian.

Supression of Ordering by Laser Radiation in Electrical Engineering Steels With High (up to 6.5 percent) Concentrations of Silicon

937D0065I Moscow IZVESTIYA VYSSHIKH UCHEBNYKH ZAVEDENIY: CHERNAYA METALLURGIYA in Russian No 9, Sep 1992 p 84

[Article by L. M. Kaputkina, A. M. Bernshteyn, and B. B. Somov, Moscow Institute of Steel and Alloys; UDC 669.018.5:621.373.826]

[Abstract] The feasibility of using laser radiation to suppress ordering in high-silicon electrical engineering steel strip was studied. Isotropic electrical engineering steel specimens 0.5-mm thick containing 6.5 percent Si and 0.01 percent C were examined. The specimens were pretreated with heat to induce full ordering by vacuum-soaking them at 1000°C for two hours, slowly cooling them at a rate of 50°C/hour to 500°C, then holding them at this temperature for 30 minutes. Subsequent radiography revealed the presence of DO_3-type ordering. The specimens were then covered with a light-absorbing compound and heat-treated with a laser on an LT1-2 laser unit. Laser intensity and specimen exposure time were varied. Metallographic analysis on a Neophot-21 showed that laser heat-treating does not significantly affect the grain structure, but the proportion of fine grains is greater than in conventionally heat-treated steel. X-ray diffraction analysis on a DRON-3M diffractometer was used to gain a more precise understanding of the evolution of the grain structure during laser heat treatment. It was shown that laser heat treatment can suppress further ordering in isotropic electrical engineering steels. Figures 1; references 2: Western.

Effect of Austenite Structure on the Elimination of Brittleness in Aging Steels

937D0065J Moscow IZVESTIYA VYSSHIKH UCHEBNYKH ZAVEDENIY: CHERNAYA METALLURGIYA in Russian No 9, Sep 92 pp 85-86

[Article by V. G. Gorbach and I. V. Sidoruk, Kiev Polytechnic Institute; UDC 669.15-194.55]

[Abstract] N27Yu2T3B iron and nickel-based alloy steel was studied to determine the link between the structure of the transformation austenite and the brittleness elimination effect of the α to γ transformation. The "brittle martensite + transformation austenite" was obtained in one of two ways. The first method entailed rapidly reheating quenched-to-martensite specimens in molten iron until the temperature of the α to γ transformation interval was reached, thus forming "martensite + flake transformation austenite." The specimens were quenched from this temperature and then aged for two hours at 480°C. The other method involved an embrittling preaging in the martensitic condition for two hours at 480°C, followed by rapid reheating to the temperature of the α to θ transformation interval and quenching. This resulted in the formation of an "aged martensite + dispersed austenite of acicular morphology". These two aging processes yielded high-strength, brittle alloys. Tensile tests were performed per GOST 1497-73 on smooth specimens 4 mm in diameter with a gauge length of 5. Dynamic bend tests were performed per GOST 9454-78 on type-7 specimens with U-shaped notches. The quantity of austenite in the specimens was determined magnetically. The results showed that, in order to bring the alloy out of its brittle state, it is necessary to obtain 10 percent dispersed or 35 percent flake austenite in its structure. To obtain a properties satisfactory for an engineering alloy, these percentages need to be 15 to 20 percent or 40 to 46 percent, respectively. Figures 1; references 4: Russian.

Corrosion-Resistant Steel Fiber Made by the Melt Spinning Method and Its Use in Refractory Materials

937D0071I Moscow METALLOVEDENIYE I TERMICHESKAYA OBRABOTKA METALLOV in Russian No 9, Sep 92 pp 24-26

[Article by Van I-Ho and Liu Ven-Nen, Central Research Institute of Steel and Cast Iron, China; UDC 669-494:669.531.262]

[Abstract] Properties and applications of refractory materials reinforced with corrosion-resistant steel fiber made by the melt spinning method are surveyed. Chemical compositions of five brands of steel fiber in the system Ni-Cr-Si-Mn-C are given. Advantages of corrosion-resistant steel fiber for reinforcing refractory concrete used in furnaces and other high-temperature equipment are described, and strength properties of such reinforced concrete are listed. Current applications of corrosion-resistant steel fiber for reinforcing refractory materials in the metallurgical, cement, and petroleum industries of China are identified.

Carburization of 20CrMnNiB Steel by Compound Treatments

937D0072A Moscow METALLOVEDENIYE I TERMICHESKAYA OBRABOTKA METALLOV in Russian No 10, Oct 92 pp 2-4

[Article by Ye.L. Gyulikhandanov, A.D. Khaydorov, and Li Tei Hen, State Technical University, St. Peterburg; UDC 621.785.5]

[Abstract] An experimental study was made concerning carburization of 20CrMnNiB steel by compound treatments and the effect of such treatments on the thickness of its cementite layer, with natural gas used as carburizing agent in each of the eight different treatments. The steel was carburized isothermally, stepwise, and cyclically. The three variants of isothermal treatment were: (1) at 925°C for four hours followed by air cooling, (2) at 1000°C for four hours followed by air cooling, (3) at 1000°C followed by two quenches. Stepwise treatment was (4) at 925°C for two hours 40 minutes, cooling to 800°C, soaking at 800°C, or one hour 20 minutes quenching. The four variants of cyclic treatment were: (5) four 925°C → 20°C → 925°C cycles with one hour soaking at each temperature and quenching from 925°C each time, (6) four 925°C → 600°C → 925°C cycles with one hour soaking at 925°C and 20 minutes soaking at 600°C followed by quenching, (7) four 925°C → 700°C → 925°C cycles with one hour soaking at each temperature followed by quenching, (8) three 1000°C → 700°C → 1000°C cycles with 80 min soaking at each temperature followed by quenching. The results indicate carburization of this steel proceeds most intensely during cyclic treatment according to schemes (7) and (8). Neither the experimental data nor a theoretical analysis of the carburization process readily reveal the diffusion mechanism, owing to its intricacy and also owing to the complexity of numerical simulation. While the high probability of many point defects (vacancies) forming in the process and giving rise to superplasticity associated with vacancy creep is certain to further complicate the diffusion process, evidently supercooling of the steel below the eutectic point

also contributes to superplasticity and "loosening" of diffusion. Figures 2; tables 2; references 4.

Dependence of Structure and Growth of Austenite + Carbide Colonies during Carburization of Chromium Steels on Ferrite Grain Size

937D0072B Moscow METALLOVEDENIYE I TERMICHESKAYA OBRABOTKA METALLOV in Russian No 10, Oct 92 pp 4-6

[Article by V.V. Vladimirova, Dnepropetrovsk Institute of Metallurgy; UDC 621.785.5:669.15'26-192]

[Abstract] Data on carburization of 08Cr20 low-alloy steel after various preliminary treatments are analyzed for a relation between structurization of γ+carbide colonies and grain size of the ferrite phase during this process. While fine carbide grains forming in the initial stage of the carburization process in the presence of still many structural defects did not interfere with the growth of these colonies, preliminary cold working to a 50 percent strain level diminished the ferrite grains sufficiently to allow the volume fraction of conglomerates in the diffusion layer to increase till colonies completely vanished. Preliminary annealing at 1200°C for eight hours, on the other hand, facilitated the growth of ferrite grains and thus also of γ+carbide colonies. Theoretical analysis of the carburization process, according to the Fe-C-Cr constitution diagram, is concerned with the thermodynamic stability of ferrite phase and with the kinetics of carbon distribution over the thickness of the receding ferrite layer in front of the growing γ+carbide layer. The results indicate that the growth of γ+carbide colonies slows down near the boundaries of original ferrite grains and that their attendant restructurization is somehow associated with diffusion of chromium as well as of carbon through the ferrite layer, a zone of thermodynamic instability of the parent phase developing ahead of the recrystallization front as this phase becomes oversaturated with both elements. Figures 1; references 6.

Structure of 50Mn Steel and Quality of Modified Layer After Nonabrasive Finishing Antifriction Surface Treatment

937D0072D Moscow METALLOVEDENIYE I TERMICHESKAYA OBRABOTKA METALLOV in Russian No 10, Oct 92 pp 14-20

[Article by L.M. Rybakova, L.I. Kuksenova, and Yu.A. Nazarov, Institute of Machine Science at Russian Academy of Sciences; UDC 669.14.018.298]

[Abstract] The structure of 50Mn steel liners on cylinders for internal combustion engines was studied after nonabrasive antifriction finishing surface treatment, of particular concern being the quality of the thus modified steel layer under the cladding. Such liners (initial hardness 45 HRC) were normalized and then washed with gasoline, whereupon their surfaces were clad with about 0.5 μm thick layers of of LS59-1 brass (57.8 Cu, 41.3 percent Zn, 1 percent Pb) by a mechanical friction process in one or two passes on a screw-cutting lathe. While the liner was turning at a speed of 250 rpm, a brass rod was fed to the liner surface at a rate of 0.3 mm/rev under a pressure of 22 MPa. This treatment decreased the microhardness of the steel surface layer from 41 DPH to 35 DPH. A subsequent 100 h friction and wear test was performed on a 77MT-1 reciprocating machine, with a clad liner in an M-10G_2K oil bath rubbing against a self-aligning stationary chromium-plated collar at an average velocity of 0.1 m/s under a 30 MPa load pressure. Both the linear wear and the wear rate were measured by the analytical weighing method throughout the 100 h test. Microhardness measurements in a PMT-3 tester under a 0.1 N load and structural examination including microgeometrical surface analysis was performed before and after the test, this being an effective procedure for nondestructive layerwise inspection of an up to 7.5 μm thick steel layer deformed by friction and including an about 3 μm thick upper steel layer modified by cladding. Structural examination and phase analysis were performed by a special method with a glancing X-ray beam in a diffractometer with a CoK_α- radiation source. The physical broadening of X-ray lines was determined from microphotometric curves by an appropriate approximation technique: physical β(200), β(211), β(200) broadening versus distance from the surface and β(hkl) broadening as a function of the reflex angle. The change of the crystal lattice period Δα from before to after nonabrasive antifriction treatment, nonmonotonically depending on the thickness of the deformed layer, was determined graphoanalytically on the basis of precise measurements made without a reference standard (B.M. Rovinskiy and Ye.P. Kostyukova; KRISTALLOGRAFIYA, Vol 3 No 3, 1958). The data on physical β(hkl) broadening were processed according to the Hall method for calculation of the relative intensity of (211) interference maxima and for analysis of substructural transformations. The results of this study indicate that nonabrasive antifriction surface treatment of a cylinder liner made of normalized 50Mn steel produces fewer structural defects in the modified steel layer and less intensely heats the very thin surface layer than does conventional finishing surface treatment. They also indicate that the 100 h friction and wear test has abated the dependence of the crystal lattice period in the deformed layer on its thickness. It thus is evidently possible, on the basis of such a comprehensive evaluation, to optimize the finishing surface treatment for maximum wear resistance of cylinder-piston pairs. Figures 7; references 15.

Thermal Reinforcement of Rolled Steel

937D0072E Moscow METALLOVEDENIYE I TERMICHESKAYA OBRABOTKA METALLOV in Russian No 10, Oct 92 pp 20-23

[Article by M.S. Podgayskiy, Donetsk Scientific Research Institute of Ferrous Metallurgy; UDC 621.789: 669.14018.298]

[Abstract] A new method of hardening rolled steel, by thermal reinforcement, has been developed at the Donetsk Scientific Research Institute of Ferrous Metallurgy: producing by conventional heat treatment techniques an internal reinforcement pattern of segments differing from the remaining segments of the structure in size and shape as well as in texture and strength. Rolled steel stock thus reinforced by local heat treatment is, in metallographic terms, a macroheterogenous composite material which to some extent duplicates its intrinsic microstructure at the macroscopic level. The heat treatment can be either unilateral or bilateral, for either superficial or completely

penetrating reinforcement, and be designed to produce a variety of preferably symmetric simple reinforcement patterns appearing on the surface as: 1) round or square spots of hardened metal amid original metal; 2) interstitial bands of hardened metal winding between spots of original metal; 3) parallel straight bands of hardened metal alternating with bands original metal, the width of hardened metal bands ranging from much smaller to much larger than the width of original metal strips; 4) "labyrinth" patterns of hardened metal around original metal sites or original metal around hardened metal sites, including checkerboard-like patterns. The method was tested on 8-20 mm thick strips of killed St-3 carbon steel and of 14Mn2 alloys steel. They were locally hardened by electric-contact heating and by plasma-arc heating with subsequent selective contact or jet cooling, selectively oriented cooling after hot rolling having been found to be most effective as well as most economical and selective jet cooling then being used henceforth. While the ultimate tensile strength of the carbon steel was raised to 600 N/mm^2 by thermal reinforcement over 60 percent of the strip surface, achieving the same result by conventional hardening would have required adding about 2.5 percent of an alloying element (Mn, Si, Cr, Cr + other). While the ultimate tensile strength of weldable steels with 4 percent and thus the maximum economically justified amount of alloying content is about 700 N/mm^2, the ultimate tensile strength of 14Mn2 steel was raised to the same level by thermal reinforcement over 45 percent of the strip surface and to the conventionally unattainable 750 N/mm^2 level by thermal reinforcement over 60 percent of the strip surface. The hardness of the carbon steel and 14Mn2 steel in the reinforcement regions was found to be as high as 220-240 Bhn and 400-420 Bhn respectively. Because standard tension and impact tests would not yield meaningful data here, specimens of both thermally reinforced steels were tested for cracking pattern and resistance to fracture under four different loading conditions: 1) axial tension (sporadic necking followed by fracture in an oblique plane preferably at a 45° angle), 2) eccentric tension (cracks propagating not in the direction of rolling but around reinforcement regions acting as barriers), 3) static bending (cracks beginning to form at much wider bending angle and thus higher deformation levels than at the same stress levels in conventional steel normalized after quenching and subsequent high- temperature tempering), 4) impact bending at room temperature and at -20°C (coexisting regions of brittle fracture and regions of ductile fracture in the carbon steel, the fraction of brittle fracture being proportional to the fraction of thermal reinforcement. A major advantage of thermal reinforcement is a buildup of residual compressive stresses in the steel strip. Figures 5; references 1.

Hot Shortness of 10Cr2MnNiMo Steel Welds

937D0072F Moscow METALLOVEDENIYE I TERMICHESKAYA OBRABOTKA METALLOV in Russian No 10, Oct 92 pp 23-26

[Article by V.M. Goritskiy, G.R. Shneyderov, Ye.A. Aksenova, and Zh.A. Lipilina, Central Scientific Research and Institute of Steel Structure Design; UDC 620.178.746: 621.791.052]

[Abstract] An experimental study of 10Cr2MnNiMo weldable low-alloy steel (0.07 percent C, 2.10 percent Cr, 1.10 percent Mn, 0.53 percent Ni, 0.52 percent Mo, 0.32 percent Si, 0.052 percent Al, 0.022 S, 0.020 percent P) used for petroleum hydrocrackers was made concerning temper brittleness of its welds in the heat-affected zone. Strips of this steel, 200 mm thick after normalization, were welded together by the electroslag process with 3 mm thick wire of nitrided 04Cr2MoN$_2$ steel and AN-22 flux. The welds were heat treated as follows: normalization from 920-930°C for eight hours producing a ferrite-bainite structure and tempering at 630-650°C for 13 hours. Bar specimens 12 mm square and 180 mm long were held in a muffle furnace at 450°C (1260 hours, 2500 hours) and at 550°C (24 hours, 1260 hours, 3500 hours), whereupon they were tested in impact bending. Subsequent examination of brittle fracture regions was done by the carbon replication method under a Tesla BS-540 electron microscope with a 120 kV accelerating voltage. Statistical analysis of brittle sites in the fracture zone was based on 500-700 fields of vision on the objective reticle under x(4000-6000) magnification. The test results and theoretical calculations regarding ductility-to-brittleness transition in martensitic-bainitic steel confirm the proneness of this steel to temper brittleness, with the fraction f_{tra} of intrarcrystalline cracks consistently larger than the fraction f_{ter} of intercrystalline ones and with the 50 percent embrittlement temperature $T_{50} \approx (1-f_{ter})/(1+f_{ter})$. This temperature rose by 60° during 2500 h long soaking at 450°C and only by 40°C during 3500 h long soaking at 550°C. For recovery of the catalysts, it thus appears to be permissible additionally soaking the hydrocracker vessel at 550° for "short" 24 h after a long soaking at 450°C. Figures 3; tables 1; references 4.

Effect of Zirconium on Sulfide Phase Formation in Medium-Carbon Steel

937D0080A Moscow METALLY in Russian No 6, Nov-Dec 92 pp 20-24

[Article by A.P. Serbin, G.N. Plotnikov, V.Ye. Sokolov, Yekaterinburg; UDC 669.14:669.296'775'784]

[Abstract] The lack of comprehensive data on Zr-doping of steels with $\leq$ 0.2 percent C and its effect on the sulfide phase formation prompted a study of the morphology and chemical composition of S-containing inclusions in medium carbon steel alloyed with Zr—the base component in a number of structural steels for crucial purposes. The smelting process is outlined. Samples for the metallographic study are selected from the surface, at the mid-radius point, and at the center of castings whose solidification rate corresponds to 2-4 t ingots. The nonmetallic inclusions are examined by metallographic analysis and X-ray diffraction microanalysis (RSMA) in JXA-5 and Camebax units. The Zr, S, and C distribution in the yellow phase cross section in steel is plotted. The study shows that two sulfide phases form in medium carbon steel inoculated with 0.04-0.10 percent Zr: Mn, Zr, and Fe sulfides and Zr, Fe, and Ti carbosulfides with $C_{1-x}S_x$. Steel having 0.3-0.4 percent C and 0.025-0.040 percent S and deoxidized with Al should have a Zr concentration within 0.05-0.08 percent. An excess phase may form in steel with $>$ 0.08 percent Zr in the form of dendrite and ribbon precipitates.

Attempts to determine its composition have been unsuccessful. The microhardness of various sulfides is discussed. Figures 2; tables 3; references 8: 2 Russian, 6 Western.

Austenite Stability and Properties of High-Manganese Medium-Carbon Steels

937D0080B Moscow METALLY in Russian No 6, Nov-Dec 92 pp 56-61

[Article by M.A. Filippov, M.R. Zilbershteyn, Yekaterinburg; UDC 621.74.002.6:669.15.24.74.194]

[Abstract] The need to develop austenitic steel for use as the base in clad metal wear resistant castings prompted a study of the thermal and strain stability of a number of austenitic steels within 0.41-1.25 percent C and 12-13 percent Mn concentration ranges as well as toughness and abrasive wear resistance after cooling and heating at different rates. The chemical composition of the steel samples under study is summarized. The phase and structural transformations occurring under quenching or annealing and normalizing in austenitic manganese steels is examined and the effect of the resulting phases and martensitic strain transformations on toughness and abrasive wear resistance is studied. Dilatograms of steel 40G13L, 60G13L, 70G13L, 95G13L, and 125G13L samples under heating at a 150° C/h rate, thermal austenite stability diagrams, and toughness and abrasive wear diagrams are plotted. An analysis shows that the abrasive wear is lower somewhat after annealing than after quenching. Samples of hardened steel 125G13L have the highest wear resistance. Wear resistance under abrasive wear depends not as much on the initial hardness as on the effective strength level reached in the surface layer under the influence of abrasive particles. Austenitic steel with 0.45-0.65 percent C and 13 percent Mn remains metastable under loading and may be used for castings operating under impact abrasive wear due to the high thermal stability of medium carbon austenite. Figures 4; tables 3; references 5.

Effect of Phase Composition and Martensite Transformation Development on Wear Resistance of Low-Carbon Manganese Steels

937D0080C Moscow METALLY in Russian No 6, Nov-Dec 92 pp 62-66

[Article by L.S. Malinov, Ye.Ya. Kharlanova, Mariupol; UDC 669.017:669.15'74-194.004.62/.63]

[Abstract] The limited applicability of test data on the relationship between wear resistance and the phase composition of low-carbon manganese steels with metastable austenite obtained at low slip rates prompted a study of the effect of martensite transformation development and phase composition on wear resistance of three classes of steel at other testing conditions. To this end, martensitic steel classes G8, G10, G14, G16, G20, G22, and G24 as well as austenitic classes G20Kh10, G20N10, 30G20, and 30G20Kh6N are examined. The initial phase composition and the austenite's stability to martensite transformations in the surface layer are controlled by manipulating the Mn concentration and also by additional alloying. The loss of mass during block-and-roll tests of various steel, the effect of Mn on the relative wear resistance, microhardness behavior and separation current, and the microhardness of manganese steel as a function of distance from the friction surface are plotted. An analysis shows than Mn affects wear resistance differently, depending on the type of steel. It is the highest in steels where the $\gamma \rightarrow \alpha'$ transformation is realized most fully in the surface layer while in steels with ε-phase in the structure, the $\varepsilon \rightarrow \gamma$ transformation occurs and the surface layer loses strength as a result with an attendant decrease in wear resistance. Alloying with Cr and C increases wear resistance while Ni lowers it. Joint Cr and Ni doping leads to an austenite stabilization and decreases wear resistance. This confirms that stable austenite is less wear resistant than metastable. Figures 3; table 1; references 13: 12 Russian, 1 Western.

On Effect of Copper and Nickel on Strength and Toughness of Aging Ni-Mn-Cu-V-C Austenitic Steels

937D0080D Moscow METALLY in Russian No 6, Nov-Dec 92 pp 67-72

[Article by O.A. Bannykh, V.M. Blinov, M.V. Kostina, Moscow; UDC 669.3+24-194.56:532.13]

[Abstract] The outlook for increasing the strength of steel by alloying and dispersion aging is discussed, and the behavior of strength and toughness of steel 40G10F1.5 with changes in the Ni and Cu concentration within a 4-13 percent and 0.01-4 percent range, respectively, is investigated. The chemical composition of steel under study is summarized. The samples for tensile and toughness tests are smelted in an induction furnace and forged. The effect of Cu on the difference between the ultimate strength and yield point ($\Delta\sigma$) in various steels after hardening and aging, the effect of percent Cu+0.5 percent Ni on the ultimate strength and yield point after hardening and aging, the behavior of the amount of VC carbide as a function of aging duration at various Cu concentrations, the behavior of yield point and toughness as a function of heat treatment conditions, the effect of percent Cu+0.5 percent Ni on toughness, and the dependence of toughness on the carbide phase amount are plotted. The findings show that an increase in the Ni and Cu accelerates the VC carbide precipitation from the γ-solid solution during aging while an increase in percent Cu+0.5 percent Ni leads to an increase in strength. All steels display a decrease in toughness after aging at 650° C for 5 and 10 h with an increase in the percent Cu+0.5 percent Ni parameter. The effect of Cu on the mechanical properties is attributed to its enhancement of dispersion aging. Figures 6; tables 1; references 2: 1 Russian, 1 Western.

Magnetic Properties of Strips of AMAG176 Glassy Alloy

937D0071G Moscow METALLOVEDENIYE I TERMICHESKAYA OBRABOTKA METALLOV in Russian No 9, Sep 92 pp 19-21

[Article by V. S. Chernov, O. G. Ivanov, B. L. Shtangeyev, and O. A. Levina, Research Institute of Electrical Equipment Materials, Kaluga; UDC 669.25'15:539.213:669.018.5]

[Abstract] Static and dynamic magnetic properties were investigated in strips of different sizes made of the cobalt-based glassy alloy AMAG176 (system Co-Fe-Ni-Si-B), in both the initial state and after heat treatment and thermomagnetic treatment in a transverse field. Strips 10-35 μm thick were made by the melt spinning method using a bronze disk with a special device for stabilizing the gap between the discharge nozzle and the disk. The following properties of the strips were measured: induction, residual induction, squareness ratio, coercive force, maximum permeability, permeability in a field of 0.08 A/m at frequencies of 1 kHz and 1 and 5 MHz, and specific losses at frequencies of 10 and 100 kHz at induction 0.2 T.

It was found that magnetic properties of strips in the initial state depend considerably on their thickness and length, indicating a connection between magnetic properties and conditions of manufacture of the strips (rate of cooling). It was also found that heat treatment and thermomagnetic treatment eliminate virtually all inhomogeneity of magnetic properties along the length of strips and substantially improve these properties. After heat treatment and thermomagnetic treatment, magnetostatic properties do not depend on the thickness of strips, and dynamic properties (permeability at high frequencies and losses) are variable: as thickness decreases, permeability increases and losses decrease.

Structure, Phase Composition and Hardness of Nitrided Titanium

937D0071K Moscow METALLOVEDENIYE I TERMICHESKAYA OBRABOTKA METALLOV in Russian No 9, Sep 92 pp 34-38

[Article by T. A. Panayoti and G. V. Solovyev, Moscow Higher Technical School im. N. E. Bauman; UDC 621.785.532:669.295.5]

[Abstract] Features of formation of the structure of hardened layers produced on the surface of titanium by ion nitriding were investigated, and the effect of different parameters of this treatment on the structure and phase composition of the hardened layers was determined. The structure and phase composition of hardened surface layers were analyzed using metallographic, electron-microscope, X-ray, microdurometric and mass-spectrometry methods. Ion nitriding of specimens was conducted at temperatures below and above titanium's polymorphic transition temperature. The studies established a sequence of formation of phases in the surface layer of unalloyed titanium after ion nitriding. A thin nitride layer (down to 5 μm) is formed on the surface, and beneath it there is a diffusion zone which is a solid solution of nitrogen in the α-phase with excess formations of the ε-phase, whose amount decreases with increasing distance from the surface, and then (down to the primary metal) there is a zone of nitrous α-solid solution. The high hardness of the diffusion zone was found to be due not only to the solid-solution mechanism of hardening, but also to heterogenization of the structure thanks to precipitation of a large amount of highly dispersed formations of the ε-phase.

Toughness of Standard Al-Si Alloys

937D0072G Moscow METALLOVEDENIYE I TERMICHESKAYA OBRABOTKA METALLOV in Russian No 10, Oct 92 pp 32-33

[Article by N.A. Belov, A.Yu. Gusev, and V.S. Zolotorevskiy, Moscow Institute of Steel and Alloys; UDC 669.715:620.178.7]

[Abstract] Eight cast Al-Si alloys (9-10 percent Si, 0.1-1.3 percent Cu, 0.25-0.4 percent Mg, 0-0.7 percent Zn, 0.1-0.8 percent Fe, six with 0.1-0.4 percent Mn, five with 0.1-0.2 percent Ti, one with 0.2 percent Be) and one high-strength cast Al-Si alloy strength (8 percent Si, 3.0 percent Cu, 0.3 percent Mg, 0.7 percent Zn, 0.2 percent Fe, 0.2 percent Ti, 0.15 percent Be) were tested for toughness after hardening by heat treatment with various crystallization rates, these alloys having been produced in a Silit furnace by adding to the charges of pure Al,Si,Cu,Mg,Zn the appropriate aluminum alloy containing Fe (0.1-0.8 percent) and also Mn (0.1-0.4 percent), Ti (0.1-0.2 percent), Mn+Ti (0.3- 0.6 percent), or Mn+Ti+Be (0.2 percent Be) respectively. They were cast into cold or 400°C hot graphite molds for cooling at a rate of 150°C/min and 30°C/min rate respectively. Ingots of the 15x30x160 mm^3 size were heat treated in a muffle-resistance furnace according to standard procedure with the temperature held constant within +/-3°C. They were then tested in bending by the three-point method at a loading rate of 5mm/min on a UME 10 TM universal machine. Structural examination was performed under a Neophot-21 microscope and under a JSM-35CF scanning electron microscope. The results reveal that the toughness of these alloys is lower after slower crystallization, that addition of impurity elements and especially of iron lower their toughness, and that all these alloys with a copper content are not as tough as the not as hard copperless Al-Si-Mg alloys such as the Al-12 Si-(Mg). Figures 1; tables 3; references 3.

Properties of AL2 Cast Aluminum Alloy

937D0072H Moscow METALLOVEDENIYE I TERMICHESKAYA OBRABOTKA METALLOV in Russian No 10, Oct 92 pp 34-36

[Article by E.V. Tataurova, Institute of Thermophysics at Russian Academy of Sciences, Siberian Department; UDC 669.715]

[Abstract] The cast Al + 12-14 percent Si alloy was tested for mechanical properties after freezing on a metal crystallizer. The alloy was produced from pigs with addition of tailings in a 7:1 ratio, the melt being heated to 620°C and then slowly cooled to 580°C while ingots were being castings were obtained by freezing on a crystallizer at either 50°C or 120°C temperature prior to solidification in a crucible. Such castings were tested for ultimate tensile

strength, percentage elongation, Brinell hardness: 1) after being frozen from 610°C to 50° and from 600°C to 120°C, 2) after aging at 50°C and 120°C respectively, 3) after rolling at 400°C (Al + 11.5 percent Si) and at 450-500°C (Al + 12.4 percent Si). The ultimate tensile strength of the alloy was found to be much higher (225 N/mm^2 after freezing from 610°C to 50°C and 265 N/mm^2 after aging, 160-165 N/mm^2 after rolling) than when cast into sand or permanent molds. Structural examination of frozen castings revealed no internal or subsurface blisters, but a nonuniform distribution of both α and eutectic phases. Spectrum analysis in an ISP-29 spectrograph, performed by successive slicing away 0.3 mm thick layers, revealed a nonuniform distribution of silicon in the castings produced by freezing of liquid melt from 610°C. This was evidently responsible for the serrate microhardness profile of the eutectic phase across such a casting. Figures 4; tables 1; references 9.

Study of α (Al)-Solid Solution Decay During Quench Heating of Cast Al + 10 Percent Mg and Al + 6 Percent Zn + 1.5 Percent Mg + 1 Percent Cu Alloys Doped With Mn

937D0080E Moscow METALLY in Russian No 6, Nov-Dec 92 pp 80-83

[Article by A.A. Aksenov, Das Goutam, V.S. Zolotorevskiy, G.M. Kuznetsov, D.V. Luzgin, Moscow; UDC 669.715'721'74+715'5'721'3'74:621.78]

[Abstract] The uncertainty about the nature of α(Al)-solid solution decay during quench heating with the formation of manganese aluminides in multicomponent alloys prompted an examination of the substructure of Al+10 percent Mg and Al+6 percent Zn+1.5 percent Mg+1 percent Cu alloys doped with 0.4 percent Mn is examined. To this end, the phase composition and decay product precipitation kinetics are studied during quench heating accompanied by the manganese aluminide formation in alloys prepared in a resistance furnace from an alloying composition and cooled at a 100K/s rate, exposed to 10 min to 20 h, and water quenched. The structure is examined under a JEM-2000EX transmission electron microscope at a 160 kV accelerating voltage. The phase morphology is analyzed in electron microscopy patterns and the solid solution decay products are identified by the microdiffraction patterns. The isothermal transformation diagram and polythermal cross section are plotted on the basis of thermodynamic analyses. The findings show that on the periphery, the dendrite cell may contain > 1 percent Mn while its concentration at the center may be only 0.06 percent. The diagram (*C*-curves) indicates that the phase composition of the aluminides and the kinetics of their precipitation during the solid solution decay are determined by the solid solution composition. Figures 2; references 4.

Change in Crystal Orientation in Subsurface Layers of Polycrystalline Aluminum During Diffusion Interaction With Gallium

937D0080F Moscow METALLY in Russian No 6, Nov-Dec 92 pp 105-110

[Article by V.I. Franchuk, L.N. Larikov, Kiev; UDC 539.319;669.176;669.87]

[Abstract] The orientation transformation due to the recrystallization processes in subsurface aluminum single and bicrystals and the phenomenon of diffusion stimulated recrystallization (DIR) are discussed, and the orientation transformations in the subsurface layers of polycrystalline aluminum during diffusion interaction with Ga are examined and compared to various structural parameters in order to clarify the interaction mechanism. To this end, samples of 99.99 percent pure polycrystalline Al reduced by 15 percent by rolling with a thickness of about 10 μm are studied. A thin layer of Ga is applied to the surface at a 301K temperature and exposed up to 1,000 h. An X-ray diffraction analysis is carried out in CuK_α monochromatic radiation and pole figures are plotted by a computer graphics printer. The texture changes on the Al surface as a function of the duration of contact with Ga and the fracture structure of Al polycrystals after the interaction with Ga are cited. The study made it possible to identify the general patterns of the phenomenon under study and the factors which facilitate and complicate slip which accompanies changes in the strength characteristics of subsurface layers. The mechanism of diffusion interaction and its effect on the metal matrix hardening and loss of strength are identified. The relaxation of stresses and defect curing under predominant volume diffusion and the secondary recrystallization processes which help to restore the original structure are discussed. Figures 2; references 16: 12 Russian, 4 Western.

Study of Effect of High-Power Current Pulses on Structure of Copper Conductors

937D0080G Moscow METALLY in Russian No 6, Nov-Dec 92 pp 117-121

[Article by V.G. Buduyeva, V.S. Kruglikov, Moscow; UDC 621.9.048]

[Abstract] The effect of structural transformations in surface layers of conductors under current pulses on efforts to optimize the design, harden the surface layers, and develop methods of increasing the wear resistance of circuit breaker contacts is discussed, and an attempt is made to identify the structural transformations in various zones of copper conductors under the effect of electromagnetic factors (EMF). To this end, hollow cylindrical copper samples with rectangular rifling on the outside surface are tested under short DC pulses whereby coated and bare samples are examined. The microstructure of the metallographic sections is examined under a Neophot-30 optical microscope and the microhardness is measured by a PMT-3 tester at a 20 gf load. The sections are etched in an acid solution. The microhardness behavior in the sample depth (from the surface inward) after the impact of electromagnetic factors is plotted. The study reveals a nonuniform structure of electric wear in different conductor zones and the presence of areas with an elevated microhardness along the recess contour. Intensive vaporization is discovered along the entire surface contour while considerable changes in the metal structure on the former ledge segments is discovered. The metal vapors are carried away by plasma flows and molten metal is gathered due to the pinch effect forces and becomes elongated toward the anodic flow, forming protrusions. Figures 3; references 4.

Ternary Scandium and Transition Metal Germanides

937D0080H Moscow METALLY in Russian No 6, Nov-Dec 92 pp 147-152

[Article by B.Ya. Kotur, Lvov; UDC 669.018:793+548.736.4]

[Abstract] Interest in alloys of scandium and other rare earth metals (RZM) due to their diverse physical and chemical characteristics and their beneficial effect on the mechanical properties is noted, and data on the constitution diagrams of ternary Sc-*Me*-Ge systems where *Me* is a *d*- or *f*-transition metal are briefly reviewed and isothermal cross sections of 17 ternary systems are tabulated at 870 and 1,070K. The chemical compositions of the alloys are summarized, and their structural characteristics are examined. The formation of solid solutions of substitution on the basis of binary compounds is noted, and scandium's tendency toward reciprocal substitution is identified. Seventy ternary germanide compounds examined belong to 23 structural groups. Tables 2; references 17: 13 Russian, 4 Western.

Phase Equilibria in Systems Formed by Aluminum With Iron, Palladium, and Cerium

937D0080I Moscow METALLY in Russian No 6, Nov-Dec 92 pp 161-165

[Article by M.V. Rayevskaya, A.L. Tatarskina, A.A. Filippova, Moscow; UDC 669.017.11]

[Abstract] The effect of the original component properties on the phase equilibria character in multicomponent alloys is outlined, and the Al-Fe system is studied at a 500° temperature within a 50-100 percent Al concentration range; the study confirms the existence of the following intermetallic compounds: $FeAl_3$, Fe_2Al_5, $FeAl_2$, and FeAl. The isothermal cross sections of the Al-Pd-Fe and Al-Pd-Ce systems at 500° C and of the Al-Fe-Ce system at 550° C in an Al-rich area and the phase equilibrium diagram in the aluminum corner of the quaternary Al-Fe-Ce-Pd system at 500° C are plotted. The structures of the ternary phases are identified. Solid solutions on the basis of the original components virtually do not penetrate the ternary systems; this is attributed to the well known solubility criteria. Figures 3; tables 3; references 18: 8 Russian, 10 Western.

Interaction of Palladium With Ruthenium and Yttrium

937D0080J Moscow METALLY in Russian No 6, Nov-Dec 92 pp 180-183

[Article by M.V. Rayevskaya, I.N. Avertseva, Moscow; UDC 669.017.11.234859]

[Abstract] Interest in alloys of Pd with transition and rare earth metals due to their potential applications in thin wall membranes for organic synthesis catalysts is noted, and the interaction of Pd with Ru and Y is examined. The phase equilibria diagram (isothermal cross section) of the Pd-Ru-Y system at 600° C within a 0-70 percent Y concentration range, the concentrational dependence of the lattice constants of various compounds, and the dependence of the alloy hardness on the composition are plotted. These phase equilibria and isothermal cross sections are examined by the methods of structural microanalysis, X-ray phase analysis, X-ray spectral microanalysis, hardness and microhardness testing, and differential thermal analysis. A study of the concentration curves of the two-phase compound lattice periods confirms the low solubility of the third component. The hardness behavior of the alloys and individual phase components attests to a considerable hardening effect of Ru, especially in the case with two-phase areas with a Laves phase. The character of phase equilibria makes it possible to clarify the homogeneity area boundaries of pure components and binary and ternary intermetallic compounds. Figures 3; tables 2; references 10: 2 Russian, 8 Western.

Optical and Luminescent Properties of $A^{II}B_2^{III}C_4^{VI}$ Where A is Tb, Eu, Sm, Ca, Sr, or Ba and C is S, Se, or Te

937D0089A Moscow NEORGANICHESKIYE MATERIALY in Russian Vol 28 No 12, Dec 92 pp 2269-2275

[Article by B.G. Tagiyev, V.A. Dzhalilov, T.A. Gyulmaliyev, G.M. Niftiyev (deceased), O.B. Tagiyev, F.B. Askerov, B.M. Izzatov, Ya.G. Talybov, Physics Institute at the Azerbaijani Academy of Sciences; UDC 535.37]

[Abstract] Optical absorption and luminescence of 80-120 μm thick $A^{II}B_2^{III}C_4^{VI}$ single crystals produced by gas transport reactions and activated with Nd, Eu, and Ce are examined, and the use of impurity doping is justified by the need for a high quantum yield under optical and electric pumping of these materials in order to transfer efficiently the excited carrier energy to 4*f* electrons. Attention is given to studying the doping of crystals containing lanthanides and alkali earth metals with trivalent rare earth metals. To this end, the coefficients of optical absorption and luminescence of the $YbGa_2S_4$ single crystals is examined in detail, and the absorption and photoluminescence (FL) spectra as well as the temperature dependence of the luminescence intensity, Nd excitation spectra at 77K, and the spectral dependence of the radiant intensity of single crystals and a luminescent lamp on its basis are plotted. In addition to the time response, the parameters of the defect levels responsible for the energy transfer to the rare earth ions are determined. Figures 6; references 9: 3 Russian, 6 Western.

Use of $TlInSe_2$ Crystals for Hard Radiation Detection

937D0089B Moscow NEORGANICHESKIYE MATERIALY in Russian Vol 28 No 12, Dec 92 pp 2404-2408

[Article by I.V. Alekseyev, Physics Institute at the Azerbaijani Academy of Sciences; UDC 539.12.043]

[Abstract] Increasing uses of $TlInSe_2$ semiconductors for penetration radiation recording and measurements are mentioned, and the interaction of $TlInSe_2$ crystals with X- and γ-radiation is examined. The use of these crystals for measuring the X- and γ-radiation dosage rate and the thermal neutron flux density is discussed. Crystals with a 10^6-10^7 Ω x cm resistivity at room temperature are examined. The samples are produced by cleaving a single crystal

ingot along two mutually perpendicular cleavability planes while In ohmic contacts are applied by soldering on the freshly cleaved sample faces. The crystal interaction with X- and γ-radiation is examined using RUM-3 and RUM-13 sources and ROKUS and AGAT units with a ^{60}Co isotope with a good geometry. The dependence of the crystal sample current on the exposure dosage rate, the dependence of sensitivity on the effective X-radiation energy of crystal samples of varying thickness, and the oscillograms of the detector signals in the gamma-neutron field are plotted. The findings demonstrate that $TlInSe_2$ crystals may serve as an effective material for hard radiation detectors characterized by a high sensitivity, a small size, a good parameter stability, and a high radiation resistance. The authors are grateful to V.M. Nazarov, I.L. Sashin, and V.N. Sysoyev (all from the Joint Institute for Nuclear Research) for helping with in-pile measurements. Figures 3; references 4: 3 Russian, 1 Western.

Strain Gauge Properties of PbTe and PbSe Crystals and Outlook for Their Use

937D0089C Moscow NEORGANICHESKIYE MATERIALY in Russian Vol 28 No 12, Dec 92 pp 2414-2418

[Article by S.S. Varshava, I.V. Kurilo, Lvov Polytechnic Institute; UDC 621.315.592]

[Abstract] Interest in the strain gauge properties of PbTe and PbSe semiconductors due to their high piezoelectric resistivity and good physical and mechanical properties is noted, and PbTe and PbSe crystals grown by chemical transport reactions (KhTR) in Pb-Te-Br_2 and Pb-Se-NH_4Br reactions, respectively, are investigated. The growth conditions are outlined in detail. The dependence of the percentage change in the PbTe and PbSe crystal resistivity and conductivity on the pressure (i.e., the hydrostatic pressure coefficient (KGD)), the dependence of the percentage change in resistivity on the geometric factor of the melt- and gaseous phase-grown crystals, and the dependence of the relative change in the sample voltage referred to the unit pressure on the current at various pressures are plotted. The effect of the geometric factor and working current in the sensor on the strain sensitivity is established. Allowing for the weak dependence of the hydrostatic pressure coefficient on temperature, the conclusion can be drawn that PbTe and PbSe microcrystals produced by chemical transport reactions are suitable for making miniature pressure gauges. One of their advantages is that there is no need for machining or chemical treatment. Ways of controlling the pressure gauge sensitivity are outlined. Figures 4; references 6: 5 Russian, 1 Western.

Light-Exciton Mixing Effects in GeS

937D0089D Moscow NEORGANICHESKIYE MATERIALY in Russian Vol 28 No 12, Dec 92 pp 2438-2440

[Article by D.O. Gamzayev, A.M. Kulibekov, R.A. Suleymanov, Physics Institute at the Azerbaijani Academy of Sciences; UDC 621.315.592]

[Abstract] The lack of data on the characteristic features of the origin of exciton states in GeS and similar semiconductor crystals prompted an experimental study of the polarization absorption spectra of single crystal GeS at low temperatures which point toward the significant role played by the polariton effects in the exciton spectra of GeS and, perhaps, other group $A^{IV}B^{VI}$ crystals with a similar crystallographic and band structure; the crystal and band structure of GeS semiconductors and their optical properties are discussed. The spectral response of absorptance at 4.2K at $E \| e$ and $E \perp e$ polarization in this crystal as a function of the angle between the crystal axis and the beam propagation direction and the temperature dependence of the exciton absorption peak are plotted. The absorption peak is found to have an exciton origin. The findings confirm the need for a detailed examination of the exciton processes in GeS-type crystals and point toward the possibility of studying the polariton effects in a new and interesting class of laminar semiconductors. The conclusion is drawn that the line observed in the absorption spectra in the specially selected geometry corresponding to the extraordinary ray propagation in GeS single crystals is due to the mixed exciton mode excitation. Figures 2; references 13: 3 Russian, 10 Western.

Reactor Graphite and Its Normal Life

937D0091A Moscow FIZIKA I KHIMIYA OBRABOTKI MATERIALOV in Russian No 6, Nov-Dec 92 pp 5-14

[Article by Yu.S. Virgilyev, Moscow; UDC 621.039.532.21]

[Abstract] The use of graphite as the core and reflector material of water moderated graphite reactors and high-temperature gas cooled reactors prompted interest in the service properties of this material. Data on the properties of both commercial and pilot domestic reactor graphites accumulated to date are considered in order to assess their normal life in operating reactors and estimate the possibility of using them as stacking elements in reactors under design. In particular, four types of graphite manufactured today—the Gr-280 for stacking blocks and the GRP2 for contact rings and the KPG, MPG, and GR-1 produced in smaller quantities—are examined in detail. The dependence of the percentage change in the graphite size and physical properties on the neutron fluence at various temperatures under different irradiation angles, the dependence of the percentage change in the modulus of elasticity, compressive strength, and thermal and electric resistance of graphite on the neutron fluence, the relationship between the neutron fluence corresponding to the secondary growth level and the irradiation temperature, and the dependence of the secondary swelling rate on the irradiation temperature are plotted. An analysis shows that the normal life of the GR-280 graphite as a stacking material in RBM-K high-power pressure-tube reactors is 40-45 years, while pilot GR-1 graphite may be recommended for use in internal reflector blocks of high-temperature gas cooled reactors. The secondary swelling rate peaks within 1,000-1,200K and increases exponentially with the graphite density. Figures 9; tables 3; references 9.

Fracture Toughness of Diamond Single Crystals

937D0042A Kiev SVERKHTVERDYYE MATERIALY in Russian No 5(80), Sep-Oct 92 pp 5-11

[Article by N.V. Novikov, S.N. Dub, V.I. Malnev, Superhard Materials Institute at the Ukrainian Academy of Sciences, Kiev; UDC 620.186.4:621.321]

[Abstract] The use of indentation for fracture toughness tests of brittle poorly machinable materials is reviewed and a formula is derived for calculating the fracture toughness coefficient K_{1c}; the constraints of the fracture toughness measurement methods and the shortcomings of published data are discussed. The crack nucleation and propagation in diamond single crystals under loading and load relieving by a Vickers indentor is studied using a PMT-3 microhardness gauge and a high-temperature microhardness gauge under loads of 0.49-10.0 N at a 1,500° C temperature. The fracture character around the indentation is studied under NU-2 and AMPLIVAL-interphako microscope in transmitted and reflected light under varying phase contrast conditions and in polarized light. Single crystals are also etched to reveal surface cracks and polished layer by layer to determine the crack shape. A diamond fracture toughness anisotropy in the (100) face is discovered and it is shown that the fracture toughness of a single crystal of synthetic Ib and natural Ia diamonds is the same at room temperature (20° C). At 800° C, the radial crack length in synthetic diamond is greater than that of natural diamond by a third while the fracture toughness decreases. These data are consistent with the temperature dependence of the diamond single crystal strength. Figures 7; tables 2; references 15: 5 Russian, 10 Western.

Natural Diamond Powder Compacts' Thermal Conductivity: Discussion

937D0042C Kiev SVERKHTVERDYYE MATERIALY in Russian No 5(80), Sep-Oct 92 pp 19-21

[Article by O.A. Voronov, A.A. Kaurov, High-Pressure Physics Institute at Russia's Academy of Sciences, Troitsk, Moscow oblast; UDC 679.826.002.2]

[Abstract] The thermal conductivity of natural diamond single crystals and polycrystals is discussed and the dependence of the thermal conductivity of diamond polycrystals on the crystal grain size at room temperature is investigated. To this end, polycrystals with various crystal grain sizes are produced by compacting powders made by grinding the diamond bort from Yakut kimberlite deposits whereby 1.0-1.2 mm diamond single crystals are crushed and separated into fractions by a sieve, resulting in 630/400, 400/250, 250/180, 180/125, 125/90, 90/63, 63/45, 45/36, and 35/25 fractions. The dependence of the thermal conductivity of polycrystals on the crystal grain size is plotted on the basis of both experimental results and analytical formulae. A small drop in thermal conductivity with an increase in the crystal grain size above 125 μm is attributed to the appearance of cracks and dislocations in some grains under powder compression. The effect of the defect concentration on the thermal conductivity behavior is discussed. The authors are grateful to V.V. Pimenov, A.V. Rakhmanina, N.F. Borovikov, and L.F. Afanasyeva for constant support. Figures 1; references 13: 6 Russian, 7 Western.

Use of Heat-Resistant Concrete With Si-Na Composite Mortar

937D0073A Moscow BETON I ZHELEZOBETON in Russian No 9, Sep 92 pp 4-6

[Article by S.F. Korenkova, candidate of technical sciences, A.I. Khlystov, candidate of technical sciences, and T.V. Sheina, engineer, Samara Institute of Construction Engineering; UDC 691.327:666.965:621.745]

[Abstract] An experimental study of four new heat-resistant concretes for liners in smelting furnaces was made, these concretes containing 25-35.5 wt. percent fireclay only as filler and correspondingly 45-35 wt. percent dry Na_2SiO_3:soil = 80:20 mixture as mortar. Replacement of aqueous sodium silicate with mixture of dry sodium and soil, a fine-disperse composite, facilitates in situ casting with a high degree of homogenization and with not only lower water content but also with less alkaline flux. Replacement of scarce magnesite, the conventional filler in heat-resistant concretes, with fireclay not only improves the thermal characteristics by virtue of its smaller coefficient of thermal expansion, but also reduces the cost. Specimens of these concretes were tested for compressive strength after desiccation and after firing at 800-900-1000- 1100-1200°C, for average density after firing at 1200°C, for shrinkage at 1200°C, and for flexural strength at 800-1100°C. The compressive strength was found to be consistently highest after firing at 1200° and the flexural strength was found to be lower at higher temperatures. This loss of flexural strength was subsequently prevented by adding 5-15 wt. percent of processed IM-2201 catalyst: a greenish fine-disperse and highly refractory (melting point 1700°C) mixture of up to 75 wt. percent α-$Al_2)_3$ powder in water and up to 15 wt. percent chromium oxide, obtained from tailings of synthetic rubber production. Such concretes were tested and approved for production. Tables 4. references 2.

Self-Stressing of Cellular Concrete Structures During Autoclave Treatment

937D0073B Moscow BETON I ZHELEZOBETON in Russian No 9, Sep 92 pp 11-13

[article by G.P. Sakharov, doctor of technical sciences, professor, and Ye.P. Skorikov, engineer, Moscow Institute of Construction Engineering, F.M. Salimgareyev, engineer, and B.G. Fedotov, engineer, Cellular Concrete Manufacturing Plant, Naberezhnyyye Chelny; UDC 69.022.326: 691.327:666.973.2]

[Abstract] Specimens of cellular reinforced concrete were treated in an autoclave for self-stressing of the reinforcing steel rods with attendant decrease of concrete shrinkage and creep, self-stressing being due to the two materials having different coefficients of thermal expansion. Batches of 0.3 m thick and 1.39 x 6 m^2 large aerated concrete wall panels were formed using: 1) mortar with a 1:1.5:0.05 cement-to-sand-to-lime ratio, average density of 700 kg/m^3 (specific surface of sand 180 m^2/kg) and compressive strength 5 MPa at a 0.62 moisture- temperature index; 2) mortar with a 1:0.25:2.86 cement-to-lime-to-sand ratio (specific sand surface 120 m^2/kg, activity of lime 45 percent), compressive strength of 4.2 MPa at a 0.55

moisture-temperature index. Into the panels were lengthwise embedded A-III rods 8 mm in diameter and transversely embedded V-I rods 4 mm in diameter, all lengthwise embedded rods in one such panel then being welded at one end only to a common anchor and markers being rigidly attached across the center line of each panel for strain measurements. After molding and subsequent 12 h soaking, these panels were steam cured in an autoclave under a pressure of 1 MPa according to an 8 + 10 + 5 h scheme. From the same two concrete mixes were also formed prisms: 1) 0.55 m long 0.145 m square prisms with prestressed reinforcing A-III rods 10 mm in diameter, 2) 0.3 m long 0.1 m square prisms with prestressed reinforcing A-III rods 0.8 mm in diameter. The rods were anchored in some prisms and not anchored in others. An additional experiment was performed with 0.3 m long 0.1 m square prisms made of cellular concrete using: 1) mortar with a 1:1.5 cement-to-sand ratio, 0.56 moisture-temperature index; 2) mortar with a 1:0.19:1.3 cement-lime-sand ratio (specific surface of sand 128 m^2/kg, activity of lime 45 percent), 0.56 moisture-temperature index. Some prisms in each batch had reinforcing A-III rods 8 mm in diameter with anchors and some had no reinforcing rods. Some were soaked 14 h for subsequent steam curing at 85°C under atmospheric pressure according to a 4+7 h scheme followed by natural cooling in an unheated chamber and some were soaked 21 h for steam curing in an autoclave under a pressure of 1 MPa according to a 7 + 11 + 6 h scheme. The results of this experiment confirm that autoclave treatment produces residual expansion of the concrete and self-stressing of the reinforcement. They also reveal that shrinkage and creep of cellular concrete at 0.05-0.1 compressive strain levels do not contribute much to the stress relief in reinforcing rods. Autoclave treatment is, therefore, recommended for construction of prestressed crack-resistant wall panels and cover plates of cellular concrete, also for both high-density and low-density compact silicate concrete. Figures 4; references 6.

Ways To Minimize Temperature Nonuniformity During Electrothermal Treatment of Structures

937D0073C Moscow BETON I ZHELEZOBETON in Russian No 9, Sep 92 pp 13-15

[Article by V.Ya. Gendin, candidate of technical sciences, Central Moscow Institute for Construction Quality Improvement; UDC 666.97.035.5]

[Abstract] A laboratory study of reinforced-concrete structures concerning their electrical heating in the field was made jointly by the Central Moscow Institute for Construction Quality Improvement and the Central Scientific Research Institute for Organization and Mechanization of Construction with Technical Assistance, the object being to minimize the temperature nonuniformity in the concrete during this treatment. Fragments of such structures were collected from various regions of the country and particularly the cold-climate ones. They were heated in a frost chamber at temperatures from -10°C to -20°C in a crate assembled from 40 mm thick boards. Uncrated concrete surfaces were covered with a polymer film and kept warm by pads of mineral wool. They were heated electrically in three ways: 1) with rod electrodes fastened to the crate panels, 2) with 40 mm wide strip electrodes spaced 200 mm apart, 3) with plate electrodes made of roofing steel fastened to the long edges of the crate. They were heated after preliminary soaking in the chamber, with 49 V or higher voltages applied so that their heating rate could be varied over the 5-20°C/h and then isothermally soaked either for 28 h at 60°C or for 11 h at 80°C. The results have revealed that both material and disposition of the electrodes as well as the disposition of reinforcing rods between electrodes determine the degree of nonuniformity of the temperature distribution in the concrete. The results did not confirm the prevailing view that temperature self-regulation takes place at lower current levels and intense heat dissipation takes place at higher current levels. For minimization of the temperature nonuniformity during bulk heating, it is recommended: 1) to use linear arrays of rod electrodes, plate electrodes, and checkerboard arrays of rod electrode to minimize respectively small, medium, and large temperature nonuniformity; 2) to lower the voltage after having decreased the distance between them; 3) to increase the distance between electrodes and reinforcing rods by appropriate design and layout, with plates or strip electrodes for peripheral unilateral or bilateral heating; 4) to lower the final isothermal treatment temperature and to slow down the prior temperature rise; 5) to effectively shield the structure with thermal insulation and to waterproof uncrated concrete surfaces. Figures 2; references 3.

Relation Between Length of Cure of Concrete in Nondetachable Reinforced- Concrete Casing and Bonding to Monolithic Concrete Structure

937D0073D Moscow BETON I ZHELEZOBETON in Russian No 9, Sep 93 pp 15-16

[Article by A.S. Nikitin, engineer, V.P. Selivanov, candidate of technical sciences, and N.S. Kazanir, engineer, St.Peterburg Higher Military School of Construction Engineering; UDC 691.620.18]

[Abstract] An experimental study of bonding between a nondetachable thin reinforced-concrete casing to a monolithic concrete underground structure was made, its purpose being to determine the dependence of the bond strength to the length of cure of the casing concrete and thus the feasibility of minimizing the volume of steel requirement. Test specimens were formed into 100 x 100 x 100 m^3 cubes with a 100 mm wide rib and into 100 x 100 x 200 mm^3 prisms, each consisting of two 50 mm thick layers. The reinforced upper half was made fine-grain concrete containing in 1 m^3: 590 kg Portland cement, 1470 kg river sand, 242 kg water, and 88 kg grade 136-41 silicone. Granitic debris of 5-10 mm and 10-20 mm fractions or metal chips were embedded in it to half height, after 8-10 mm deep parallel grooves spaced 20-30 mm apart had been cut in it from the outside surface at a 45° angle. The monolithic lower half was made of high-density concrete containing in 1 m^3: 440 kg Portland cement, 1160 kg granitic debris of 5-10 mm and 10-20 mm pebble size fractions, 176 kg water, and 3 kg grade S-3 modifier. The grade-400 Portland cement was supplied by the Pikalevo plant. Specimens were tested for strength of the bonding contact seam with reinforced concrete aged 3-7-14-28 days. The strength was found to be consistently lower with longer aged concrete, only 3-7 days long aged reinforced

concrete being adequate for bonding to monolithic concrete. Figures 1; tables 1; references 4.

Strength of Compressed Reinforced-Concrete Columns in Oblique Sections

937D0073E Moscow BETON I ZHELEZOBETON in Russian No 9, Sep 92 pp 20-21

[Article by V.A. Otsmaa, candidate of technical sciences, and I.E. Pello, engineer, Tallinn Technical University; UDC 624.073.23]

[Abstract] While a longitudinal compression force is known to enhance the resistance of reinforced-concrete columns, not much is known about its effect on their strength in oblique sections. Ensuring the required load capacity of columns in normal sections ensures also the required load capacity in oblique sections, according to Russian design practice, so that columns are not checked for the transverse force. Control calculations according to the CNiP Construction Norms and Rules indicate, however, that strength in oblique sections is not automatically ensured. Experiments concerning this problem were performed with 20 half-size models of a K5a-3-2 column. A longitudinal force was applied by means of a 500-ton hydraulic press, while application of a transverse force and a bending moment required a device with jack and clamp specially designed for this purpose. Fracture was found to occur in flexure: under higher than 500 kN compression forces, only when the actual bending moments exceeded their design limits. This validates the practice of ignoring the transverse force in the design of reinforced-concrete columns. While calculations by the CNiP method yield a smaller transverse force (smaller by a factor of 1.5 for K5a-3-2 columns), calculations according to the "European Community Commission for Industrial Processes, Buildings, and Civil Engineering" Eurocode No. 2 (design of concrete structures) yield a resistance to transverse forces close to the experimentally determined one. Figures 4; references 3.

Experience With Use of Ash + Slag Mixture in Production of Concrete and Reinforced-Concrete

937D0073F Moscow BETON I ZHELEZOBETON in Russian No 9, Sep 92 pp 29-30

[Article by N.A. Rakitina, engineer, Industrial Association "Burzhelezobeton" (Buryat Reinforced Concrete), A.V. Kirpichnikov, engineer, P.K. Khardayev, candidate of technical sciences, and A.B. Pavlov, candidate of technical sciences, East Siberian Institute of Technology; UDC 662.613.1:61.32]

[Abstract] The feasibility of using ash and slag tailings from central heat and electric power plants such as the Ulan-Ude TETs-1 in production of concrete and reinforced concrete is being studied, in an attempt to replace some of the sand with ash+slag mixture and effect some saving of cement. The mixture used for experimentation with high-density concretes is a polydisperse product of coal combustion (70-80 percent anthracite from Gusinoozersk deposits, 20-30 percent anthracite from Irkutsk deposits). Inasmuch as it consists of ash with a specific surface of 1400-1600 cm^2 and 50.98 percent SiO_2 + 20.86 percent Al_2O_3, its density of 800-900 kg/m^3 and 0.7 bulk modulus do not satisfy the applicable GOvernment STandard and, therefore, the ash + slag content in the concrete must be properly optimized. It was optimized for concretes of high-density classes classes V15-V25. These concretes for the study were produced with Portland cement (grades 400 and 500) from three plants (Timlyuysk, Angarsk, Achinsk), sand having been extracted from sand-gravel mixtures through sieves and combined with granite-diorite debris of the 20-40 mm largest pebble size fraction. The concrete mixes were prepared in a laboratory mixer and then molded into cubes with a 100 m wide rib. These were stored in vats so as to prevent loss of water by evaporation prior to their heat-and-moisture treatment. All specimens were cured identically according to standard industrial practice. Tests for strength were performed 4 h after isothermal heat-and-moisture treatment at 80°C for eight h, after such a treatment and 28 days long curing, and after 28 days long storage under normal conditions. Tests for frost resistance were performed on V15 concrete in two steps: first by the accelerated method according to the 1976 GOvernment STandard at a freezing temperature of -50 +/- 2°C without ash and slag, then according to the 1987 GOvernment STandard with ash+slag mixture replacing 30 percent and 50 percent of the sand. Specimens of concrete without and with ash +/- slag mixture replacing 30 percent of the sand also tested for frost resistance after freeze-thaw cycling. Watertightness tests were performed on high-density concretes by the "wet spot" method. The results of the tests indicate that replacement of sand with ash+slag mixture does not degrade the quality of concrete, except only slightly its frost resistance, and even improves its surface characteristics. They thus confirm the suitability of such heavy-density concretes for reinforced-concrete structures exposed to the severe climate of Buryat-Mongolia. References 3.

Refraction and Molar Volume of Bismuth-Bearing Gallate Glass

937D0077A Moscow STEKLO I KERAMIKA in Russian No 9, Sep 92 pp 8-9

[Article by A.I. Rabukhin, G.V. Belousova, Moscow Chemical Engineering Institute imeni D.I. Mendeleyev; UDC 666.113'681'87:666.117.9]

[Abstract] The lack of published data on the quantitative dependence of such gallate glass properties as density and refractive index on the glass composition prompted an examination of the concentrational dependence of the specific and molar refraction and molar volume as well as the above two properties of Bi-containing glass synthesized from $CdO-Bi_2O_3-Ga_2O_3$ and $PbO-Bi_2O_3-Ga_2O_3$ systems. The compositions of the glass under study are selected within the vitrification ranges stipulated in U.S. patents 4456692 and 4483931. The glass for the study was founded in corundum crucibles in a silite electric furnace at a 1,050-1,100° C temperature; the melt was cast onto a cooled metal plate and the glass was annealed at a 350-400° C temperature. The chemical composition was studied using a Camebax X-ray spectral microanalyzer; the glass density was determined by hydrostatic weighing in toluene and the refractive index was measured by a GS-5 goniometer at λ = 0.6328 μm. The dependence of the glass refractive index on its density, the dependence of the glass Lorenz molar refraction on its molecular mass, and the

dependence of the partial refraction of cations on their radius is plotted. The refractive index of the synthesized glass as a function of density is approximated by a linear dependence which corresponds to the generalized Beer-Gladston-Dale expression for specific refraction with a standard deviation of 0.0003 (or < 0.16 percent). The concentration dependence of the glass density, molar volume, refractive index, and molar refraction is approximated by an additive formula. It is shown that the cation refraction in oxides increases in proportion to the cation volume or polarizability. The constant specific refraction values with changes in the glass composition and the additive character of properties attest to the fact that the character of the structural groups present in the glass does not change within the concentration range under study. The findings make it possible to develop gallate glass with the necessary properties. Figures 3; tables 4; references 5.

Fluorine-Bearing Lanthanum-Borate Glass Tinted With *d*-and *f*-Element Oxides

937D0077B Moscow STEKLO I KERAMIKA in Russian No 9, Sep 92 pp 11-12

[Article by V.D. Khalilev, V.G. Chekhovskiy, M.A. Amandikov, A.R. Kuznetsov, St. Petersburg Technological Institute; UDC 666.11.01:535.343.666.24:546.4/.8]

[Abstract] The high refractive indices of superheavy crown glass which make it possible to use it for costume jewelry and the lack of known studies of tinted crown glass prompted an examination of stained glass produced on the basis of heavy crown glass which, in turn, is made on the basis of the $Zn_{0.5}Cd_{0.5}B_2O_4$-$La(BO_2)_3$-YF_3 system. The glass for the study is founded in glass-carbon crucibles in an electric furnace at 1,100° C with a melt shielding from the air. The coloring agent concentration on the glass and the main characteristics of their absorption spectra and ultraviolet absorption edge are summarized. The absorption spectra are recorded by a Specord M40 spectrophotometer. An analysis reveals that the ion line positions of not only *f*-, but also *d*-elements in the absorption spectra are generally consistent with the line positions of the same ions in silicate glass; a noticeable line shift is noted only for Cr^{3+} ions. The glasses under study have a good translucence and high refractive indices and may be used for making decorative consumer goods. Tables 1; references 5.

Aspherical Part Forming From Optical Glass Under Exposure to External Force and Temperature Fields

937D0077C Moscow STEKLO I KERAMIKA in Russian No 9, Sep 92 pp 12-14

[Article by A.A. Frolov, Optika Scientific Production Association; UDC 666.22]

[Abstract] Interest in aspherical optical parts due to the fact that their use makes it possible to improve the optical characteristics, eliminate numerous errors, and improve the optical system image quality and the possibility of controlling the surface shape by manipulating the external parameters and thus giving the surface the necessary configuration prompted an analysis of the deformation of thin planar optical part blanks under the external action of temperature and force fields. It is speculated that by selecting the external parameters, the forming of aspherical surfaces can be controlled and surfaces with the requisite shape can be produced. The effect of the temperature field on a planar optical glass part blank is considered and formulae are derived for analyzing the plate surface strain under the effect of the temperature field. Then the aspherical surface forming by an external force action is considered in a similar fashion. It is shown that surfaces with a much greater asphericity degree can be produced under a force loading than under the effect of temperature fields. The above methods can be used for making optical elements, both with a small asphericity under the temperature exposure and with a significant deviation from the initial surface under the force loading. References 1.

Superconducting Glass Ceramics in Bi-Sr-Ca-Cu-O System: Review

937D0077D Moscow STEKLO I KERAMIKA in Russian No 9, Sep 92 pp 16-21

[Article by N.V. Shishkov; UDC 666.263.2:666.113.42'41'21'087'056:537.311]

[Abstract] Bi-containing high-T_c superconducting (VTSP) ceramics with copper oxides in the Bi-Sr-Ca-Cu-O system, particularly the 2201, 2212, and 2223 phases (according to the number of Bi, Sr, Ca, and Cu cations), and their structure are considered, and their synthesis methods are divided into three groups: rapid melt quenching with annealing, casting into ready products with subsequent annealing, and fiber pulling from a melt or an amorphous blank. Most attention is given to the first method. A large volume of published data is summarized, and phase transformation are examined by the differential thermal and thermal gravimetric analysis methods (DTA and TGA). The magnetic susceptibility and electric resistivity of the samples is examined, and the sequence of phase formation is traced. The effect of oxygen on T_c is plotted, and the design of a device for fiber production by laser floating zone melting is cited. The specific synthesis techniques are described in detail, and the effect of the composition and quenching and annealing conditions on the sample properties is examined. Figures 3; tables 2; references 25: 8 Russian, 17 Western.

Determining Qualitative Ceramic Phase Composition by X-ray Phase Analysis Method

937D0077E Moscow STEKLO I KERAMIKA in Russian No 9, Sep 92 pp 23-24

[Article by Ye.M. Dyatlova, N.M. Bobkova, T.N. Yurkevich, Ye.M. Kupran, Belarussian Technological Institute; UDC 666.762:539.26]

[Abstract] The shortcomings of the chemical and microscopy analysis methods of determining the elemental composition and the advantages of qualitative X-ray phase analysis based on establishing the dependence of the diffraction peak intensity of the phase under study on its concentration in the sample aroused increased interest in all types of X-ray qualitative analysis methods due to their versatility and suitability for automation, making it possible to use them for determining virtually any crystalline phase concentration. The stages of qualitative phase analysis are outlined and a ceramic material characterized by a

range of elevated thermal and mechanical indicators is examined. The ceramic material is synthesized on the basis of the Al_2O_3-TiO_2-SiO_2 system; an attempt is made to find the qualitative and quantitative phase composition of this material by quantitative X-ray phase analysis. The diffraction patterns are recorded in CuK_α radiation in a Dron-2 unit at a 1°/min scanning rate using model compositions. The calibration curves of the ceramic are plotted in order to determine the unknown concentrations of various components. An analysis of the melt:solid phase ratio shows that the liquid phase amounts to 43.5 percent and the solid phase consists of 44.6 percent tialite and 11.9 percent rutile. A slight discrepancy between the theoretical and experimental ceramic compositions is attributed to the impurities present in the clay ray material mixture. The findings provide the most complete information to date about the ceramic composition, making it possible to ensure oriented synthesis of ceramic materials and program their properties. Figures 1; references 6.

Effect of Ampoule Annealing on Medical Preparation Contamination With Glass Dust

937D0077F Moscow STEKLO I KERAMIKA in Russian No 9, Sep 92 pp 24-25

[Article by Y.L. Belousov, BTISM; UDC 666.176: 666.1.038.002.68]

[Abstract] The effect of annealing on ampoule and medical preparation rejection due to the ingress of mechanical particles and two mutually opposite processes occurring with temperature variation during annealing—separation of glass particles from the ampoule surface and adhesion of particles from inside or outside to the glass surface—are considered. The effect of annealing and temperature gradients on the residual stress distribution in the ampoules is discussed, and an optimum cooling rate is identified for each wall thickness. The temperature, residual stress, and dust distribution during the ampoule forming, the effect of residual stress of the ampoule preparation rejection, and the dependence of the ampoule rejection on the annealing temperature are plotted. An analysis of the ampoule forming characteristics and residual stress distribution shows that the temperature gradient along the ampoule length has a greater effect that that in the wall thickness. These stresses reach 300-600 nm/cm and are normal to the surface. The conclusion is drawn that cassette annealing of several ampoules at once has advantages over other methods despite its greater duration and complex heat exchange conditions. It is speculated that ampoule rejections can be decreased considerably by using gradual cassette annealing (Patent No. 1551665) but it is stressed that the number of rejects can be reduced significantly only by brief annealing in an individual minifurnace whose design and operating conditions were developed at BTISM. Figures 3; references 2.

Production of Quartz Ceramic Rolls

937D0077G Moscow STEKLO I KERAMIKA in Russian No 9, Sep 92 pp 27-28

[Article by A.M. Akhyan, Kvarts Scientific Production Association; UDC 666.192.2:658.51:621.824]

[Abstract] The uses of quartz ceramic rolls for plate glass annealing in horizontal conveyors (including shatter proof sheet glass) and the type of rolls used for these purposes are outlined and the results of studies aimed at determining the degree of roll homogeneity and sintering and their physical and chemical properties are reported. The water absorption, density, open, close, and total porosity, and cristobalite concentration in various sections of rolls made in France and the United States are summarized and discussed. Two types of rolls—solid and hollow (tubular)—manufactured at the Kvartz Scientific Production Association and their production methods are described; the former are made by traditional ceramics compaction and sintering methods and the latter—by spin casting. Three specific types of spin quartz ceramic casting are considered and machining methods are analyzed. Rolls made by the Kvarts Association were tested and passed the tests. They have been in operation since June 1990 and their quality is comparable to that of imported rolls. Figures 3; tables 1.

Graphite With Corrugated Layers Under High Pressures

937D0042B Kiev SVERKHTVERDYYE MATERIALY in Russian No 5(80), Sep-Oct 92 pp 12-16

[Article by V.D. Andreyev, A.F. Goncharov, M.T. Muinov, Superhard Materials Institute at the Ukrainian Academy of Sciences, Kiev and Crystallography Institute at Russia's Academy of Sciences, Moscow; UDC [538.69:539.121.14]:666.233]

[Abstract] The studies of graphite behavior under high pressures (see *ZhETF* Vol. 96 No. 8, 1989, *Pisma v ZhETF* Vol. 51, 1990, and *ZhETF* Vol. 98, 1990 and Vol. 100, 1991) in the diamond's thermodynamic stability region are continued, and an attempt is made to attain the line of direct graphite → diamond transition at room temperature. To this end, various graphite samples are subjected to several loading cycles at a ≈800 Mbar pressure in order to stabilize the high-pressure amorphous phase containing carbon in the sp^3 state. Raman spectra (KRS) of compressed graphite samples produced by graphitization of the ASM 28/20 synthetic diamond during isothermal annealing for 30 min at 1,900° C at various pressures (of up to 95 GPa) with and without a pressure transmitting medium, Raman spectra of various carbon modifications at high pressures, and a phase constitution diagram of various forms of graphite, diamond, carbon, and liquid are plotted. An analysis demonstrates that the graphite-like carbon modification transformation into the amorphous phase at high and low (room) temperatures is a characteristic feature of carbon's phase diagram. A typical graphite brightening in the visible spectrum at pressures above 60 GPa is noted and attributed to the π-bond localization between the layers, thus depriving the lattice of free electrons responsible for absorption and reflection and sharply increasing the resistivity. Figures 4; references 17: 7 Russian, 10 Western.

Thermal Patterns of Diamond Grinding of Tool Ceramics

937D0042F Kiev SVERKHTVERDYYE MATERIALY in Russian No 5(80), Sep-Oct 92 pp 40-43

[Article by V.I. Lavrinenko, A.A. Sytnik, V.V. Shklyarenko, Superhard Materials Institute at the Ukrainian Academy of Sciences, Kiev and Svetlovodsk Hard Alloy and Refractory Metals Works; UDC 621.923: 666.3:621.922]

[Abstract] The effect of tool ceramics' heating during grinding on the quality of surfaces machined by them is discussed, and the thermal patterns of diamond grinding of tool ceramics are examined; the lack of published data on this problem is noted. The grinding temperature is measured by an insulated thermocouple placed in a cut between two ceramic tips and calibrated with the help of an electric furnace. The parameters which affect the grinding zone temperature are analyzed, and the dependence of the machining zone temperature on the cross-feed parameter during grinding of VOK71, VO13, and nitride ceramics as well as the temperatures measured in the near-surface layers during grinding of VOK71, VOK95S, and nitride ceramics and silinite and cortinite and the approximating curves are plotted. Formulae which reflect the correlation of the grinding parameters and temperature are derived and it is shown that the temperature follows a square law in the grinding zone. The effect of the grinding wheel binder on the thermal processes is investigated and it is demonstrated that the highest temperature is reached during grinding of tool ceramics using diamond grinding wheels with the M2-01 binder. The earlier assumption that oxide binder-based ceramics can be machined using grinding wheels with metal binders without excessive heating is confirmed. The finding make it possible to draw the conclusion that diamond grinding wheels with polymer binders ensure the lowest temperature for grinding polyhedral cutting ceramic inserts regardless of the ceramic base. The relationship between the force and temperature parameters is examined. Figures 2; tables 1; references 7.

Producing Hexagonal Tube From Boron Steel

937D0054H Moscow STAL in Russian No 9, Sep 1992 pp 48-49

[Article by N. P. Karpenko, V. I. Ryabushkin, I. I. Sergeyev, and A. A. Fedorov, Chelyabinsk Tube-Rolling Plant; UDC 621.774.35]

[Abstract] The tube is made from hot-rolled 04Kh14T3R1F boron steel and is 289 by 11 mm by 5.8 to 6.3 m long. After straightening on a press, the tube is bored out to an internal diameter of 271.5+1/-0.5 mm. Depending on inspection results, the nominal external diameter is set after turning to obtain an average wall thickness of about 6.4 mm. The tube is then chamfered externally at the front end and internally at the back end relative to turning position. If necessary, external surface defects are attended to, wall thickness is tested by ultrasound, and the product is degreased, induction heat-treated, and inspected non-destructively. After drilling the fastener holes, the tubes are salt greased and thermally roll-formed to a module pitch of 257.5 mm. After degreasing, they are heat-treated in a chamber furnace, press-straightened, and, after trimming, inspected with a gauge along their entire length. Finally, they undergo final surface finishing, testing, and inspection. The finished tubing is 4330 mm in length, the module pitch is 257 + 2 mm, wall thickness is 6 + 1.75/-1 mm, total deflection is no more than 3 mm, and distortion of any one side does not exceed 2°15' along the entire length of the tubing. An inspection gauge four meters long with a module pitch of 237 mm and a diameter of 271.5 mm can pass through the tubing. The mechanical properties of the tubing metal are: $\sigma_B \geq 450$ N/sq mm; $\sigma_T \geq 250$ N/sq mm; and $\delta_5 = 10$ percent. The metal can pass an intercrystalline corrosion test. There are no surface defects deeper than 0.5 mm and no flaw-detected hidden defects deeper than 0.6 mm. The authors claim that this product and the technology used to produce it is superior to any similar product or technology in the world. References 2: Russian.

Laws Governing the Formation of the Structure and Properties of Powder Carbon Steels During Laser Thermal Modification. 2. The Properties of Modified Steels

937D0056D Kiev POROSHKOVAYA METALLURGIYA in Russian No 9, Sep 92 (manuscript received 12 Jun 89) pp 91-95

[Article by V.N. Antsiferov, A.M. Shmakov, and S.V. Shtennikov, Republic Powder Metallurgy Engineering and Technology Center, Perm; UDC 621.762:621.375]

[Abstract] Specimens of the various powder carbon steels (including SP20-2, SP60-2, SP70-2, and SP90-2) were subjected to metallographic and electron microscopy studies to determine effects of laser thermal modification on the formation of their structure and properties. The studies established the presence of martensite and residual austenite in the fused zone of the steels SP60-2 through SP90-2. Products of the decomposition of inhomogeneous austenite were also found in the laser-affected zone. In addition, a shallow layer of transition to the base that contained a cementite mesh was also found in the specimens of SP90-2 steel. The depth of the laser-affected zone increased as the carbon content in the steels was increased to 0.8 percent. At room temperature, the steels' thermal conductivity decreased by 35 to 40 percent as the carbon content was increased from 0.1 to 1.0 percent. A significant dependence between the depth of the phase transformation zone and the laser thermal modification regimen was established. The deepest laser-affected zone in the steels SP20-2 through SP60-2 was achieved when a radiating power of 2 kW was used and when the specimens were moved at a rate of 10 m/h. In the steels SP70-2 through SP90-2, the deepest laser-affected zone was obtained with a radiating power of 1.5 kW while the specimens were moved at a rate of 10 m/h (with a scanning zone 6 mm wide and scanning frequency of 3.7 s^{-1}). Further increases in radiating power did not result in any further intensification of the processes of total and selective vaporization from the surface of the base. The hardened region of the study specimens is divided into zones with high and medium microhardness. The low microhardness corresponds to the starting material of the base, whereas the highest (up to 500 HV for SP20-2 steel and up to 1,200 HV for SP90-2 steel) corresponds to the material after two or three cycles of surface hardening with laser radiation. The microhardness of both zones increases as the concentration of carbon in the steels increases. The amount of residual austenite in the steels changes as a function of the initial composition and structure of the steels and ranges from 15-20 percent in SP70-2 steel to 50-55 percent in SP90-2 steel. The residual austenite content was lowest at the minimum specimen feed rate (3-5 percent). Under such conditions, doubling the radiating power reduces the fraction of residual austenite by a factor of 1.5 to 2. CO_2 laser thermal modification also induced changes in the fracture toughness of the steels studied: Fracture toughness decreases as radiating power is increased due to the increase in the dimensions of the embrittled layer in the laser-affected zone with a martensite structure. Fracture toughness decreases as the starting concentration of carbon in the steels increases. The intensity of the wear of low-carbon steels with a modified surface is a factor of 1.5 to 5 less than that of nonhardened steels depending on the treatment parameters. SP90-2 steel treated with radiation at a power of 2 kW as the specimens and fed in at a rate of 10 m/h was found to possess the best wear resistance. The method of laser thermal modification was thus found to be promising for use in the production of powder steel components with a locally hardened surface. Figures 4, table 1; reference 1: Russian.

The Structure and Electrophysical Properties of Hot-Compacted Ceramic Materials in the System Si_3N_4-SiC. 3. The Effect of Electromagnetic and Heat Fields on Electrophysical Properties

937D0056E Kiev POROSHKOVAYA METALLURGIYA in Russian No 9, Sep 92 (manuscript received 13 Nov 90) pp 95-99

[Article by A.A. Kasyanenko, V.Ya. Petrovskiy, L.A. Shipilova, and Ye.I. Gervits, Materials Science Problems Institute, Ukraine Academy of Sciences, Kiev; UDC 621.762.4:621.55:546.28:661.66.1:537.3.3:537.312.6]

[Abstract] A study examined the effect of electromagnetic and heat fields on the structure and electrophysical properties of hot-compacted ceramic materials of the system Si_3N_4-SiC. Twelve different specimens with SiC concentrations of 10 to 20 vol.- percent, SiC grain sizes of 1 to 120 μm, and MgO concentrations of 5 to 10 vol.- percent were studied. The temperature and frequency dependences of their electric resistance were determined, their volt-ampere characteristics were measured, and the temperature coefficient of their electric resistance and coefficient of the nonlinearity of their volt-ampere characteristics were calculated. The temperature dependence of the bulk electric resistance of all of the ceramic specimens studied had the form of a straight line in half-log coordinates, which means that the temperature dependence of their electric resistance is of an activation nature and subjected to the law $\rho \approx (\Delta E_\sigma/kT)$. The frequency dependence of the electric resistance of several of the Si_3N_4-SiC materials was found to be between 10^4 and 10^8 Hz. The effect of the frequency of the applied voltage on the materials' electric resistance was found to increase as the average grain size and amount of activator increased. All of the specimens were found to be characterized by a jump mechanism of conduction. The volt-ampere characteristics of the Si_3N_4-SiC materials were found to manifest a slight nonlinearity in cases of low currents and voltages. When the materials were under high loads, their volt-ampere characteristics were practically linear, which means that resistive elements based on the Si_3N_4-SiC composites studied may be recommended for use within a broad range of working currents and voltages. Powders with grain sizes ranging from 28 to 120 μm or silicon carbide produced by the method of self-propagating high-temperature synthesis were recommended for use as a conductive phase. Figures 4, table 1; references 9: 8 Russian, 1 Western.

Effect of Comprehensive Chemical and Heat Treatment Conditions on Residual Stress Distribution

937D0057I Lviv FIZIKO-KHIMICHESKAYA MEKHANIKA MATERIALOV in Russian Vol 28 No 1, Jan-Feb 92 pp 116-118

[Article by M.F. Berezhnitskaya, A.K. Tikhonov, I.V. Bogdanova, Physical Mechanics Institute imeni G.V.

Karpenko at the Ukrainian Academy of Sciences, Lvov; UDC 539.319:621.785.532/533]

[Abstract] The use of low-temperature gaseous nitriding to increase the wear resistance of the cam pair parts and the development of new comprehensive chemical and heat treatment methods are discussed, and it is noted that neither one solves the attendant problem the nitrided layer peeling. To address this issue, the residual stress distribution and the microhardness behavior, phase composition, and wear resistance of the surface layers of Volga Automotive Plant parts under various comprehensive chemical-heat treatment conditions are investigated. Six steel 40Kh nitriding conditions are summarized, and the residual stress distribution in the surface layers of samples after nitriding and comprehensive treatment is plotted. The favorable effect of temperature on the residual stress formation is recorded. The high hardness and residual compressive stresses supply the nitrided layer with a high brittle fracture resistance under severe operating loads. The conclusion is drawn that of the six conditions under study, Nos. 3 and 6 are optimal (620 and 580°C with a 14-18 and 14-16 μm layer, respectively). Figures 1; tables 1; references 5.

Hydrogen in Electroslag Refining Processes That Use a Liquid Starting Flux

937D0065C Moscow IZVESTIYA VYSSHIKH UCHEBNYKH ZAVEDENIY: CHERNAYA METALLURGIYA in Russian No 9, Sep 1992 pp 11-17

[Article by O. N. Romanov, I. A. Novokhatskiy, and V. Ya. Kozhukhar, Odessa Polytechnic Institute; UDC 669.187.26+669.046.58- 154]

[Abstract] Electroslag refining with liquid starting flux was studied to determine how the hydrogen concentration of the starter affects the absorption of hydrogen by the metal. In the first part of the study, granulated ANF-6 flux from the same production batch was melted in a graphite crucible that also served as a ladle. The flux was either air-dried or specially moisturized by adding water to an airtight container containing the flux one day prior to melting. The flux was also melted directly from ANF-6 components air-dried or moisturized as just described. It was found that the level of hydrogen absorption by the melted flux was insensitive to the hydrogen concentration of the original granulated flux or the components used to make it. A quasi-equilibrium concentration of hydrogen in the melted flux melt was determined primarily by the humidity of the air and by the temperature of the flux. In the second part of the study, ESR test heats of 12Kh18N10T and 40KhN steels were run under production conditions using liquid starting fluxes made as previously described from ANF-6 and ANF-29 fluxes or their individual components in three different variations: air-dried (regular), pre-calcined, and specially moisturized. It was found that, at any particular time, the hydrogen concentrations in both the metal and the flux during open electroslag processing are not related to the initial hydrogen concentration in either the granulated fluxes or their individual components. It was concluded that predegassing of centrally produced granulated fluxes for electroslag processing with a liquid starting flux is both ineffective and unnecessary. Figures 1, tables 3; references 16: Russian.

Deep Treatment of Melts With High-Temperature Media

937D0067A Moscow LITEYNOYE PROIZVODSTVO in Russian No 9, Sep 92 pp 5-6

[Article by V.L. Naydek, A.V. Narivskiy, V.I. Sinichak, Yu.P. Lenda; UDC 621.745.55:669.715]

[Abstract] The possibility of improving the quality of nonferrous and Fe-C alloy properties by plasma treatment, particularly deep treatment of the melt with high-enthalpy gaseous reagent media for the purpose of degassing, prompted an investigation into the process of H_2 removal from the melt during its treatment with cold and high-temperature argon jets using the AK7 alloy hydrogenated beforehand at a 730-740° C metal temperature. To eliminate the effect of oxygen and the surface metal oxidation on refining, the alloy was treated under different conditions under a layer of conventional flux. The melt was blasted with cold and plasma jets at the same Ar rate and the gas content was determined by vacuum H_2 extraction directly from the melt through a Pd filter while correcting the measurements by degassing control samples. Kinetic curves of H_2 removal from the AK7 alloy by deep cold and plasma jets and the characteristics of the AK7 alloy degassing process during treatment with gaseous reagent jets at various temperature states of the melt are plotted. The quality of untreated and treated (by both types of jets) aluminum alloys are summarized; they show that plasma treatment ensures a 70-80 percent refining degree for hydrogen and 50-55 percent for oxide inclusions. The high efficiency of the new methods enables the enterprises to use recovered and nonferrous alloy chips as a burden. The study makes it possible to recommend the procedures for implementation. Figures 2; tables 1; references 4.

Laser Impact on Liquid and Liquid-Solid State of Aluminum Alloys

937D0067B Moscow LITEYNOYE PROIZVODSTVO in Russian No 9, Sep 92 p 8

[Article by V.A. Pereloma, V.P. Likhoshva; UDC 621.74:669.715-154:621.375.8]

[Abstract] Experiments with laser treatment of the Al25 alloy with CW Kometa-2 laser radiation and pulsed periodic Kvant-15 laser radiation are reported. Two crucibles with the same composition—experimental and control samples—are heated in a resistance furnace to a temperature 100° C above the liquidus point and the melt is exposed to a constant temperature for 5 min after which the working sample is treated with laser radiation by scanning it with focused or unfocused laser beams. The power density was manipulated in both modes within 10^2-10^6 W/cm^2; the samples were cooled with the furnace at a 10° C/min rate. The structural characteristics of the melt are studied by metallographic, X-ray diffraction, and X-ray structural microanalysis and by Auger spectroscopy.

The hardness and microhardness are measured by a PTM-5 microhardness and hardness gauges. The structure and phase composition behavior are reflected on the physical and mechanical properties of the alloy; the sample hardness after treatment with CW radiation increases by 1.6 times compared to that of the untreated sample. The most significant changes occur in the melt treated with pulsed radiation at a higher energy density per unit volume of material. Given subsequent treatment of the sample with a carbon powder layer applied to it, the sample hardness increases by more than twofold. References 2.

New Production Practices of Quality Superalloy Items

937D0067E Moscow LITEYNOYE PROIZVODSTVO in Russian No 9, Sep 92 pp 14-16

[Article by N.M. Kochegura, Ye.A. Markovskiy; UDC 621.74.011:669.245]

[Abstract] An attempt is made to develop certain aspects of the theory of cast structure formation of multicomponent corrosion resistant alloys from the liquid state with predictable performance and effectively controllable properties and to develop on this basis commercial processes with regulated melt treatment during casting in order to produce materials with improved and stable performance. To this end, ZhS alloys used for making nozzle vanes and blades and cast rotors of gas turbines for various purposes are examined. The properties of these alloys are controlled by treating the melts. In selecting the treatment method and its condition, the structure-sensitive characteristic of the melt which responds most fully to this treatment and can be measured with the least error is selected as the efficiency criterion. The polythermal density curves of these alloys and the temperature-time conditions of the alloy heat treatment are plotted. The melt passes from the metastable to stable state at a diffusion annealing temperature whereby diffusion annealing is related to additional energy outlays for reordering in the liquid state which occurs under thermal cycling (TVO). Thermal cycling leads to a twofold increase in the alloy resistance under high-temperature extended strength tests; TVO helps to form an optimum microstructure. Thermal cycling also reduces the amount of rejects and increases the usable blade yield to 80 percent from 60 percent. The use of the new technology makes it possible to control the shape and size of inclusions thus improving the alloy properties. Figures 2; tables 1; references 2.

Liquid Fe-Ni-C Alloy Structure Under Various Temperature-Time Conditions

937D0067F Moscow LITEYNOYE PROIZVODSTVO in Russian No 9, Sep 92 pp 19-21

[Article by A.A. Sheyko; UDC 621.745.56]

[Abstract] An X-ray diffraction study of a liquid Fe-Ni-C alloy carried out in a high-temperature diffractometer in Mo-K_α monochromated radiation scattered by the alloy's free surface in order to examine the alloy structure is reported. The molten sample was heated before recording the diffraction patterns to a 1,773-1,793K temperature for 5-15 min in order to obtain a pure specular surface, then the temperature was lowered to a set level, the sample exposed to it for 10-15 min, and the diffraction pattern recording was taken. The alloy was smelted from pure components (21.4 percent Ni, 3/35 percent C, and 75.15 percent Fe) in alundum crucibles in an induction furnace. The diffraction patterns of the alloy at various temperatures and the radial distribution function of the distance from the central atom are plotted; the latter is plotted on the basis of a Fourier analysis of the diffraction patterns on a computer. The findings show that the graphite dissolution in the liquid Fe-Ni-C alloy is an extended process whose length largely depends on temperature. Graphite dissolution is accompanied by the formation of carbide clusters highly enriched with carbon which consist mostly of metal atoms and whose structure does not change with temperature. The atomic packing arrangement types in clusters with carbon impoverishment changes substantially with temperature. Reversible BCC-FCC structural transitions typical of liquid iron and some alloys are noted. Figures 2; tables 1; references 6: 4 Russian, 2 Western.

Partially Graphitized Pig Iron and Its Application

937D0067G Moscow LITEYNOYE PROIZVODSTVO in Russian No 9, Sep 92 pp 21-22

[Article by I.G. Neizhko; UDC 621.74:669.13]

[Abstract] The properties of mottled or partially graphitized pig iron (ChGCh) whose structure contains both graphite and structurally free cementite and its behavior under chilling are studied. Attention is focused on a method of producing partially graphitized pig iron by partial graphitizing annealing of white pig iron castings which makes it possible to attain a uniform ChGCh structure throughout the casting and examine the relationship between its HB hardness, KC toughness, and ultimate strength. To this end, breaking and impact tests of samples with an ingot skin and, in some cases, internal defects (microporosity) in the central area are examined. The microstructure of partially graphitized pig iron is shown and the dependence of its hardness on toughness and strength is plotted. As expected, the toughness and ultimate strength are in the mid-range between white and pearlitic malleable pig iron while the wide spread of parameters is due to casting defects. An analysis of available experimental and theoretical data makes it possible to confirm the high utilization efficiency of partially graphitized pig iron and the need for subsequent studies of this material as well as for expanding its use as a wear resistant friction material. Figures 2; tables 1; references 1.

Thin-Walled Light Alloy Casting Production in Traveling Magnetic Field

937D0068A Moscow LITEYNOYE PROIZVODSTVO in Russian No 10, Oct 92 pp 6-8

[Article by B.V. Rabinovich; UDC 621.74.002.6:669.715]

[Abstract] The importance of decreasing the casting mass in machine building and decreasing the ratio of the machine or device mass to its output (an indicator attesting to the technology development level) and ways of attaining these goals are discussed. A new process developed for meeting the increasing demand for lightweight aluminum alloy castings—making thin-walled castings in a traveling electromagnetic field (LBEMP) which requires a

special magnetohydrodynamic (MGD) mold design and an MHD chill—is considered. The essence and characteristic features of the LBEMP method are considered and its advantages and shortcomings are compared to those of alternate methods, e.g., permanent-mold casting and die casting. The MHD mold design is considered and the LBEMP method's advantages and applications are summarized in detail. The behavior of the piezometer tube head along the casting channel and the behavior of the aluminum alloy flow front rate along the channel are plotted. The LBEMP method makes it possible to resolve the conflict between designers and production engineers and make castings and thin-walled parts from lightweight nonferrous alloys with a large surface and local bulges, primarily for machines and devices whose operating characteristics directly depend on their mass. It is especially efficient in the aerospace, rocket, automotive, and other advanced industries. The method also makes it possible to use high-strength alloys and cheaper chills and eliminates such operations as forging, stamping, rolling, and welding. Figures 3; tables 2; references 6: 3 Russian, 3 Western.

Blast Furnace Foundry Pig Iron

937D0068B Moscow LITEYNOYE PROIZVODSTVO in Russian No 10, Oct 92 pp 12-13

[Article by V.A. Kurganov, V.V. Lesovoy, L.A. Krauze, Donetsk Scientific Research Institute of Ferrous Metallurgy; UDC 621.74:669.162/.163]

[Abstract] Blast furnace cast iron (ChDP)—one of the most common materials whose hereditary properties may significantly affect the technical and economic foundry indicators—is considered in detail and attention is focused on ladle refining of foundry cast iron as the most realistic and efficient from the energy viewpoint. Since most of foundry cast iron is used in subsequent process stages, its gas saturation, impurity concentration, and initial structure are ignored. Liquid foundry cast iron is characterized by the lack of "genetic memory" since it is produced from ore materials by oxide reduction and foundry cast iron properties are formed at a 1,570-1,300° C temperature. The use of inoculation to control the cast iron properties is examined and the properties of foundry and conversion pig iron are compared. The correlation of mechanical properties and casting and conversion pig iron production methods is discussed and it is noted that this relationship can be used to program the casting properties in making conversion pig iron by using early treatment and late inoculation. This conclusion is borne out by a study of the effect of heredity on the pig iron solidification parameters during the second remelting. The graphitizing and refining effects produced by means of inoculation are preserved after the second remelting. The findings make it possible to raise the issue of actively controlling the hereditary properties of the original conversion pig iron by ladle refining. The need for further scientific and engineering studies for implementing the new technology is stressed. References 3: 2 Russian, 1 Western.

Increasing Cast Iron Ingot Mold Plate Durability

937D0068C Moscow LITEYNOYE PROIZVODSTVO in Russian No 10, Oct 92 pp 14-15

[Article by I.A. Malykhin, S.V. Milyukov, B.V. Shakhtarina, Yu.N. Selivanov, R.Ya. Kutuyeva, Magnitogorsk Mining and Metallurgy Institute and Magnitogorsk Integrated Iron and Steel Works; UDC 621.74.002.6:669.13]

[Abstract] The limited durability of cast iron bottom plates used at the Magnitogorsk Integrated Iron and Steel Works due to the development of through cracks and bottom plate welding to the steel ingot in the open hearth furnace prompted a study of the structure and properties of the bottom plate cast iron aimed at increasing its durability. The chemical composition of cast iron in bottom plates which had not been used was examined and found to be roughly the same in the three layers under study. It is speculated that the low cast iron strength in the working layer which picks up the principal mechanical and thermal loads greatly lowers the plates' operating resistance and causes their premature failure. This discovery led to the development of a new procedure of extending the plate life by increasing the metal uniformity and inoculating it with byproducts of rolling mills—low-carbon discards of plate edges (OBKL) which are added during suspension casting. The OBKL distribution patterns in the plate are examined in a lab by approximate simulation. The distribution of sodium thiosulfate and OBKL particles in the bottom plate surface (where sodium thiosulfate simulates the OBKL particles) is plotted. The study shows that thick-walled castings can be made by suspension casting with an addition of OBKL chilling inoculants, making it possible to increase the uniformity of pig iron properties and control the structure of massive pig iron casting by manipulating the inoculant rate. In 1991, the economic impact of the new method in Magnitogorsk was 400,000 rubles. Figures 2; tables 2; references 3.

Increasing Durability of Cast Mining and Metallurgical Equipment Parts

937D0068D Moscow LITEYNOYE PROIZVODSTVO in Russian No 10, Oct 92 pp 15-16

[Article by V.V. Lunev, Ye.I. Ivakhnenko, V.A. Fedkov, V.I. Minakova, Zaporozhye Mechanical Engineering Institute; UDC 621.74:669.018.4:620.178.169]

[Abstract] Extensive mining and metallurgical ore dressing equipment downtime due to an unacceptable durability of rapidly wearing parts usually made from high alloy Cr-Ni steels 40Kh24N12SL, 35Kh23N7L, and 35Kh18N24S2L according to GOST 977-88 prompted attempts to increase the durability of cast parts for mining and metallurgical equipment and develop abrasion resistant alloys for this purpose by optimizing their compositions, designing efficient inoculation techniques, and using new heat treatment conditions. To this end, the composition of existing alloys is optimized in order to lower the P and S concentration and new alloys which ensure an elevated level of physical, mechanical, and operating properties are developed. Pilot alloys are smelted in 10 and 50 kg lab RF induction furnaces and in commercial 6 ton DSP-6 arc furnaces with basic lining by remelting and fusing. The chemical composition of four alloys is summarized and the results of mechanical tests (ultimate strength, elongation, reduction in area, mass loss, and wear resistance) are presented. High-temperature wear is examined by simulating the operation of commercial concentration equipment. The study makes it possible to recommend a low-alloyed metal for crucial parts operating under high-temperature wear

conditions which extends the service life of mining equipment by 1.5-2 times and makes it possible to shorten equipment downtime and save scarce and expensive nickel. Figures 1; tables 2; references 3.

Ways of Decreasing Foundry Worker Efforts in Casting Alloys From Crane-Mounted Ladles: Discussion

937D0068E Moscow LITEYNOYE PROIZVODSTVO in Russian No 10, Oct 92 pp 25-26

[Article by L.M. Goncharov, I.N. Polukhina, I.I. Guralnik, GP Sevmorzavod; UDC 621.74.224]

[Abstract] The effort required to tilt a manually operated crane ladle for pouring alloys consists of the restoring moment and friction torque which are specified by the Safety Engineering and Occupational Safety Rules for Machine Building Industry Foundries. Yet the design and operation experience of crane-mounted ladles shows that the actual manual force required for operating these ladle conflicts with said Rules. This prompted an examination of methods of increasing the manual efforts, especially since Roper ladles (from Britain) which have been in operation for almost 20 years in St. Petersburg require little effort to tilt and their reduction gears have not broken down even once during this time. A new formulation of the Rules is suggested and the tilting moment behavior for various types of ladle journals is plotted. The importance of preventing the ladle from self-tilting is stressed; it is noted that this requirement should replace the one mandating that the center of gravity be lowered. Figures 1; tables 1; references 8.

Electric Furnace Impoverishment of Slags for Flash Smelting at the Nadezhdinsk Metallurgy Plant

937D0069A Moscow TSVETNYYE METALLY in Russian No 10, Oct 92 pp 7-10

[Article by G.V. Vostrikov, Z.V. Zoriy, and V.N. Ampilogov, Gipronikel and Norilsk Mining and Metallurgy Combine imeni A.P. Zavenyagin; UDC 669.243.88: 621.365.3]

[Abstract] The system for flash-smelting nickel and copper sulfide concentrates at the Nadezhdinsk Metallurgy Plant was put into operation in 1981. Round three-electrode electric furnaces produced by Krupp (Germany) with self-sintering electrodes measuring 1,270 mm in diameter and horizontal suspended arches were installed to impoverish slag. It was originally planned that all nickel slags from the flash smelting furnaces and the converter slags from the nickel production process would be impoverished in the electric furnaces of the nickel line and that all of the copper slags of the flash smelting furnaces and converter slags from the copper production process would be impoverished in the electric furnace on the copper line. The heavy ore fraction from the Komsomolskiy ore mine was to be used as a sulfidizing agent. Because of irregular supplies of needed materials, however, the plant experienced start-up problems and was rather slow in reaching its design capacity. In order to meet its state-assigned quotas, the plant began processing more than twice the planned amount of solid metal-containing burden (wastes, agglomerate). This practice was continued until 1986. Because of the converter slags' low silicon dioxide content, sandstone was smelted at twice the planned rate. The distribution of the amount of liquid slags between electric furnaces continued to differ from the planned distribution until 1988: All the converter slag of the nickel and copper lines, all the slag of the nickel flash smelting furnace, and up to one-third the slag of the copper flash smelting furnace were processed together in the electric furnace of the nickel line. The electric furnace of the copper line processed virtually only slag from the copper flash smelting furnace. The practice of processing materials with an elevated moisture content (ore, sandstone, reducing agent) resulted in frequent repairs to the central portion of the arches owing to "pops" in 1981-1984. Leaks in the arches made it impossible to use the planned amount of coal culm in the furnaces. Joint research conducted by associates of the State Institute for the Design of Nickel Industry Enterprises [Gipronikel] and the Nadezhdinsk Metallurgy Plant's own specialists resulted in the development of a set of measures to reduce the content of nonferrous metals in the waste slag. The new measures made it possible to achieve an 8-hour impoverishment cycle tied to the operating graphs of the converters and flash smelting furnaces operating in pairs with the electric furnaces. The amount of nickel in the waste slag from the nickel line was reduced from 0.19-0.22 to 0.10 percent, and the amount of cobalt was reduced from 0.125-0.130 to 0.096-0.1 percent. A ratio of components in the metal-containing burden was determined that made it possible to produce mattes with a copper:nickel ratio not exceeding 4. The planned content of nonferrous metals in the waste slag was achieved with respect to all metals except cobalt (because of the large amount of liquid and solid slag with a nondesign composition that had to be processed). The impoverishment process at the Nadezhdinsk Metallurgy Plant currently boasts the highest slag and burden processing indicators of all its counterpart enterprises (higher by a factor of 1.5 to 2) and the lowest energy consumption. The plant's specialists are continuing their work with the Gipronikel to further improve and intensify the plant's slag impoverishment process. Preliminary impoverishment directly in the converter by blasting with natural gas will make it possible to reduce the amount of magnetite in the converter slag to 11.8-13.7 percent and to boost the amount of SiO_2 to 20.9-22.8 percent. This will further reduce the energy required for the process. A method of using natural gas to mix the slag bath and thus increase the melting of solid burden is currently being introduced. The process of pouring slag into the electric furnaces has been speeded up by a factor of 1.5 by increasing the discharge hold of the sleeve to 120 mm. The problem of improving the process of granulating the waste slag of impoverishment electric furnaces has also been receiving a great deal of attention. Lengthy tests of different methods (water stream, basin, mechanical) of slag granulation and dewatering processes are under way, and a basin method of granulating ferrous slag with a discharge intensity of > 1.0 metric ton/min has been introduced in two electric furnaces. The new process is distinguished by it safety from explosions and low energy consumption. Tables 4; references 11: Russian.

Vibroacoustic Diagnosis of the Process of Converting Nickel-Containing Copper Mattes in a Vertical Oxygen Converter

937D0069B Moscow TSVETNYYE METALLY in Russian No 10, Oct 92 pp 11-14

[Article by A.I. Vaganov, A.N. Korneyev, Ye.A. Boshnyakov, V.D. Zhidovetskiy, and V.V. Novokreshchenov, Severonikel Combine and Odessa Polytechnic Institute; UDC 669.243]

[Abstract] A system has been developed for vibroacoustic diagnosis of the process of converting nickel-containing mattes in a vertical oxygen converter. A piezoelectric accelerometer with a linear amplitude characteristic in the frequency range up to 20 kHz was used as a transducer in the body noise measurement system. A KSP-4 automatic recording device connected to an SK4-56 spectrum analyzer continuously records vibroacceleration spectra. Electrical noise in the measurement line is eliminated by electrical isolation of the vibration sensor from the converter body, elimination of the cable line between the sensor and emitter repeater, and the use of a low-noise preamplifier mounted in direct proximity to the sensor. Two characteristic sources in the body noise spectrum are observed while the vibroacoustic characteristics of an oxygen converter for producing blister copper are recorded: The first source, i.e., the high-speed oxygen stream, has a frequency range of 4000 to 6000 Hz. The second source, which has a frequency range of 150 to 300 Hz, cannot be classified as a resonance phenomenon. The source of this low-frequency noise is the reaction zone in which the oxidation reaction occurs. the behavior of this low-frequency noise source has been correlated with changes in SO_2 content, which in turn reflect the dynamics of the oxygen processes occurring in the melt. The aerodynamic noise (frequency, 4000 to 6000 Hz) in the tuyere is an important information source in that it makes it possible to reduce the risk of a partial burnthrough of tuyeres, especially when the aerodynamic noise of the oxygen tuyere of a converter is screened by other equipment. The new system includes the capabilities of listening to signals via head telephone or microphone in cases in which the converter control panel is located in a sealed room. The new vibroacoustic diagnosis system is currently undergoing pilot industrial tests at the Severonikel combine. Figures 7; references 5: Russian.

The Change in the Properties of Copper Foil as Its Thickness Increases

937D0069C Moscow TSVETNYYE METALLY in Russian No 10, Oct 92 pp 14-16

[Article by A.A. Kucherov and V.N. Samoylenko, Uralelektromed Combine; UDC 621.357:669.387]

[Abstract] The changes occurring in the properties of copper foil as its thickness is built up were studied. Samples of foils produced under conditions of commercial electrolysis at shops in the Uralelektromed Combine were used for the studies. The foils were produced in electrolyzers with insoluble anodes and titanium drum-cathodes that had first been either machined or subjected to anode oxidizing. The electrolyte consisted of the following (mol/l): 1.10 $CuSO_4$, 0.63 H_2SO_4; and 0.3 x 10^{-3} Cl^-. The gelatin was metered in at a rate of up to 1 x 10^{-3}. The electrolyte was kept at a temperature of 309.5 K, and a cathode current density of 2,500 A/m^2 was used. Foil samples were subjected to tests on a type TsT-4-40 tensile testing machine, and segments of foil with different thicknesses were subjected to x-ray crystallographic analysis on a URS-2.0. Roentgenograms were also taken and processed on an MD-100 microdensitometer. The studies established an obvious link between the ultimate breaking strength and porosity of foil and thickness. This link is due largely to a decrease in porosity, i.e., to the formation of a more monolithic layer of foil all the way to thicknesses of 17-20 μm. Beginning at $h \geq 21$ μm, pores become sparse. At $h \geq 29$ μm, the number of pores decreases practically to 0. It turned out to be extremely difficult to produce pore-free foil less than 25-30 μm thick on a titanium cathode without additional surface treatment (such as mechanical polishing) because of the polycrystalline structure of the cathode. Another way of reducing the porosity of the cathode precipitate was to use anodically oxidized titanium. Foil produced on an oxidized titanium surface manifested a less sharp increase in ultimate rupture strength as the thickness of the precipitated layer increased. The studies thus established that when producing thin electrolytic foil, it is advisable to use amorphous or nearly amorphous materials, especially anodically oxidized titanium, as the cathode base. Figures 2; references 6: Russian.

Determining the Optimum Shape of the Working Space of an Aluminum Electrolysis Bath

937D0069D Moscow TSVETNYYE METALLY in Russian No 10, Oct 92 pp 28-31

[Article by Ya.Zh. Freyberg, Ye.I. Shilova, and E.V. Shcherbinin, Physics Institute, Latvia Academy of Sciences; UDC 669.713.7]

[Abstract] The effect that the shape of the working space of an aluminum electrolysis bath has on the static skew of the heel of metal was examined. A mathematical model was developed that gave consideration to the magnetic forces in an electrolysis bath that result from the interaction of the vertical component of the magnetic induction vector (B_z) and horizontal components of current density (j_y). A numerical experiment was then conducted to determined the effects of the skull size and shape on the operation of an aluminum electrolyzer. The PIAP software package for calculating electromagnetic and hydrodynamic fields and current efficiency was adapted for use on IBM PC AT-type computers. Four shapes of hearth skull were studied: no hearth skull ($\delta = 0$); a skull with a width equal to half the side-to-anode distance ($\delta = 0.15$ m); a skull with a width equal to the side-to-anode distance ($\delta = 0.3$ m); and a skull with a width of about 2 side-to-anode distances ($\delta = 0.53$ m). No dependence of the nature of the electrolyte flow on skull dimensions was visually evident; however, the integral value of the electrolyte flow rate changed somewhat as δ increased. The maximum electrolyte flow rate increased, whereas the mean square flow rate (within the confines of skull shapes 1 through 3) decreased somewhat. A clear dependence of the integral characteristics of the internal field on skull shape was discovered in the cases of skull shapes 1 (no skull) and 4 (the elongated skull). The highest current efficiency (89 percent) was found in the case of

skull shape 4 (versus 82.43 percent in the case of skull shape 1). The studies thus confirmed the hypothesis that the shape of the working space of an electrolysis bath is optimal when the size of the hearth skull equals the side-to-anode distance. The skew of the metal-electrolyte surface in electrolyzers with the current supply design examined is decreased thanks to a decrease in j_y and, consequently, the specified value of B_z. Another way of reducing j_y is to optimize the shape of the electrolysis bath's working surface. Another possible way of reducing the skew of the heel of metal in an electrolysis bath is to place discrete non-current-conducting zones along the lengthwise sides of the bath so as to periodically change the direction of j_y in the melt and the lengthwise skew of the interface surface (in turn reducing the resultant amplitude of lengthwise skew). Figures 4; references 2: Russian.

Processing Hard-To-Concentrate Low-Grade Tungsten Raw Material To Produce an Iron-Tungsten Alloy

937D0069H Moscow TSVETNYYE METALLY in Russian No 10, Oct 92 pp 42-46

[Article by V.I. Maslov and N.I. Kopylov; UDC 553.463:669.275.669.11/15]

[Abstract] A series of large-scale laboratory experiments and pilot-commercial tests was conducted to develop a process for direct recovery of tungsten from poor intermediate products to produce an iron-tungsten alloy. The experiments were performed in a 50-kW two-electrode furnace with 100-mm-diameter electrodes. Sodium sulfate containing 70 percent Na_2SO_4 and 30 percent Na_2CO_3 was used as a flux. The smelting process resulted in the formation of an iron-tungsten alloy with a tungsten content of 6.6 percent and with an extraction of 89.3 percent; 16.5 kg of alloy was produced. The alloy had a melting point that was less than the bath temperature; it was nonviscous and easily discharged from the furnace. Next, a process for direct extraction of tungsten from poor intermediate products and production of an iron-tungsten alloy was tested. The new process included reduction ore smelting of the tungsten intermediate product with sodium-containing flux at a temperature of 1,150 to 1,200°C. The intermediate product used for the tests contained the following (percent): WO_3, 2.53; Fe, 10.68; CaO, 21.28; SiO_2, 18.5; S, 12.68; F, 11.4; and moisture, 6.5. Sodium sulfate containing 34 percent Na and 21.9 percent S was used as a flux, and metallurgical coke containing 83 percent C was used as the reducing agent. The electric furnace smelting was conducted with an electrode current strength of 5,000-6,000 A, a voltage of 93-100 V, a flue gas temperature under the furnace arch of 900-1,100°C; and a rarefaction under the arch of 10-20 Pa. The amount of burden loaded was controlled as a function of fluidity and kept at a level of 1.5 metric tons/h. During the course of the tests, 20,914 kg of burden was fed in, and 11 batches of melt were produced, resulting in the following: 14,000 kg of sodium-containing melt with a content of 0.13 percent W and 8.7 percent F (with an extraction into the melt of 7 percent W and 99.6 percent F) and 1,150 kg of iron-tungsten alloy. This iron-tungsten alloy contained the following (wt.-percent): Fe, 82.40; W, 7.0; P, 6.0; C, 1.2; S, 0.39; and Si, 3.0 (extraction into the melt: W, 93 percent; and Fe, 98.8 percent). Per metric ton of burden, 646 kWh of electricity and 15 kg of electrode were required. The resultant alloy was a dark gray nonuniform material that included light gray (possibly eutectic) formations of different sizes. Coke particle inclusions were also noted in the materials formed. Each of the different phases formed was analyzed. The new process makes it possible to increase start-to-finish extraction of tungsten from ore to 76 percent. Figures 4, tables 2; references 5: 3 Russian, 2 Western.

The Adsorption of Uncontrolled Impurities on the Polished Surface of Silicon Wafers

937D0069I Moscow TSVETNYYE METALLY in Russian No 10, Oct 92 pp 48-50

[Article by A.G. Vorobyev, L.Ye. Loskutov, A.V. Aleksakhin, B.F. Bogatikov, and M.N. Volkov, Moscow Institute of Steel and Alloys; UDC 543.53:546.27]

[Abstract] The neutron activation method with autoradiographic termination was used to analyze the degree of adsorption of uncontrolled impurities on the polished surface of silicon wafers. This analysis method made it possible to determine a large number of impurities with a sensitivity ranging from 10^{-9} to 10^{-6} wt.- percent and with a precision of 5 to 20 percent. Silicon wafers measuring 40 mm in diameter and 1 to 1.5 mm thick were first subjected to standard polishing by using copper ions, chromium oxide, or zirconium oxide. A γ-spectrometer outfitted with a PPD-56 germanium-lithium detector and 4,000 channel analyzer was used to measure the γ-spectra of the samples after they had been irradiated with a thermal neutron flux (1.2×10^{13} n x cm^{-2}/s for 100 hours. The impurity elements in the spectra were identified from the quantum energy of radioactive isotopes formed in an n-γ-reaction during the irradiation process. The impurity concentrations of specimen silicon wafers prepared by each of the three different polishing methods were determined. Of all of the impurities present in the different reagents used, Cu, Au, and Fe were mainly absorbed. The appearance of Cr and Na was also observed. Other impurities such as Pb and Mn, while present in the reagents, are not adsorbed by the wafer surfaces. Two groups of elements were identified to be present in the specimens: 1) slowly diffusing elements located in a thin, near-surface layer and 2) quickly diffusing elements (Na, Cu, Au). The elements belonging to the first group may be eliminated by etching 5 μm of the surface; however, the elements of the second group are not as easily removed. It was determined that Cr, W, Zr, Cu, and Au get into the silicon when the wafers are polished; the Fe comes from the chemical reagents as well as from the polishing agents, and the Na comes from the wafers as a result of the manufacturing process used. Figure 1, tables 3.

The Use of Ultradisperse Powders of Chemical Compounds When Casting Ingots of Aluminum and Forming-Quality Aluminum Alloys

937D0069J Moscow TSVETNYYE METALLY in Russian No 10, Oct 92 pp 56-58

[Article by T.N. Krushenko, T.N. Miller, M.N. Filkov, B.A. Balashov, and Z.A. Vasilenko, Computer Center, Siberian Department, Russian Academy of Sciences; UDC 669.715:621.74]

[Abstract] A study examined the use of ultradisperse powders to produce aluminum and forming-quality aluminum alloys with finer structures. The term "ultradisperse powder" refers to intermediate phases characterized by a high melting point (about 2,273 to 3,273 K depending on their composition) and a small particle size (4 to 80 nm). Existing methods of adding modifying powders to a melt cannot be used with plasma-chemical ultradisperse powders because they are easily compacted, oxidize at comparatively low temperatures, and form dustlike suspensions in air despite their density. A new method of manufacturing modifying rods was therefore developed. The surface of the aluminum particles was clad with particles of ultradisperse powder. The said composition was poured into a thin-walled aluminum container measuring 165 mm in diameter, subjected to the required temperature, and pressed into rods of different diameter on hydraulic presses. The work was performed under metallurgy and aluminum plant conditions. The modifying rods studied were pressed from D16 alloy and different ultradisperse powders. The effectiveness of the new modifying technique was confirmed in tests in which the modifying rod was added to the alloy AMg6 cast into 420-mm-diameter ingots by the semicontinuous method. The average grain size of ingots cast according to the standard series production process (modification with an Al-Ti foundry alloy) is 0.322 m^2. When SiC ultradisperse powder was added by the new process, the average grain size decreased to 0.123 mm^2 (a factor of 2.6). The addition of a BN ultradisperse powder resulted in a decrease in the average grain size to 0.146 mm^2 (a factor of 2.2), and the addition of a TaN ultradisperse powder resulted in a decrease in grain size to 0.078 mm^2 (a factor of 4.1). Studies of the effect of modification by ultradisperse powders of the alloys D16 and D1 on the mechanical properties of shaped sections pressed from aluminum and forming-quality aluminum alloy ingots confirmed that the new technique of adding ultradisperse powders (whether TaN, SiC, or BN powders are used) results in stronger products than the currently existing technique does. What has been termed "induced" activity evidently occurs when rods of ultradisperse powders ar used to modify aluminum and forming-quality aluminum alloys. This "induced" activity results from two phenomena: 1) the contact between the powder particles and the aluminum particles during the pressing process and 2) the formation of a layer of aluminum on the powder particles that then serves as a substrate for crystallization. Figures 2, table 1; references 4: Russian.

The Effect of the Conditions of Pouring Cadmium Bronze on Ingot Structure

937D0069L Moscow TSVETNYYE METALLY in Russian No 10, Oct 92 pp 60-62

[Article by R.K. Mysik, Yu.P. Poruchikov, S.N. Chukhlantsev, V.N. Rudnev, and I.A. Vays, Ural Polytechnic Institute imeni S.M. Kirov, and Kamensk-Ural Plant OTsM; UDC 621.746.62.047:669.735]

[Abstract] A series of laboratory and industrial tests were conducted to determine the effect of the conditions of pouring cadmium bronze on the structure of the resultant ingots. Specifically, the studies were designed to determine the effect that the temperature at which the alloy is poured into the ingot mold, the heat-accumulating capacity of the mold, and the alloying method used have on ingot structure formation. Under laboratory conditions, cadmium bronze ingots were cast in steel, copper, and fireclay ingot molds measuring 30 x 30 x 150 mm. Casting temperatures of 1,150, 1,130, and 1,100°C were used. When a casting temperature of 1,130°C was used, cooling of the cadmium bronze alloy was fastest in the copper molds and slowest in the fireclay molds. The use of ingot molds with different heat storage capabilities was reflected in the structure and properties of the ingots formed. Metallographic studies and other tests were performed to determine the mechanical properties of samples cut from the ingots. The formation of structural zones in the ingots was found to be dictated mainly by the intensity with which the molten alloy cooled and by the temperature gradient in the melt. The macrostructure of the ingots cast in the steel and copper molds was characterized by the presence of all three zones: a surface zone of fine crystals, a zone of columnar crystals, and a central zone of equiaxial crystals. The columnar crystals of the ingots cast in the steel molds were five to six times shorter than those of the ingots cast in the copper molds. The crystals formed in the two types of molds had respective grain sizes of 0.720 and 0.684 mm and dendrite cell sizes of 1.96 and 1.40 μm. The ingots cast in the fireclay molds did not have any zone of columnar crystals at all, and their grains were much larger. The higher the rate at which the melts were poured, the quicker they cooled. The ingots cast at 1,150°C had a zone of columnar crystals, and in a narrow bottom part of the ingot there was a pronounced transcrystallization. As the casting temperature was decreased to 1,100°C, the zone of columnar crystals decreased significantly and was completely absent in the upper broad portion of the ingot. Such a structure may be produced by continuous casting with late alloying. Three different methods of alloying the copper with cadmium were studied: two conventional methods (i.e., alloying the copper melt in the melting furnace with pieces of 1) pure cadmium or 2) Cu-Cd foundry alloy) and one new method (i.e., late alloying of the copper melt in the continuous casting mold with a bimetal wire consisting of a copper sheathing and cadmium core). Cadmium loss was cut in half when the bimetal wire was used, thus eliminating the release of toxic cadmium vapors when the alloy was poured from the melting furnace into the mixer. A series of commercial tests was then conducted on ingots with a cross section of 100 x 100. The use of the new process of adding the alloy-forming component in the form of a bimetallic wire made it possible to conduct the alloying process at lower temperatures. The grain size of alloys produced in that manner was also smaller (0.37 mm in the case of the bimetallic wire versus 1.39 mm when pure cadmium was used and 1.02 mm when the Cu-Cd foundry alloy was used). Figures 3, table 1.

Plasma Synthesis of Oxides in the System Y-Ba-Cu-O

937D0070A Kiev POROSHKOVAYA METALLURGIYA in Russian No 10, Oct 92 pp 7-10

[Article by O. M. Grebtsova, Ye. P. Domashneva, Ye. N. Kurkin, and A. A. Budanov, Institute of New Chemical Problems, Russian Academy of Sciences, Chernogolovka; UDC 621.762:533.92:537.312.62]

[Abstract] Decomposition of nitrate and oxalate mixtures of yttrium, barium and copper in microwave-generated oxygen plasma was investigated. Physicochemical analysis established that the synthesis products are ultradispersed powders with an average particle size of less than 0.1 μ and consisting of several phases. It is possible to obtain a superconducting phase $YBa_2Cu_3O_{7-x}$ with $T_c \approx 99$ K only after heat treatment of plasma powder compacts in an

oxygen jet. The lower temperature limit for formation of the superconductive phase was found to be 850° C.

Effect of Fraction Composition of Charge on Sintering of High-Speed Steel Powder

937D0070B Kiev POROSHKOVAYA METALLURGIYA in Russian No 10, Oct 92 pp 15-20

[Article by G. A. Baglyuk, S. N. Kaplya, L. A. Poznyak, and O. Yu. Kononenko, Institute of Materials Science Problems, Ukrainian Academy of Sciences, Kiev; UDC 621.762]

[Abstract] The fraction composition of gas-atomized R6M5K5 high-speed steel powder was investigated for its effect on regularities of activated sintering of billets which undergo subsequent hot plastic working. An activator was used which consisted of nickel powder and 30 wt. percent boron. It was found that as average particle size decreases, shrinkage after sintering increases, but the dependence of the shrinkage of compacts on the fraction composition differs in character for monodispersed and polydispersed compositions. While maximum particle size of powder in polydispersed compositions does not have a significant effect on shrinkage, in the case of monodispersed mixtures there is a pronounced increase in the density of compacts after sintering as particle size decreases. At a sintering temperature of 1200° C, there is a significant increase in density yielding a closed porosity (90-93 percent); to achieve such a density in a mixture that does not contain an activator, a temperature of at least 1230° C is necessary.

Laser Treatment of Plasma-Sprayed Coatings on Powder Steel

937D0070C Kiev POROSHKOVAYA METALLURGIYA in Russian No 10, Oct 92 pp 25-28

[Article by V. N. Antsiferov, A. M. Shmakov, and N. N. Ivshina, Research Institute of Powder Technology and Coatings, Perm; UDC 621.762:621.793.7:621.375.862]

[Abstract] Results are presented of studies of the structure and phase and chemical compositions of coatings sprayed with plasma onto powder steel and treated with a high-power CO_2 laser. Comparative analysis is made of the coatings' homogenization conditions, and the nature of crack formation in their surface layers is investigated. Characteristics of the composites' structure formation in the course of laser thermal modification are established. The alternative effect of the energy contribution on the set of physicomechanical properties and tribotechnical characteristics of the materials is demonstrated.

Thermodynamic Properties of Vanadium Monoboride in the Temperature Range 150-2300 K

937D0070D Kiev POROSHKOVAYA METALLURGIYA in Russian No 10, Oct 92 pp 29-31

[Article by A. V. Blinder, A. S. Bolgar, and V. R. Sidorko, Institute of Materials Science Problems, Ukrainian Academy of Sciences, Kiev; UDC 536.722+546.271]

[Abstract] Heat capacity and enthalpy of vanadium monoboride in a wide range of temperatures were investigated for the first time. Parameters are calculated for temperature dependences of heat capacity, entropy, enthalpy, and reduced Gibbs free energy. Comparison of the obtained results with previously published data makes it possible to estimate the coefficient of thermal expansion of vanadium monoboride.

Regularities of Low-Temperature Synthesis of Tungsten Carbide and WC-Co Mixture in Methane-Hydrogen Gas

937D0070E Kiev POROSHKOVAYA METALLURGIYA in Russian No 10, Oct 92 pp 31-35

[Article by A. S. Petukhov, I. V. Uvarova, V. P. Bondarenko, E. G. Pavlotskaya, L. M. Martynova, L. D. Konchakovskaya, and T. N. Kosenko, Institute of Materials Science Problems and Institute of Superhard Materials, Ukrainian Academy of Sciences, Kiev; UDC 621.762]

[Abstract] Regularities of low-temperature (to 900° C) carbidization of tungsten and tungsten-cobalt powders of different degrees of dispersion in methane-hydrogen gas were investigated. It was found that in carbidization in a H_2+CH_4 gas medium, to obtain a dispersed mixture of WC-Co, tungsten or tungsten-cobalt powders with a specific surface of at least 2-3 m^2/g and 4.5 m^2/g, respectively, should be used. Cobalt, which promotes carbidization of tungsten, has a negative effect on dispersion of products when carbidization takes place in a methane-hydrogen medium.

Thermophysical Properties of Iron-Copper Pseudoalloy

937D0070F Kiev POROSHKOVAYA METALLURGIYA in Russian No 10, Oct 92 pp 38-42

[Article by S. V. Demidkov, L. N. Dyachkova, Ye. V. Zvonarev, I. I. Krasnyakov, A. Kh. Nasybullin, and B. M. Khusid, Belarus Republic Powder Metallurgy Scientific and Production Association, Minsk, and Institute of Heat and Mass Transfer, Belarus Republic Academy of Sciences, Minsk; UDC 536.21]

[Abstract] A thermophysical model of Fe-Cu pseudoalloy is constructed which permits determination of the alloy's thermal and temperature conductivity both before and after deformation. Formulas for the thermal and temperature conductivity have an analytical form and permit a fast estimation of thermophysical parameters of the composite, which is important for the designing of products made from it.

Effect of Graphite Content on Structure and Properties of Bronze-Graphite Materials

937D0070G Kiev POROSHKOVAYA METALLURGIYA in Russian No 10, Oct 92 pp 47-51

[Article by L. V. Zabolotnyy, N. G. Baranov, V. S. Ageyeva, A. I. Ilnitskaya, V. S. Mokrovetskaya, and Ye. A. Ganusets, Institute of Materials Science Problems, Ukrainian Academy of Sciences, Kiev; UDC 621.891]

[Abstract] Graphite content in antifriction bronze-graphite powder material made by double compaction and sintering was investigated for its effect on the material's structure and mechanical and tribotechnical properties was. It was found that at a graphite content of 7-9 percent

and sliding rates of 11 and 22 m/s bronze-graphite possesses a low (0.07-0.1) friction coefficient and a negligible wear intensity (3-6 μm/km). The material can be recommended for practical application in high-speed friction assemblies.

Hydrogen Sorption Properties of $LaNi_4Al$ Powder With Different Particle Surface States

937D0070H Kiev POROSHKOVAYA METALLURGIYA in Russian No 10, Oct 92 pp 56-61

[Article by M. M. Antonova, L. L. Kolomiyets, T. V. Khomko, Yu. N. Ivashchenko, and A. A. Malyshenko, Institute of Materials Science Problems, Ukrainian Academy of Sciences, Kiev; UDC 539.21:669.01:548]

[Abstract] Long-term (up to 7 months) exposure to air of powders of the electron compound $LaNi_4Al$ with different grain sizes was studied for the exposure time's effect on hydrogen capacity, rates of hydrogen sorption and desorption, and the level of equilibrium pressure of the system $LaNi_4Al$-H_2 in the region of plateau pressures. It was demonstrated that long-term exposure to air affects the hydrogen capacity of electron compound powders with different grain sizes in different ways: in fine-grain powders the effect is decreased by almost two times, in coarse-grain powders the effect increases, and in powders with grain size of 40-80 μm the effect is practically unchanged. The electron compound's hydrogen sorption rate depends largely on H_2 temperature and pressure, and is hardly affected by exposure time to air. When powders are exposed to air, the level of equilibrium plateau pressure moves to higher values.

Microstructure of Shock-Compacted Polycrystalline Aluminum Nitride

937D0070I Kiev POROSHKOVAYA METALLURGIYA in Russian No 10, Oct 92 pp 65-69

[Article by G. S. Oleynik, V. V. Yarosh, O. A. Shevchenko, and D. Z. Yurchenko, Institute of Materials Science Problems, Ukrainian Academy of Sciences, Kiev; UDC 669.018.45:539.5]

[Abstract] Shock-wave treatment of aluminum nitride powders produced compacted specimens with a density of 0.93-0.94 of the theoretical density. Examination of their microstructure by transmission electron microscopy of thin foils showed that polycrystalline AlN in such conditions is formed as a result of structural transformations which are characteristic for sintering of AlN at high temperatures and static compression pressures, in particular: plastic deformation, relaxation dislocation rearrangements, and primary and collective recrystallization. Plastic deformation of AlN is accomplished by full basal dislocations, which determines both the absence of deformation polytypism in it and the transition to a sphalerite modification.

Mold for Compacting Articles Made of Powders

937D0070J Kiev POROSHKOVAYA METALLURGIYA in Russian No 10, Oct 92 pp 70-71

[Article by K. A. Gogayev, V. A. Shtakun, and V. G. Bondar, Institute of Materials Science Problems, Ukrainian Academy of Sciences, Kiev; UDC 621.762]

[Abstract] A design of a multipurpose mold for compacting low-plastic, hard-to-deform powders is presented. The mold has a moveable die which permits both static and bilateral static-dynamic compaction. The mold's operational efficiency can be evaluated using diagrams of the dependence of articles' density on the powder compaction force and method.

Cold Forming of Long Rods Made of $YBa_2Cu_3O_{7-x}$ Powder

937D0070K Kiev POROSHKOVAYA METALLURGIYA in Russian No 10, Oct 92 pp 72-75

[Article by A. V. Stepanenko, L. A. Isayevich, A. A. Veremeychik, and Ye. V. Lyakhovets, Belarus Polytechnical Institute, Minsk; UDC 621.762]

[Abstract] The character of compaction of the superconductive powder $YBa_2Cu_3O_{7-x}$ under conditions of unilateral and hydrostatic compaction was investigated. The existence of a threshold density was established. Methods for periodic forming of long rods made of the high-temperature superconductive powder were developed.

Carbide Steels Based on Titanium Carbide From Titanium Alloy Shavings

937D0070L Kiev POROSHKOVAYA METALLURGIYA in Russian No 10, Oct 92 pp 78-82

[Article by Yu. V. Levinskiy, Ya. P. Kyubarsepp, and A. P. Petrov, Moscow Institute of Precision Chemical Engineering; UDC 621.762]

[Abstract] Properties and microstructure of carbide steels made with alloyed titanium carbide were investigated. TiC powder was obtained from shavings from the titanium alloys VT1-0, VT20, VT3-1, VT25, VT5-1 and OT4-1 using three techniques: nitriding-carbidization, binary carbidization, and oxidation-carbidization. It was found that the presence of even comparatively small amounts of nitrogen in titanium carbide has a negative effect on the properties of carbide steels. It was found that strength and hardness are high when the techniques of oxidation-carbidization and binary carbidization of shavings of alloy VT5-1 are used, indicating that it is advisable to use them for making carbide steels.

High-Strength Glassy Alloys Hardened With Carbide

937D0071A Moscow METALLOVEDENIYE I TERMICHESKAYA OBRABOTKA METALLOV in Russian No 9, Sep 92 pp 3-5

[Article by A. M. Glezer, Yu. Ye. Chicherin, V. I. Shvarts, and S. V. Shalin, Central Research Institute of Ferrous Metallurgy im. I. P. Bardin and All-Union Steel Research Institute; UDC 669.018.5:539.213.27]

[Abstract] The structure and mechanical properties of glassy Fe-Cr-B alloys containing crystalline WC particles were investigated. A mixed glassy-crystalline state was obtained directly during quenching of melts by alloying with carbides. For the study, alloys of the systems Fe-Co-Cr-B and Fe-W(Zr)-C- Cr-B were melted, and tapes in the glassy state were made of them. Alloys containing 1-3

percent Zr and 3 percent W were excluded from further study, as they turned out to be brittle.

It was found that a glassy alloy of Fe-15 percent Cr-15 percent B possesses the highest strength and thermal stability. It was demonstrated that an optimum (up to 2 percent) equiatomic amount of W and C added to this alloy results in WC particles forming in the glassy matrix, which substantially raises the Young's modulus and the yield point of the alloy without lowering its ductility and thermal stability. On the basis of the research, a carbide-hardened glassy alloy 15KhUVR was developed which possesses an ultimate strength of 3500 N/mm^2.

Ways of Making AMAG Magnetically Soft Glassy Alloys, Their Properties and Application

937D0071B Moscow METALLOVEDENIYE I TERMICHESKAYA OBRABOTKA METALLOV in Russian No 9, Sep 92 pp 5-8

[Article by V. S. Chernov, A. S. Yevteyev, V. A. Tatarinov, O. G. Ivanov, and F. Ye. Pashchenko, Research Institute of Materials for Electronic Equipment, Kaluga; UDC 669.25'15:539.213:621.318.13]

[Abstract] The technique for making glassy alloys in the form of ribbon by spinning off a melt was analyzed for the controllability of the process. Three variants of the process were discerned depending on the size of the gap between the discharge nozzle and the rotating disk, and on this gap's correlation with the width of the nozzle. The optimum variant was found to be in the system nozzle-gap-disk; it is the gap that is the "bottleneck" for the movement of the melt, and the melt pool between the nozzle and the disk is movable only in the direction of movement of the disk. It is in this variant that the process was found to be most stable and controllable.

The process was used to make ribbon from magnetically soft glassy alloys that have the general name AMAG (systems Co-Fe-Si-B, Co- Fe-Ni-Si-B, Fe-Ni-Si-B), and magnetic properties of the product after different types of heat treatment and treatment with a magnetic field were ascertained.

Low-Temperature Structural Relaxation of FeBSiC Glassy Alloys

937D0071D Moscow METALLOVEDENIYE I TERMICHESKAYA OBRABOTKA METALLOV in Russian No 9, Sep 92 pp 11-12

[Article by Yu. N. Starodubtsev, V. A. Katayev, and Yu. V. Matveyev, Verkh-Isetsk Metallurgical Plant; UDC 669.1'781'782'784.5:539.213:620.186.5]

[Abstract] The effect of Si, B, and C content (in atomic fractions) on magnetic induction, solidification temperature and structural relaxation of glassy alloys of the FeBSiC type was investigated. Contents of metalloids in specimens studied were in the ranges: 3.5-4.5 percent Si, 1.2-2.2 percent C, 9-14 percent B. Magnetic induction was measured in strip specimens 10 mm wide and 110 mm long after annealing at 370° C for 45 minutes without a magnetic field. Solidification temperature was determined by differential thermal analysis, and structural relaxation was evaluated according to residual deformation. It was found that the lower the total content of metalloids in the alloy, the higher the residual deformation of specimens. In the indicated range of metalloid contents, magnetic induction in a field of 100 A/m was found to fluctuate significantly and to vary in a linear fashion. Solidification temperature decreased in a linear fashion with a lower content of metalloids, the dependence being due to destabilization of the alloy's amorphous structure. Such processes intensify low-temperature structural relaxation of the FeBSiC alloy immediately after casting.

Magnetoelastic Properties of Amorphous Materials and Transducers Based on Them

937D0071F Moscow METALLOVEDENIYE I TERMICHESKAYA OBRABOTKA METALLOV in Russian No 9, Sep 92 pp 16-18

[Article by A. Ye. Yermakov, M. D. Avramenko, M. V. Shevchenko, A. I. Pyatygin, and Yu. N. Starodubtsev, Institute of Physics of Metals, Urals Branch, Russian Academy of Sciences, and Verkh-Isetsk Metallurgical Plant; UDC 669.018.5:539.213.27]

[Abstract] Magnetic and magnetoelastic characteristics of five Fe-based magnetically soft glassy alloys containing B, Si, C, Ni and Co were investigated. Tests were done on doughnut-shaped specimens of different sizes which were annealed at 325-400° C in a transverse magnetic field with a strength of 11,000-23,500 A/m. Studies focused on the dependence of magnetic and magnetoelastic properties on annealing temperature and the strength of the constant polarizing field, frequency dependences of magnetic losses at different levels of strength of the polarizing field, and the possibility of using these glassy alloys as compressive force transducers, emitters, and ultrasound sensors.

It was demonstrated that magnetically soft amorphous materials can be used as various transducers and electroacoustic emitters in place of traditional magnetostriction materials. Such materials can be used in transducers operating at high frequencies (up to 200 kHz).

Morphological and Performance Characteristics of Silicon Nitride Powder Produced by Method of Self-Propagating High-Temperature Synthesis

937D0090A Kiev POROSHKOVAYA METALLURGIYA in Russian No 11 (359), Nov 92 pp 16-21

[Article by S.Yu. Sharivker, I.P. Borovinskaya, G.A. Vishnyakova, Yu.N. Barinov, A.S. Mukasyan, A.M. Knyazik, Structural Macrokinetics Institute at Russia's Academy of Sciences, Chernogolovka; UDC 621.762+546.28.17]

[Abstract] Extensive pilot production of α- and β-modifications of silicon nitride by self-propagating high-temperature synthesis (SVS) and the lack of data on this material's performance which constraints its commercial applications prompted an investigation into the behavior of the α-silicon nitride powder (TU 88-1-143—88)—produced by the SHS method at the Structural Macrokinetics Institute at Russia's Academy of Sciences—under cold compaction and sintering and the correlation between the character of compaction under these processes and the morphology of the powder particles. The sample

preparation procedure by planetary and ball mill grinding is outlined, and the structure of the silicon nitride powder produced by the SHS method is shown. The statistical distribution of the powder particle size, cumulative size curves of four types of powder, the effect of the compaction pressure on the sample density, the effect of the process temperature on the volume shrinkage, density, and loss of mass under single- and double-stage sintering, and the effect of the factors which characterize the powder morphology on the relative bulk density and shrinkage during sintering of SHS silicon nitride are plotted. An analysis shows that there is no one-to-one correspondence between individual morphological powder characteristics and the powder behavior under compaction and sintering. The effect of the fraction ratio and form factor on the powder's bulk density and packing is discussed. It is noted that the grinding and milling processes must be optimized in order to improve the sintering ability of SHS Si_3N_4 powders. The best shrinkage during sintering should be expected in a close-to-spherical isotropic powder with a broad range of particle sizes due to the presence of submicrometer fractions. Figures 6; tables 2; references 3: 2 Russian, 1 Western.

Sintered Mg_2N Intermetallic Compound as Hydrogen Accumulator. II. Effect of Impurities on Hydrogen Sorption Properties of Intermetallic Compound

937D0090B Kiev POROSHKOVAYA METALLURGIYA in Russian No 11 (359), Nov 92 pp 44-46

[Article by M.M. Antonova, T.V. Khomko, O.T. Khorpyakov, Institute of Materials Science Problems at the Ukrainian Academy of Sciences, Kiev; UDC 621.762.4+669.01:669.721:669.21:669.788]

[Abstract] A study which suggested that the hydrogen absorption capacity of the Mg_2Ni intermetallic compound depends on the original metal purity (*Poroshkovaya metallurgiya* No. 9, 1992) is continued. In so doing, the sorption abilities of the materials sintered from commercial Mg and Ni powders of varying purity and size in a Mg:Ni=2:1 ratio are compared. Purified hydrogen is used as the shielding gas since the structure of the material sintered under such conditions is favorable for rapid hydrogen sorption and desorption. The characteristics of the initial powders and samples sintered from them and the sorption properties of the sintered intermetallic compound produced from powders of varying purity are summarized. The findings indicate that in producing Mg_2Ni intended for hydrogen accumulation, one should be guided by the specific application features. If the hydrogen capacity must be maximized, the purest and smallest powders of MPF-2 magnesium and carbonyl nickel should be used; if the hydrogen capacity is unimportant, the material should be sintered from coarser and less pure powders. Tables 3; references 3: 2 Russian, 1 Western.

Production of Cast Higher Chromium Carbide by Method of Self-Propagating High-Temperature Synthesis

937D0090C Kiev POROSHKOVAYA METALLURGIYA in Russian No 11 (359), Nov 92 pp 57-60

[Article by V.A. Gorshkov, G.N. Komratov, V.I. Yukhvid, Structural Macrokinetics Institute at Russia's Academy of Sciences and Branch of the Chemical Physics Institute at Russia's Academy of Sciences, Chernogolovka; UDC 546]

[Abstract] The requirement that the initial charge combustion temperature exceed the melting point of the combustion products necessary for producing inorganic refractory compounds by self-propagating high-temperature synthesis and the patterns of SHS in cast Cr_3C_2 higher chromium carbide are discussed. It is noted that by optimizing the initial charge composition, one can synthesize a higher carbide with 1.5-3 percent Al which can be then reduced to 0.2 percent by acid treatment. The synthesis conditions are described. The effect of the aluminum concentration in the initial mixture on the phase separation and chemical content of the product and the effect of the acid solution on the fraction and chemical composition of the cast carbide are plotted. The findings of the chemical and X-ray phase and diffraction analyses of the carbide are summarized. The results demonstrate that by manipulating the Al concentration in the original charge, one can control its content in the final product within a broad range and produce a virtually single-phase high carbide which can be then purified in hydrochloric acid; this removes the Al impurity while the cast product disperses into individual grains. Figures 3; tables 1; references 5.

Chemical Reaction Initiation Under Shock Wave Compression of Liquid Explosives Containing Glass Microspheres

937D0092D Moscow KHIMICHESKAYA FIZIKA in Russian Vol 11 No 11, Nov 92 pp 1588-1600

[Article by B.A. Khasainov, B.S. Yermolayev, Chemical Physics Institute imeni N.N. Semenov at Russia's Academy of Sciences, Moscow; UDC 533.6.011.72]

[Abstract] The use of commercial water-emulsion explosives (VV) sensitized by glass microspheres (MS) is discussed, and the lack of published data on the shock wave sensitivity of such explosives is noted. As a result, an attempt is made theoretically to analyze the sensitizing effect of the glass microspheres during the compression of liquid explosives by shock waves using a viscoplastic model. The use of the model is justified by the fact that under standard conditions, glass has a very high viscosity which, however, rapidly decreases with an increase in the medium temperature. The model is described and the findings obtained for a model explosive, i.e., nitromethane thickened with a small amount polymethyl methacrylate (PMMA), are presented. The principal properties of the materials used in the analysis are summarized, and the effect of the microsphere diameter, viscosity, and other parameters is examined. The temperature distribution in the effective model cell, the temperature behavior on the nitromethane/microsphere interface, the dependence of the ignition delay on the pressure amplitude at various MS parameters and shock wave amplitude, and the behavior of the microsphere and cavity temperature at a given glass viscosity are plotted. For the explosive under study, the sensitizing effect is determined by the ratio of the MS arc to its diameter, the mass fraction of MS, and the initiating pulse duration if it is shorter than the standard ignition delay. The authors are grateful to Dr. H.N. Presles (France) and Dr. P.A. Taylor (United States) for interest in the effort and constructive remarks. Figures 5; tables 5; references 12: 3 Russian, 9 Western.

Selecting Irradiation Conditions of W-Co Hard Alloy Laser Machining

937D0042D Kiev SVERKHTVERDYYE MATERIALY in Russian No 5(80), Sep-Oct 92 pp 22-27

[Article by S.I. Yaresko, A.A. Aleksandrovich, N.P. Ilyukhina, T.K. Kobeleva, Samara Branch of the Physics Institute at Russia's Academy of Sciences; UDC 621.373.826:621.78+669.018.25]

[Abstract] Laser pulse machining of hard alloys and the formation of wear resistant structures in the laser heat affected zones (ZLV) which can be subsequently used for a finishing hardening operation without violating the surface layer integrity are discussed, and it is noted that the issue of the criteria for proximate selection of the laser irradiation conditions remains unresolved. An attempt is made to develop and justify the criterion for proximate selection of the W-Co hard alloy laser machining conditions in the tool hardening operation. The micro- and macrostress redistribution in the hard alloy ZLV under irradiation is outlined. The dependence of the energy density limits corresponding to the appearance of incipient visible cracks on the irradiation ratio in VK6, VK6M, and VK20 alloys, diffraction patterns of VK6 samples in the initial state and after single and multiple exposures, the dependence of the energy density limits corresponding to the appearance of visible incipient cracks on the exposure ratio during machining of the VK6 and VK8 alloys, and the surface cracking probability as a function of the energy density in the VK6 alloy are plotted. Based on the findings, a laser treatment selection criterion is proposed whereby the values of energy density and exposure ratio at which the first microcracks appear in the ZLV are found; then the energy density is lowered by 20-25 percent. Figures 4; tables 1; references 7.

Effect of Subcritical Temperature Tempering on Failure Strength of Structural Medium Carbon Steel

937D0063A Moscow METALLOVEDENIYE I TERMICHESKAYA OBRABOTKA METALLOV in Russian No 8, Aug 92 pp 10-13

[Article by A. P. Gulyayev, V. N. Zikeyev, Yu. V. Kornyushchenkova, and S. V. Zemskiy, Central Research Institute of Ferrous Metallurgy im. I. P. Bardin; UDC 669.14.018.298:621:785.796]

[Abstract] The possibility of raising the resistance of 30KhMA alloy pipe steel to hydrogen sulfide cracking by forming a fine subgrain structure in the process of heat treatment in the subcritical ($<Ac_1$) temperature range was investigated. Objects of study were carbon diffusion, fine structure of the matrix, and resistance to brittle failure and hydrogen sulfide cracking. The effect of diffusion mobility of carbon atoms in the course of tempering of 30KhMA steel in the subcritical range was confirmed, as was the positive effect of such treatment on the steel's resistance to hydrogen sulfide cracking. It was demonstrated that the effect of diffusion mobility of carbon atoms in the subcritical range during tempering can be used to obtain a higher failure strength than with ordinary martempering. The improved properties that are achieved are due to finely divided grain (to No. 14) and subgrain (to d_c = 0.25 μm) structures and to more complete globularization of carbide particles and their uniform distribution.

High-Strength Structural Shapes With Structural Anisotropy

937D0063B Moscow METALLOVEDENIYE I TERMICHESKAYA OBRABOTKA METALLOV in Russian No 8, Aug 92 pp 13-17

[Article by P. D. Odesskiy and V. T. Chernenko, Institute of Ferrous Metallurgy, Dnepropetrovsk, and Central Research Institute of Construction Structures; UDC 621.771.09]

[Abstract] Properties of high-strength structural shapes for construction structures were investigated. The effect of structural anisotropy on performance properties of St3ps steel shapes hardened from the rolling heat in a high-speed mill was examined. It was determined that it is possible to produce high- strength structural shapes (σ_T = 400-600 N/mm^2) with structural anisotropy of properties. The presence of structural anisotropy of properties contributes to high performance and technological properties, primarily to high resistance to cold and good weldability of structural shapes. Shapes with such properties can be made from inexpensive steels of ordinary quality, for example, from semikilled low-carbon steel of the type St3ps. This rolled product is recommended for structures used in especially harsh environments, particularly lightweight structures in northern regions.

Properties of Welded Rotor Element Made of 25Kh2NMFA Steel After Final Heat Treatment

937D0063C Moscow METALLOVEDENIYE I TERMICHESKAYA OBRABOTKA METALLOV in Russian No 8, Aug 92 pp 18-20

[Article by V. S. Sheyko, T. G. Cherednichenko, and A. V. Kovalchenko, "Energomashspetsstal" Plant, Kramatorsk; UDC 621.14.018.298:621.125.62-251]

[Abstract] Results are presented of a study of the quality of metal in the large welded rotor element—the stem—of the K- 1000-60/1500-2 low-speed turbine. The stem is made from a 131- ton ingot with a central channel intended for removing the most defective metal from the central zone of the ingot and improving the final heat treatment, which consists of hardening from 850- 870° C with water quenching, and high-temperature tempering at 640-650° C for 20 hours. Objects of analysis were the metal's macro- and microstructure, mechanical properties, critical brittle temperature, and distribution of nonmetallic inclusions. It was found that special quenching conditions in the hardening process can ensure sufficiently uniform distribution of strength properties in both cross-sections of the stem. On the whole, the quality of the stem in all characteristics was found to satisfy the specifications for elements of welded rotors of low-speed turbines.

Effect of Organic Compounds on Mechanical Properties of Material of Steam Lines

937D0063D Moscow METALLOVEDENIYE I TERMICHESKAYA OBRABOTKA METALLOV in Russian No 8, Aug 92 pp 21-23

[Article by N. N. Kotov, A. A. Savikov, and I. A. Khodashinskiy, "Tomskenergo" Heat and Electric Power Plant 3; UDC 621.186.3:620.172]

[Abstract] In connection with the problem of damage to steam lines caused by organic compounds getting into boilers together with recycled condensate in heat and electric plants of petrochemical refineries, an attempt was made to determine experimentally the effect of organic compounds on the strength of steam lines. The steam line material tested was 12KH1MF steel, and organic compounds tried were surface-active agents, phenol and glycerol. It was found that in the ferritic-pearlitic steel 12Kh1MF, which is alloyed with chromium, molybdenum and vanadium to increase the strength of the ferrite matrix, under high operating temperatures and contamination of the heat-transfer agent by organic impurities there occurs disintegration of the solid solution with formation of carbide inclusions. As a result, the strength of the ferrite matrix is decreased, and micropores form which may lead to microcracks.

A system for predicting the service life of steam lines was developed on the basis of results of the experiments and mathematical modeling. The system is a set of multipurpose algorithms and programs which can be adjusted to experimental data, and a computer models the effects of chemical compounds on mechanical properties of steel.

Structure and Properties of Metal of Centrifugally Cast Steam Pipe of Industrial Manufacture

937D0063E Moscow METALLOVEDENIYE I TERMICHESKAYA OBRABOTKA METALLOV in Russian No 8, Aug 92 pp 23-28

[Article by I. I. Mints and S. A. Zakomaldina, Urals Affiliate, All-Union Heat Engineering Research Institute; UDC 669.14.018.298:621.643.2-034.14]

[Abstract] The structure and properties of metal of large-diameter steam pipe made by the centrifugal casting method were investigated. Specimens were cut from four pipes and chips (microspecimens) were taken from 126 pipes made of 15Kh1M1FL steel. Metallographic analysis showed that the structure of the metal in centrifugally cast pipes differed not only from pipe to pipe, but in different zones of the same pipe. The structure could vary lengthwise, throughout the thickness, and around the perimeter of the pipe, from a fine-grain ferrite-carbide structure to a coarse-grain bainite structure. Nonhomogeneity in the structure of metal of centrifugally cast pipe was found to be considerably greater than in hot-rolled pipe of the same size. Long- and short-term strength of centrifugally cast pipe from industrial heats was lower than in pipe from test heats, and did not always satisfy requirements of standards for manufacture of pipe. Also, long-term ductility of centrifugally cast pipe from industrial heats was appreciably lower than in pipe from test heats, and it was in the ductility range of hot-rolled pipe.

Isothermal Disintegration of Austenite in Powder Steels Alloyed With Chromium and Molybdenum

937D0063F Moscow METALLOVEDENIYE I TERMICHESKAYA OBRABOTKA METALLOV in Russian No 8, Aug 92 pp 28-32

[Article by V. N. Antsiferov, L. M. Grevnov, and O. M. Perelman, Perm Polytechnical Institute, Republic Powder Metallurgy Engineering and Technical Center, Perm; UDC 621.762:620.186]

[Abstract] Chemical nonhomogeneity and defects in the crystal structure of steels are interlinked, because the dissolving of the alloying element is accompanied by an increase in the proportion of areas with varying compositions, and consequently the number of defects. On the other hand, homogenization taking place over the course of the sintering period tends to reduce the number of these defects. Thus during homogenization in powder steels, two oppositely acting processes take place which affect the $\gamma \rightarrow \alpha$ phase transition. These processes in chromium and chromium-molybdenum powder steels were analyzed to determine the effect of structural features of powder steels on transformation of supercooled austenite. Specimens for study were prepared using the same mixture consisting of iron powder, a colloid-graphite preparation, chromium, and molybdenum. Different degrees of chemical nonhomogeneity were obtained by sintering for different periods of time; porosity varied by 2-3 percent, and the austenite grain size was constant. Specimens were compressed at 800 MPa. Sintering was conducted at 1200° C for periods from 0.5 to 4 hours, and the rate of cooling of specimens after sintering was 6-10°/min.

It was found that the position of critical points and the character of isothermal diagrams of austenite's disintegration depend on the nonhomogeneity of the solid solution, as well as the density of crystal structure defects, the presence of complexly alloyed areas, and redistribution of carbon atoms in the solid solution. Linear dependences which were established between certain phase transformation parameters and the degree of chemical nonhomogeneity of powder steel can be used to select process conditions which yield desired structures. Addition of molybdenum to chromium steel intensifies the destabilizing role of defects, but at the same time chromium dissolves more intensely and complexly alloyed areas are formed, which increases the stability of supercooled austenite in the pearlite region.

Structural Transformations in VT22 Titanium Alloy During Aging

937D0063G Moscow METALLOVEDENIYE I TERMICHESKAYA OBRABOTKA METALLOV in Russian No 8, Aug 92 pp 33-37

[Article by V. V. Shevelkov, Pskov Affiliate, St. Petersburg State Technical University; UDC 669.295.5:620.186]

[Abstract] Selecting optimum conditions for final heat treatment of titanium alloys on the basis of regularities of change in their structure and mechanical properties during aging at different time periods and in a wide temperature range is discussed. Possibilities for controlling the kinetics and morphology of the process are evaluated for high-strength two-phase titanium alloys of the VT22 type, which undergo complex structural transformations during the aging process and in which a 100 percent β-phase may be obtained after hardening.

VT22 alloy was quenched in water from 950° C (1 hr) and aged in a temperature range 200-800° C for up to 5,000 hours. Results of electron-microscope and X-ray diffractometer studies established some regularities of the disintegration of the metastable β-solid solution for titanium alloys of the VT22 type. The presence of an incubation period of formation of the α-phase during the aging process

is characteristic for two-phase high-strength alloys of the VT22 type. Disintegration of the β-solid solution in alloys of this type is a multistage process which includes formation of segregates (beginning of exfoliation of the β-solid solution), of regions of the Guignet-Preston zone type, of different intermediate states, coherent states of the formed α-phase, and finally appearance of an independent α-phase having an interface with the matrix β-solid solution.

Tendency of 28Kh3SNMVFA-Sh Annealed Steel Sheet to Brittle Fracture

937D0063H Moscow METALLOVEDENIYE I TERMICHESKAYA OBRABOTKA METALLOV in Russian No 8, Aug 92 pp 37-39

[Article by V. P. Ilina and V. Ye. Yegovtsev, "Kompozit" Scientific and Production Association; UDC 669.14.018.298:621.7.044]

[Abstract] Two batches of 28Kh3SNMVFA-Sh steel sheet (thicknesses of 5.0 and 5.6 mm) produced at the "Zaporozhstal" Plant and possessing different formability in explosive forming were investigated for their microstructure, mechanical properties, and tendency to brittle fracture. The chemical composition of the steel in these batches differed little (carbon content was 0.26 percent), but they had shown a different tendency to fracture during explosive forming. It was found that steel with a finer grain and a more dispersed carbide phase uniformly distributed in the grain possesses a lower tendency to brittle fracture and better formability in explosive forming. A higher tendency to brittle fracture and, consequently, failure under explosive forming was found to be associated with unsatisfactory structure: a coarse carbide phase unevenly distributed in the ferrite matrix. Formation of such a structure is presumed to be due to sheets being annealed too long at the manufacturing plant. It was determined that the structure of the original steel can be improved by heat treatment. Resistance to crack propagation in this case increases by 3-8 times.

Effect of Asymmetry on Rolling Parameters

937D0065D Moscow IZVESTIYA VYSSHIKH UCHEBNYKH ZAVEDENIY: CHERNAYA METALLURGIYA in Russian No 9, Sep 92 pp 18-20

[Article by V. A. Nikolayev, Zaporozhye Industrial Institute; UDC 621.771.7:621.7.014]

[Abstract] Three asymmetrical rolling parameters were studied to determine their effect on the rolling process. The ratios of small (upper)-to-large (lower) roll diameters fell within 0.94 to 0.967 for five pairs of rolls. Microroughness for one pair of rolls, which was measured with a portable Kaliber-M-283 profilometer, was 4 to 4.1 for the upper roll and 0.6 to 0.8 for the bottom roll. These values were reversed for another pair of rolls. The other two pair of rolls had matched roughnesses of 4 to 4.1 and 0.6 to 0.8. The other parameter tested was the angle at which the strip is inclined in a vertical plane towards the bottom (large) roll. To test rolling asymmetry, aluminum strip was rolled with a draft of 0.3 to a thickness of 1.24 mm and a width of 20.5. To test the effect of the incline angle, the same type of strip was rolled with drafts of 0.23, 0.33, and 0.43 to a thickness of 1.03 mm and a width of 18.2 mm. The strip, which had a roughness of approximately 7μm, was coated with a lubricant similar to brand T coolant. Rolling force was measured with hydraulic capsules, and the torque on each roll with pressure transducers affixed to the spindles. The readings were amplified and recorded by an N338-4 plotter. Forward slip on the top and bottom surfaces of the strip was measured from centered markers without straightening the curvature that resulted from the rolling process. It was found that, during asymmetrical rolling, the effect of reducing the average normal pressure did not exceed about 5 percent in comparison with symmetrical rolling. Reducing the small-to-large roll diameter ratio to 0.91 makes it possible to reduce the average pressure by 15 to 20 percent, which is akin to reducing roll diameter from 100 to 91. Inclining the strip in a vertical plane before feeding it into the rolls somewhat reduces rolling forces and greatly affects the redistribution of torque between the rollers. Figures 3; references 9: Russian.

Effect of Heat Treatment on the Mechanical Properties of Three-Layered Bimetal Strip

937D0065E Moscow IZVESTIYA VYSSHIKH UCHEBNYKH ZAVEDENIY: CHERNAYA METALLURGIYA in Russian No 9, Sep 1992 pp 30-32

[Article by A. V. Voronin, V. T. Zhadan, V. A. Osadchiy, and A. V. Rumyantsev, Moscow Institute of Steel and Alloys; UDC 621.78.011:669-419.8]

[Abstract] Three-layered bimetal strip made of equal thicknesses of steel 45 and a high-chromium ledeburite reinforcing alloy was studied to determine how heat treatment affects its mechanical properties. The strip was made by hot-rolling bimetal bars cast in a double-casting metal mold that employed a container holding the alloy in powder form as the solid insert. After cooling and cleaning, the bars were reheated in a two-chamber furnace at 1150°C for one hour. They were then rolled width-wise on a two-roll 600 rolling mill to a thickness of 10 mm at a rolling rate of 1 m/second. The rolled bars were sent hot to guillotine shears, where they were cut into stock 10 x 412 x 450 mm, reheated at 1150°C for 30 minutes, rolled lengthwise into strip 4.5 mm thick, cut while cold into 4.5 x 45 x 215-mm lengths, and annealed in an electric furnace by heating at 1000°C, holding for one hour, cooling with the furnace to 650°C, holding for four hours, cooling with the furnace to 300°C, then air-cooling. Flat three-layered specimens were prepared on a milling machine per GOST 1497-84. The specimens were quenched by heating them in the furnace at 1000°C for 15 minutes, then cooling them in air or water. The air-quenched specimens were tempered in an electric furnace at 200, 300, 400, and 500°C for 1.5 hours. The reinforcing layers of the specimens were tested for Rockwell hardness, and the specimens for tensile strength on an Instron tester with a grip displacement rate of 5 mm/minute. Each type of heat treating procedure was represented by three specimens. It was found that optimal mechanical properties were obtained when the specimens were air-quenched at 1000°C and annealed at 300°C for 1.5 hours. Tables 1; references 3: Russian.

Speed Conditions of the Process of Rolling Foil

937D0069K Moscow TSVETNYYE METALLY in Russian No 10, Oct 92 pp 58-59

[Article by M.A. Tikhachev, All-Union Scientific Research Institute of Standardization; UDC 621.771.016.3.01-416:669.71]

[Abstract] The main problem of the foil-rolling industry is to produce very thin aluminum foils that are free of shape flaws. One of the key factors affecting the stability of the rolling process and the capacity of foil-rolling equipment is the speed of the metal in the exit plane of a deformation site. For this reason, a study was conducted to examine the effect of key rolling process parameters (rolling tension, force, and speed) on the rate of metal output. The study aluminum foil was rolled in accordance with a 0.1-0.05-0.028-0.014 mm scheme on 280/850 x 1,850 mm (first pass) and 260/850 x 1,850 mm (second pass) foil-rolling mills. The thickness of the foil during the course of the rolling process was measured by a precision isotope thickness gauge and then checked against samples by using a vertical telescope caliper. A standard computer program was used to process the experimental data and derive models of the change in rolling process coefficients as a function of the thickness of the foil produced. An analysis of the experimental data and mathematical models derived revealed that as the thickness of the foil being rolled is decreased, the efficiency of the effect of rolling speed and force decrease, whereas that of tension increases. The efficiency of the effect of rolling force on the rate of metal output during the rolling of foil 0.05 mm thick is 2.5 to 3 times higher than when foil 0.014 mm thick is rolled. The effect of rolling speed begins to diminish significantly in cases of foil less than 0.03 mm thick. This change is associated with the decrease in the effect of rolling speed on relative and absolute reduction. The coefficient of the intensity of the effect of tension on the rate of metal output has a tendency to increase as the thickness of the foil decreases. It was thus recommended that the following actions be taken to regulate the rate of metal output during the process of rolling aluminum foil for the purpose of increasing the capacity of foil-rolling mills: When the foil is between 0.1 and 0.03 mm thick, rolling force and speed should be regulated; when the foil is less than 0.03 mm thick, the front and back tensions should be regulated. A tension equal to 0.25 to 0.35 of the yield point of the metal being rolled should be used. Figures 4; reference 1: Russian.

Structure and Properties of Rapidly Quenched Microcrystalline Fe-Si Alloy

937D0071C Moscow METALLOVEDENIYE I TERMICHESKAYA OBRABOTKA METALLOV in Russian No 9, Sep 92 pp 8-11

[Article by B. V. Molotilov, N. M. Zapuskalov, and A. N. Savin, Central Research Institute of Ferrous Metallurgy im. I. P. Bardin; UDC 669.15'782-194:669-494:621.785.6]

[Abstract] Homogeneity of the structure and mechanical and magnetic properties of cast ribbon made of the single-phase alloy Fe-4.5 percent Si were investigated. Two techniques of air cooling of this product were compared: during continuous winding of the ribbon into a roll as it was made, and without winding it. Ribbon 150 mm wide and 140-200 μm thick was produced on a two- roll mill with bronze water-cooled rolls 440 mm in diameter. Metallographic structure of ribbon in the free (unwound) state and wound into a roll as it emerged from the rolling mill was examined with an optical microscope, magnetic properties were measured according to hysteresis cycles, and mechanical characteristics were determined by breaking tests, with fractographic analysis of fractured specimens done with a scanning microscope.

It was found that in rapidly quenched ribbon left in the free state, the structure and mechanical and magnetic properties demonstrate inhomogeneity in both lateral and longitudinal directions. When the technique of continuous winding of ribbon into a roll as it emerges from the mill is used, this inhomogeneity is decreased. The winding technique can be used to control the structure and properties of the product.

New Phases in Fe-Nd Alloys Obtained by Hardening From Molten State

937D0071E Moscow METALLOVEDENIYE I TERMICHESKAYA OBRABOTKA METALLOV in Russian No 9, Sep 92 pp 13-16

[Article by Ye. V. Obrucheva, V. P. Menushenkov, A. M. Gabay, and N. V. Belaya, Moscow Institute of Steel and Alloys; UDC 669.15'857-158:621.785.6]

[Abstract] The effect of non-equilibrium cooling conditions (hardening from the molten state) and subsequent annealing on the phase composition and magnetic properties of Fe-Nd alloys was investigated. Six different alloys with Fe contents from 7 percent to 58 percent were tested. The alloys were melted in an inert atmosphere and cast into an iron ingot mold. The central part of each ingot was used for hardening from the molten state by the spinning method. Specimens were obtained in the form of strip fragments 10-15 mm wide and 30-50 μm thick. Structural analysis of specimens was done with a diffractometer and a scanning electron microscope, and magnetic studies were done with a vibromagnetometer in fields of up to 2 MA/m. Curie temperatures were determined by thermomagnetic analysis.

Three phases were found in Fe-Nd alloys: P_1 with Curie temperature of 240° C for Fe content of 28-58 percent; P_2 with Curie temperature of 220 +/- 5° C for Fe content of less than 28 percent, and P_3 with Curie temperature of 160° C for an alloy containing 23 percent Fe and 5 percent Co (presumably amorphous). The presence of phase P_1 in alloys containing 37-58 percent Fe causes the coercive force to increase to 0.4 MA/m. In the annealing process, the amount of this phase decreases and a stable phase Nd_2Fe_{17} appears, which is accompanied by a sharp drop in the coercive force. In the alloy containing Co, a phase P_4 is formed after annealing (Curie temperature 340° C), which results in a coercive force of 1.52 MA/m.

Effect of Quenching Rate on Physical Properties of Thin Metal Filaments

937D0071H Moscow METALLOVEDENIYE I TERMICHESKAYA OBRABOTKA METALLOV in Russian No 9, Sep 92 pp 21-24

[Article by M. N. Vereshchagin, Gomel Polytechnical Institute; UDC 669.1'24'781.5-494:539.213]

[Abstract] A melt spinning process for producing metal filaments on a split disk which separates the melt into two filaments is described. The process permits filaments to be made in different geometrical shapes and to alter their cross-section. The effect of the quenching rate on the vitrification and solidification temperatures of an Fe-Ni-B alloy was investigated for this process. The mechanism of solidification of the glassy alloy was examined, and the microhardness and resistivity of the alloy after annealing at different temperatures were determined.

It was found that as the quenching rate increases, the vitrification temperature of the Fe-Ni-B alloy tends to be higher, while its solidification temperature virtually does not change. Solidification of the alloy in the process of isothermal annealing proceeds by the mechanism of eutectic crystallization. The alloy's microhardness in the annealing process has two maximums. The first maximum (about 280° C) is connected with peculiarities of the vitreous state near the vitrification temperature, and the second (360° C) is connected with the appearance of a boride phase in the solidification stage. In the temperature range 15-23 K, the glassy alloy's electrical resistance drops sharply.

Heat Treatment of Cast Aluminum Alloys Crystallized Under Regulated Pressure

937D0072I Moscow METALLOVEDENIYE I TERMICHESKAYA OBRABOTKA METALLOV in Russian No 10, Oct 92 pp 36-39

[Article by A.S. Petrov and V.F. Korostelev, Vladimir Polytechnic Institute; UDC 669.715-143.6:621.785]

[Abstract] Heat treatment of the Al + 8 percent Si alloy with a standard composition was studied in an experiment concerning the liquation of its constituent elements: principal ones (Al,Si,Cu) and secondary ones (Mg,Mn). Castings of this alloy in the form of cups with a not larger than 10:1 ratio of length to wall thickness are produced by crystallization under internal pressure, such a pressure being obtained and regulated by insertion of a plunger into the melt. Castings for this study were made from rods 50 mm in diameter, a material deformed by rolling. Liquation levels $L_{max} = \Delta C/C$ and liquation rates $L_P = \Delta C_{n+1}$ (C—lowest or highest concentration of element near nominal average, ΔC - maximum concentration difference within a grain of alloy material, ΔC_{n+1} - difference between concentrations of an element at two neighboring sites) in rods and in castings were measured by Auger spectroscopy with a JEOL-10 spectrometer yielding data on intragranular diffusion with a 0.5-1.0 μm resolution. Castings were then homogenized at 450° and at 470°C for four hours, eight hours, 12 hours. Optimum homogenization with minimum liquation of aluminum and copper was attained by an 8 hour long treatment (silicon liquation level greatly reduced, to zero in some sites), their liquation increasing during longer treatment. Hardness measurements were made after supplementary heat treatment, a maximum hardness of 72-74 HRB having been attained by homogenization at 470° C for eight hours with subsequent quenching from 500-505° C in water and aging at 150-170° C for 2-2.5 hours or continued for 1.5 hours longer without danger of overaging. The hardness was lower, 58-59 HRB minimum, after homogenization at 450°C for eight hours followed by quenching from 505-510°C in water and aging at 165° C for two hours but not longer so as to prevent overaging. Figures 6; tables 3; references 4.

Isothermal Pressing of VBr3 Casting High-Temperature Alloy

937D0075A Moscow KUZNECHNO-SHTAMPOVOCHNOYE PROIZVODSTVO in Russian No 9-10, Sep-Oct 92 pp 8-10

[Article by B.D. Kopyskiy, I.S. Zonnenberg; UDC 621.77.7.001]

[Abstract] The low ductility and unstable strength properties of items cast from the VBr3 complex alloyed bronze which make traditional pressing and plastic forming methods unsuitable prompted a study of the possibility of using isothermal pressing at an 850, 900, and 950° C temperature with a 1 MN force in a unit developed on the basis of the D0430 hydraulic press using dies made from hardened ZhS6U Ni-based superalloy. To this end, commercial castings of various sizes with holes drilled in them beforehand are used for making pipes. The test conditions are outlined in detail and a formula is derived for calculating the instantaneous pressing force and time. The mechanical properties of the VBr3 alloy are summarized, and isothermal process diagrams (force vs. time) are plotted. The tool resistance and reliability conditions under extended operation are determined as a function of the load bearing capacity of the die and the container. The pressing conditions and the values of the drawing coefficient, temperature-time conditions, mean long-term and instantaneous pressure, permissible pressure under various conditions, and safety margin under various conditions are tabulated for rods and tubes. An analysis of the findings shows that isothermal pressing is a stable process for making friction unit parts from bronze VBr3 which improves the performance of this alloy. Its implementation makes it possible to save expensive nonferrous metal and labor outlays for its machining yet the high straining resistance of this alloy calls for taking into account the effect of forming conditions on the tool resistance and reliability. Figures 1; tables 2; references 13.

Experience of Cold Extrusion of Cylindrical Part With Hollow Tag and Flange at its Central Section

937D0075B Moscow KUZNECHNO-SHTAMPOVOCHNOYE PROIZVODSTVO in Russian No 9-10, Sep-Oct 92 pp 11-12

[Article by Yu.A. Zhogolev; UDC 621.777.002]

[Abstract] The labor intensity, low efficiency, extensive metal waste in the form of chips, and the need for a broad range of machine tools for making parts with a hollow tag and a flange in its center by turning prompted a study of the process of making "nipple housing" parts by cold extrusion from the AMg2 aluminum alloy. A schematic diagram of the axisymmetric step-shaped part under study is cited, and six specific cold extrusion practices used for this purpose are considered. These versions differ in the sequence of the cutting, upsetting, extrusion, punching,

and flash trimming operations. An automatic multistation cold forging machine for making nipple housing parts was designed and is being produced by the Central Research and Design Office of Forging and Stamping Machine Building on the basis of the AV1819 automatic cold forging multistation machine used for making M8 nuts. The transition from cutting and turning to cold forging increased the equipment unit productivity by fourfold. Figures 3.

Implementation of High-Strength Steels in Automotive Part Production

937D0075C Moscow KUZNECHNO-SHTAMPOVOCHNOYE PROIZVODSTVO in Russian No 9-10, Sep-Oct 92 pp 13-15

[Article by A.F. Osipov; UDC 621.983.3: 669.14.018.262.004.122]

[Abstract] The need to use elevated-strength steels for increasing the strength and endurance and decreasing the mass of passenger car bodies and other parts prompted a comparative analysis of the ductility properties of the low-alloyed elevated-strength steels (SPP) with a yield point of $\geq$ 240 MPa and ultimate rupture strength of 400-500 MPa. To this end, ultimate strain and Woehler fatigue diagrams of steels 08GSYuT and 08GSYuF, duplex steel 03KhGYu, and phosphorus-containing steel 08YuP are plotted for various taut strained state conditions. An analysis of the curves shows that steel 08YuP is the most suitable for car bodies since it combines the necessary high ductility and endurance. The specific features of the stamping and forging of sheet blanks from these steels and the problems accompanying the production process, such as punch jamming, are examined in detail. An analysis of the experience of making car parts from high-strength steels at the Volga Automotive Plant (VAZ) and the factors which hold back extensive implementation of rolled plate and sheet metal made it possible to develop practical recommendations for eliminating the most significant shortcomings. The economic impact from implementing SPP steels in forging and stamping operations at the plant in 1983-1988 reached 1.3 million rubles and 4,000 tons of rolled stock at an annual consumption rate of 49,000 tons. Figures 2; references 4.

Increasing Manufacturing Accuracy of Parts From Sections in PGR Numerical Control Machine Tools

937D0075D Moscow KUZNECHNO-SHTAMPOVOCHNOYE PROIZVODSTVO in Russian No 9-10, Sep-Oct 92 pp 17-20

[Article by N.M. Bodunov, I.M. Zakirov; UDC 621.981.2.001]

[Abstract] The specific operating conditions of PGR machine tools with numerical control (ChPU) for rolled section bending with tension are outlined, and ways of increasing the manufacturing precision are considered. Attention is focused on developing a mathematical model which makes it possible to describe with sufficient accuracy the actual bending process allowing for the geometrical nonlinearity and finite forming. Formulae are proposed for computing the chuck displacement and determining the strained state of the blank, and force parameters and a system of nonlinear differential equations is derived. The boundary value conditions are formulated, and the boundary value problem is solved. An algorithm for solving the PGR tool displacement problem is developed, and the calculation results are summarized. An analysis of the proposed mathematical model and algorithm for taking into account the part's geometrical nonlinearity in analyzing the tool displacement makes it possible to realize different straining methods. Figures 1; tables 1; references 5.

Procedure of Optimum Design and Assembly of Tubular Units by Electromagnetic Swaging

937D0075E Moscow KUZNECHNO-SHTAMPOVOCHNOYE PROIZVODSTVO in Russian No 9-10, Sep-Oct 92 pp 20-22

[Article by S.M. Kolesnikov, A.G. Golushin, S.F. Golovashchenko; UDC 621.983.044.7]

[Abstract] Expanding uses of electromagnetic swaging on mandrels with circular grooves necessitated by the axial strength requirements of modern tubular assemblies and the negative impact of random groove configuration selection on the resistance of the magnetic pulse unit (MIU) parts prompted an attempt to solve this problem in a design-process formulation by selecting the most practicable joint design which minimizes the energy consumption of the assembly process allowing for the axial strength requirements and joint length constraints. To this end, mathematical models of electromagnetic tube swaging in a circular groove are developed, the relationship between the joint size and its load bearing ability under axial loading is established, and a procedure for optimizing the design and process parameters is developed. The specific steps and methods used in solving the above three problems are outlined in detail and attention is focused on the method of optimizing the parameters of joints with grooves. The optimization criterion is formulated and straining pressure formulae are derived. A block diagram of the joint dimension optimization algorithm is cited. The proposed CAD procedure makes it possible to determine the optimum joint design and the parameters of electromagnetic swaging of tubular parts rather efficiently in an automatic mode on a computer. Figures 2; references 9.

Deuterium Segregation in V-D Alloys Under Ion Irradiation

937D0091B Moscow FIZIKA I KHIMIYA OBRABOTKI MATERIALOV in Russian No 6, Nov-Dec 92 pp 15-18

[Article by V.L. Arbuzov, V.B. Vykhodtsev, S.M. Klotsman, A.D. Levin, V.A. Pavlov, G.A. Raspopova, Yekaterinburg; UDC 621.039.539.219.17]

[Abstract] Interest in metal-hydrogen systems due to the development of fission and fusion power prompted numerous studies of the effect of hydrogen segregation in

metals under ion irradiation which may lead to high local ion concentrations. Yet existing experimental procedures call for introducing an uncontrolled factor to the system under study; this factor can be eliminated by using the beam of ions under study as the irradiation source. To this end, the interaction of the D atoms dissolved in V with the deuteron-induced radiation defects is investigated. The experimental procedure and materials are outlined in detail. The effect of the irradiation dose on the V-D alloy surface enrichment with D, the effect of the alloy composition on the D segregation magnitude, and the energy states of the D atoms in the irradiated state are plotted. The study is carried out by nuclear microanalysis using a 700 keV deuteron beam and D(*d,p*)T reaction. All measurements are taken at room temperature. The findings show that ion bombardment of vanadium alloys with 0.01-0.1 percent D leads to a D-enrichment of the sample surface; this phenomenon is attributed to segregation under ion irradiation. A segregation model is developed for V-D alloys; it takes into account the high dissolved D mobility in the V lattice and the capture of a proportion of D atoms by the radiation-induced defects. Figures 3; references 3: 2 Russian, 1 Western.

Effect of High-Power Pulsed Ion-Beam Treatment on Physical-Chemical State of Surface Layers and Endurance Strength of EP718ID Alloy

937D0091C Moscow FIZIKA I KHIMIYA OBRABOTKI MATERIALOV in Russian No 6, Nov-Dec 92 pp 28-35

[Article by V.A. Shulov, G.Ye. Remnev, V.A. Koshcheyev, Ye.V. Fedorova, I.S. Isakov, I.G. Karpova, Moscow; UDC 539.213.612.17.533]

[Abstract] The outlook for using high-power nanosecond pulse ion beam treatment (MIP) for improving the performance of part surfaces is assessed, and the lack of published data on the functional link between the irradiation conditions and the physical and chemical state of the surface is noted. The effect of the ion beam treatment conditions on the chemical composition and structural and phase state of the surface layers of the EP718ID superalloy is examined, and an attempt is made to determine one of the most important performance characteristics of parts from this high-temperature material—the endurance strength. Gas turbine engine blades are used in the study. The sample preparation and experimental technique are outlined in detail, and the chemical composition of the nickel-based alloy is summarized. The curves of the quantitative Auger spectroscopy after various treatment conditions, the effect of the ion pulse current on the (311) X-ray line parameters, the effect of the number of pulses on the surface layer microhardness, and the effect of the ion beam treatment on the fatigue strength are plotted. The effect of irradiation on the exoelectron emission, microhardness, and surface roughness of the superalloy is tabulated. The findings confirm that ion beam treatment can substantially improve the endurance properties at a current density of close to 60 A/cm^2. Greater current densities may lead to crater formation; if this problem is resolved, an even higher surface layer hardening can be attained at 100-200 A/cm^2 levels. Figures 6; tables 3; references 10: 7 Russian, 3 Western.

Structure of 50N and 79NM Nickel-Based Alloys After Multiple-Pulse Laser Treatment

937D0091D Moscow FIZIKA I KHIMIYA OBRABOTKI MATERIALOV in Russian No 6, Nov-Dec 92 pp 48-52

[Article by A.A. Uglov, V.A. Grebennikova, S.N. Zibrov, Moscow; UDC 535.211:669.24]

[Abstract] The effect of pulse laser treatment on the metal surface morphology as well as the structural changes and the development of various phases and chemical compounds under laser irradiation are discussed and the lack of data on the weld formation during pulse laser welding in a free lasing mode is noted. Consequently, the structure and strain developing in Ni-based alloys treated with laser radiation at a λ = 1.06 μm wavelength at a 1 ms pulse duration are investigated. To this end, samples are irradiated in a KVANT-16 unit at a 100 mm focal length, zero defocusing, 1 ms pulse duration, and 5+/-1 J pulse energy using different gaseous media. X-ray analyses are carried out by a DRON-UM1 diffractometer in Fe*K* radiation; the calculations are made for the (311) line. The dependence of the integral spectral reflection line width and lattice parameters on the number of pulses under treatment in various media is plotted. Laser exposure leads to a grain fragmentation into blocks with a 1,200-1,300 A mean size. Although both alloys under study are monophase, the substructure distortions caused by irradiation point toward the presence of impurity phases in the grains; impurity are clustered along the grain boundaries under the effect of irradiation. The lattice spacing behavior during irradiation attests to a decrease in the relative Fe content in the irradiated surface layer. The authors are grateful to T.Ya. Zmeyeva for help with metallographic studies. Figures 3; references 16: 14 Russian, 2 Western.

Cesium Behavior Under High-Temperature Reprocessing of Solid Radioactive Waste

937D0091E Moscow FIZIKA I KHIMIYA OBRABOTKI MATERIALOV in Russian No 6, Nov-Dec 92 pp 58-62

[Article by I.A. Knyazev, I.D. Tolstov, S.V. Stefanovskiy, Moscow; UDC 621.039.73]

[Abstract] Previous studies of the mechanism of cesium immobilization during the plasma reprocessing of solid radioactive waste are continued; in particular, ^{137}Cs behavior is examined using actual ash of incinerated solid radioactive waste (TPO) with a specific cesium activity of 2.3 x 10^6 Bq/kg. To this end, a ceramic pipe with a 0.05 m diameter sealed on one end is stuffed with a charged and placed in a furnace shaft heated by an arc plasma generator for 0.5 h. After this heat treatment, the pipe is extracted and cut into sections, and samples are taken for radiometry and X-ray diffraction analyses using SI-8B counter and DRON-4 diffractometer in Cu*K* radiation. The temperature distribution in the plasma furnace height, the ^{137}Cs distribution in the plasma furnace shaft height as a function of the charge heat treatment temperature, and the ^{137}Cs distribution in the vertical pipe after heat treatment are plotted. The solid radioactive waste and the plasma fuel move in a counterflow. The curves demonstrate that radioactive cesium in solid radioactive waste is localized

during the reprocessing operation in the shaft furnace in areas with a temperature level of 2,000-1,600, 1,200-800, and below 750K due to the absorption of cesium compound vapors by the molten slag as well as due to the Cs binding by vitrification and other mechanisms. The integral Cs radionuclide loss resulting from the addition of aluminosilicate-and carbon-containing materials to solid radioactive waste drop, especially when the solid radioactive waste and aluminosilicate are charged into the furnace layer by layer. Cesium is immobilized to an extent where it is below the detection threshold. Figures 3; references 11: 9 Russian, 2 Western.

Properties and Application of Zinc-Based Microcrystalline Solder Alloy TsAG

937D0071J Moscow METALLOVEDENIYE I TERMICHESKAYA OBRABOTKA METALLOV in Russian No 9, Sep 92 pp 28-30

[Article by V. S. Chernov, A. S. Yevteyev, V. A. Tatarinov, F. Ye. Pashchenko, and V. S. Khozikov, Research Institute of Materials for Electronic Equipment, Kaluga; UDC 669.5'71'855.5- 158:621.785.6]

[Abstract] The zinc-based alloys Zn-Al and Zn-Ge with eutectic melting points of 382° and 398° C are of interest for use as a solder to replace gold alloys in attaching silicon crystals to substrates in semiconductor instruments and integrated circuits. Trinary TsAG alloy (system Zn-Al-Ge), which cannot be made in sufficiently thin strips by conventional pressure-working methods, was produced in ribbon form by the melt spinning method. Ribbon was produced with widths of 3-10 mm and thicknesses of 30-90 μm; thickness could be varied by changing the pressure of the argon gas forcing the melt through the discharge nozzle and by changing the speed of the spinning disk. The resulting ribbon had a microcrystalline, homogeneous structure with adequate resistance to heating to comparatively high temperatures. Analysis of performance properties of the ribbon alloy indicated that it has potential for use as a solder material in semiconductor instruments and integrated circuits.

Using New Class of Composites for Surfacing Wear Resistant Protective Layers

937D0076A Kiev AVTOMATICHESKAYA SVARKA in Russian No 5 (470), May 92 pp 8-11

[Article by V.K. Lebedev, T.I. Martynova, V.M. Mozok, G.N. Gordan, L.P. Krzhyzhanovskaya, Electric Welding Institute imeni Ye.O. Paton at the Ukrainian Academy of Sciences; UDC [621.791.927.5:669.018.25]:62-419]

[Abstract] The difficulty of ensuring the composition stability of the multicomponent mechanical mixtures used for restoring the surfaces of parts and applying protecting and hardening coats by arc hard-facing with the help of a fluxed core wire of band and coated electrodes as well as the problem of attaining an identical chemical composition and properties of the hard-faced metal at each point and ensuring the necessary product quality as a whole prompted the Electric Welding Institute imeni Ye.O. Paton at the Ukrainian Academy of Sciences and the St. Petersburg State University to develop, produce, and test new surfacing materials whose charge contains composite granules produced by direct solid phase synthesis. The results of a study of the structure and properties of the metal surfaced with a self-protecting powder wire with such composite granules consisting of metal and nonmetal components in the charge are presented and ten versions of composite powders, the nickel concentration in 12 batches of composite granules, and the chemical content of the surfaced metal are summarized. Two batches of self-protecting fluxed core wire whose charge contains a mixture of ferroalloy, pure metal, and flux-forming material powders were tested with samples of steel St3 with beads made with two- and three-layer surfacing. The carbon, nitrogen, and oxygen distribution in the nonmetal inclusions in the hard-faced metal from both batches, the shape of nonmetallic inclusions and their energy spectra, and the Ti distribution in the surfaced metal are plotted. The HRC hardness of the surface metal measured at a 5 mm step and the impact abrasive wear resistance of the hard-faced coats are examined. The experimental findings demonstrate that charge preparation by solid phase synthesis is more efficient than the traditional practices, especially with respect to the surfaced metal hardness and impact abrasive wear resistance. The difficulty of explaining the physical origin of this phenomenon is noted. Figures 7; tables 5; references 2.

Effect of Defects on Welded High Pressure Vessel Strength

937D0076B Kiev AVTOMATICHESKAYA SVARKA in Russian No 5 (470), May 92 pp 12-15

[Article by G.S. Vasilchenko, A.V. Ovchinnikov, Ye.Yu. Rivkin, Scientific Production Association of the Central Scientific Research Institute of Mechanical Engineering; UDC [621.791:621.039]:539.4]

[Abstract] The findings of the Program for the Inspection of Steel Components (PISC-I) initiated by Prof. R.W. Nicols in Western Europe for checking the capabilities of a nondestructive ultrasonic testing (UZK) procedure developed for the American Society of Mechanical Engineers are discussed and it is noted that PISC-I data have a wide spread while the procedure can detect only defects with a size of more than 50 mm in the thickness direction. Subsequent inspections under the PISC-II program revealed that the data spread can be narrowed considerably by classifying the defects by categories. Efforts initiated by the State Committee on Nuclear Power and undertaken by the Scientific Production Association of the Central Scientific Research Institute of Mechanical Engineering and other enterprises in order to increase the confidence of nondestructive ultrasonic testing at nuclear power plants are described. The dependence of the detection frequency (i.e., probability) of various categories of defects on their dimensions according to PISC-II data and a graphic procedure for calculating the design ranges of breaking stress, brittle area, quasibrittle area, and viscous area are plotted. The efforts of PISC and domestic tests are aimed at detecting flaws in welded pressure vessels and other NPP structures with cracks in order to assess their strength and notch sensitivity index (KIN) under such conditions as normal operation (NUE), normal operation violations (NNUE), hydrostatic tests (GI), predicted earthquake (PZ), an emergency (AS), and maximum design earthquake (MRZ). The proposed technique was implemented for determining the dimensions of permissible defects; it is noted that the ASME procedure is virtually inapplicable for analyzing the permissible defect sizes in NPP elements under the effect of thermal exposure while the criterion described in the article makes it possible to assess correctly the role of each stress category. Figures 2; tables 1; references 9: 6 Russian, 3 Western.

Assessing Stressed State of Welded Steelwork by Magnetoelastic Stain Measurement Method

937D0076C Kiev AVTOMATICHESKAYA SVARKA in Russian No 5 (470), May 92 pp 16-18

[Article by V.G. Petushkov, A.G. Bryzgalin, V.A. Titov, V.M. Pervoy, Electric Welding Institute imeni Ye.O. Paton at the Ukrainian Academy of Sciences; UDC [621.791:62-112.81]:531.781.2]

[Abstract] The problem of using the most reliable and accurate stress measurements which call for destroying the tested sample and makes them unsuitable for monitoring the stressed state of actual structures, primarily welded steelwork, and the shortcomings of known nondestructive testing methods which are vulnerable to external factors and surface state and are difficult to implement stimulated interest in the magnetoelastic strain measurement method based on employing the dependence of the magnetic permeability of ferromagnetic alloys on their stressed state. Certain shortcomings inherent in the method are discussed, and it is stressed that several modifications of the method can be effectively used for taking practical measurements of uniaxial stresses as well as evaluating the planar stressed state of metal structures. Magnetoelastic strain measurement can be used for measuring the difference in the principal stresses before and after a change in the structures stressed state. For illustration, typical cases where the problem of quantifying stresses can be solved by utilizing *a priori* data on the structure loading character are considered. Residual stress diagrams of a condenser wall's vertical weld, outer surface of the base metal, horizontal weld, and inner surface of the base metal and hoop stress diagrams of a generating unit of a pumped storage hydroelectric power plant before and after explosion treatment are plotted. The mechanical strain is measured using a strain gauge with a 2 μm graduation while magnetoelastic strain measurement are taken by a Paton Institute instrument. The study confirms the possibility of using magnetoelastic strain measurement together with mechanical strain measurement for solving a broad range of practical tasks; the method is characterized by its simplicity and the fact that it requires low capital outlays and does not call for violating the structure integrity. Its shortcomings include a relatively high measurement error compared to destructive methods. Figures 3; references 3: 2 Russian, 1 Western.

Selecting Weld Doping System in Low-Alloy High-Strength Steel Welding

937D0076D Kiev AVTOMATICHESKAYA SVARKA in Russian No 5 (470), May 92 pp 19-25

[Article by O.G. Kasatkin, L.I. Mikhoduy, Electric Welding Institute imeni Ye.O. Paton at the Ukrainian Academy of Sciences; UDC 621.791.75.053:669.15-194.2:51.001.57]

[Abstract] The effect of the weld metal whose quality must match that of the base metal without additional heat treatment on the service properties of the weld, especially with a high yield point, and the need to develop welded structures with sufficient cold resistance, prompted a study aimed at analyzing and selecting the systems of doping the low-alloy high-strength weld steel with a yield strength of 700-900 MPa which ensure a toughness of $\geq$ 0.4 and $\geq$ 0.3 MJ/m^2 in samples with a sharp notch at a temperature of -40 and -70° C, respectively, and a satisfactory level of elongation and reduction in area. To assess the general character of the dependence of the weld's mechanical properties on its composition, data from an experimental and computational database and the results obtained in tests of low-allow samples are used. The effect of the alloying addition and impurity content on the yield point, ultimate strength, elongation, reduction in area, and toughness of the 10KhGN2M steel weld at various temperatures is plotted. The weld metal cooling duration (from 850 to 500° C) was manipulated between 7 and 30 s. Regression models are derived and the residual standard deviation and multiple correlation are calculated by processing the experimental data. An analysis shows that to attain high-strength cold resistant steel, it is necessary to minimize the impurity concentration, especially P, N, and O by using a reduced welding energy per unit of length. This also decreases the negative effect of Mn and Cr on the weld toughness. Simple alloying systems, such as 10G2N3MF or 10GN4MF ensure a good combination of strength, ductility, and cold resistance indicators at a 10-15 s cooling duration and low impurity concentrations. Figures 6; references 5.

State of the Art and Outlook for Electroslag Welding of Large-Section Aluminum Busbars

937D0076E Kiev AVTOMATICHESKAYA SVARKA in Russian No 5 (470), May 92 pp 29-31

[Article by B.A. Gubin, A.Ya. Ishchenko, V.A. Knigel, Electric Welding Institute imeni Ye.O. Paton at the Ukrainian Academy of Sciences and All-Union Aluminum and Magnesium Institute, St. Petersburg; UDC 621.791.793.002:669.715:621.316.35]

[Abstract] The shortcomings of electroslag welding (EShS) in such labor consuming processes as erection and repairs of aluminum electrolyzer busbars and the increasing use of large electrolyzer busbars with a 650 mm height and 70, 140, and 210 mm cross section prompted a comparative analysis of the efficacy of manual arc welding, argon arc welding, and electroslag welding of large-section busbars with a 650 mm-long weld. The urgency of the task of developing methods and practices of electroslag welding of large-section busbars during the construction, erection, and repairs of high-output aluminum electrolyzers and similar units is stressed, and the specific difficulties of the method due to the physical and chemical properties of the welded metal and chloride and fluoride fluxes used, i.e, a high thermal conductivity, low density, low melting point, high affinity of the metal for oxygen, as well as a high molten slag fluidity and its high electric conductivity and chemical activity at operating temperature, are outlined. Methods of overcoming these problems and their shortcomings are summarized in detail, and the welding machines developed for aluminum busbar welding are described. The need for further studies of electroslag aluminum welding applications in the industry and analyses of the process under the effect of strong magnetic fields is emphasized. Figures 4; tables 1; references 24.

Effect of Filler Wire Composition on Al-Li Alloy 01421 Fracture Resistance

937D0076F Kiev AVTOMATICHESKAYA SVARKA in Russian No 5 (470), May 92 pp 36-38

[Article by T.M. Labur, R.V. Ilyushenko, Electric Welding Institute imeni Ye.O. Paton at the Ukrainian Academy of Sciences; UDC 621.791.04:669.715'884:539.4.011.25]

[Abstract] The lack of proper attention to the fracture resistance of welded joints from Al-Mg-Li-Sc alloys with the Sc-doped AMg4 and AMg63 filler wire, particularly the nominal breaking stress and specific crack propagation work (URRT) which must be known for analyzing the strength of structures from alloy 01421, prompted a study of the effect of the filler wire composition on these characteristics. To this end, alloy 01421 joints are made by argon arc welding with a nonconsumable electrode while adhering to all specifications stipulated for welding of Al-Li alloys. In so doing, AMg4 and AMg63 with various Sc concentrations. The fracture resistance characteristics are determined under offset tension using flat samples with a sharp notch with a 0.1 mm radius and 11 mm depth. The test results are tabulated in order to optimize the weld metal composition produced using different filler wires and the fractograms of the welded joint metal are cited. An analysis of the fractograms and test data shows that the AMg4 filler wire with 0.25 percent Sc improves the operating reliability of welded joints which combine better fracture resistance indicators than other wires—a breaking stress of 340-360 MPa and crack propagation work of 6.5-8.0 J/cm^2—which is 20-25 percent and 50-100 percent better than the figures attained without scandium doping which refines the fracture microrelief, reduces the amount of coarse intermetallic phases, and shortens the length of intergranular cracks. Figures 2; tables 1; references 5.

Two-Sided Electron Beam Welding of Thick Walled Cylindrical Billets From PT-3V Titanium Alloy

937D0076G Kiev AVTOMATICHESKAYA SVARKA in Russian No 5 (470), May 92 pp 46-47

[Article by V.N. Zamkov, V.Ye. Lokshin, O.K. Nazarenko, K.S. Khripko, A.D. Shevelev, L.V. Boykov, I.V. Suzdalev, Electric Welding Institute imeni Ye.O. Paton at the Ukrainian Academy of Sciences and Prometey Central Scientific Research Institute of Composite Materials, St. Petersburg; UDC 621.791.72:[62-413.1:669.295]]

[Abstract] The need to join cylindrical billets with a thickness of up to 400 mm and 2,000 and 1,200 mm outside and inside diameter, respectively, in order to enlarge of build up titanium alloy semifinished products and the lack of detailed data on electron beam welding of such thick walled titanium items prompted a study of the characteristics of weld formation on thick walled cylindrical titanium alloy billets by an electron beam and the development of sound double-sided welding practices. The parameters of the inner and outer pass in electron beam welding of cylindrical billets and the sequence and weld surface facing conditions of cylindrical billets from the PT-3V alloy at a 60 kV accelerating potential and a welding rate of 9 m/h are summarized, and the macrorelief of the welded joint surface after two-sided electron beam welding (ELS) and weld surface facing is cited. The welds are linked up by gradually lowering the electron beam current while maintaining the optimum focal plane position. The edges are prepared for welding by making a rectangular groove. An analysis confirms the absence of large voids in the weld and a small number of weld root defects. Figures 3; tables 2.

Argon Arc Welding of Niobium Chemical Reactor Units

937D0076H Kiev AVTOMATICHESKAYA SVARKA in Russian No 5 (470), May 92 pp 47-48

[Article by S.P. Zabolotin, Ye.A. Asnis, M.M. Nerodenko, V.K. Shapran, Electric Welding Institute imeni Ye.O. Paton at the Ukrainian Academy of Sciences; UDC 621.791.754'293:[62-112.669.293]]

[Abstract] The increasing use of niobium for making chemical reactor components and the high corrosion resistance of welded joints made by argon arc welding with tungsten electrodes prompted the Electric Welding Institute imeni Ye.O. Paton at the Ukrainian Academy of Sciences to develop practices of welding together chemical reactor units using different welding conditions, depending on their configuration. The specific difficulties of welding thick walled niobium are outlined, and it is noted that the Paton Institute unit makes it possible to overcome these problems and produce quality welded joints using nonconsumable tungsten electrodes with local protection equipped with specialized heat removing clamps and welding observation and control systems. It is capable of joining sheets with an up 2,000 mm-long weld and welding shells with a 400-3,000 mm diameter and 0.5-2.0 cm wall thickness. The edge and equipment preparation processes are described, and it is noted that that the use of welded assemblies from Nb in chemical devices considerably prolongs their overhaul period and improves the product quality. Figures 2; references 1.

Experiments of Welding Tubes Spin Cast From Pig Iron With Globular Graphite

937D0076I Kiev AVTOMATICHESKAYA SVARKA in Russian No 5(470), May 92 pp 50-51

[Article by V.A. Metlitskiy, A.N. Pavlenko, L.Yu. Sorokina, Electric Welding Institute imeni Ye.O. Paton at the Ukrainian Academy of Sciences; UDC 621.791.75.042:621.643.22]

[Abstract] The valuable physical, mechanical, and operating properties of spin cast tubes from pig iron with globular graphite (ChShG), particularly their relatively high strength and corrosion resistance, prompted a study of the possibility of producing quality butt joints by mechanized arc welding of cast iron tube rings using solid section electrode wires. To this end, tubes with a 100 mm diameter and 8 mm wall thickness made by the Lipetsk Metal Works according to TU 14-3-1446-86 are used. The tube metal contains fine globular graphite in the pearlitic matrix and has an ultimate strength of 630-650 MPa, a yield point of 470-490 MPa, an elongation of

12-16 percent, and an HV hardness of 192-215. The structure and mechanical properties of the welds produced by butt welding 35 mm wide rings with 50-60° bevels blunted to 0-2 mm with a 0-2 mm clearance are tested in templates cut across the weld. The sample microstructure is examined by electrolytic etching. The mechanical properties are measured during tensile tests according to GOST 6996-66 and hardness is measured in a Leko gauge. The welding conditions and mechanical properties of welds made with Sv-08A, Sv-08G2S, PANCh-11 and -12, and experimental copper wires are summarized. An analysis confirms the possibility of producing quality welds by mechanized arc welding with solid wires and attain a weld strength at a level of 70-90 percent of the base metal. Hardening weld alloying can be used to increase the weld strength further. It is noted that the tubes must be preheated before using the Sv-08A and Sv-08G2S wire. Figures 2; tables 1; references 2.

Polymorphous Calcium Carbonate Family and Synthesis of $CaCO_3$-II Single Crystals Under High Pressure

937D0039A Moscow RAZVEDKA I OKHRANA NEDR in Russian No 9, Sep 92 pp 13-14

[Article by L.V. Gorbunov; UDC [552.54:546.41]: [549.057:539.893]]

[Abstract] The polymorphous calcium carbonate family, including the biogenic modifications, and phase transitions in $CaCO_3$ at high pressures first discovered by Bridgman in 1939 are discussed, and synthesis of acicular $Ca_{1-x}Me_xCO_3$ single crystals which are an analogue of the metastable $CaCO_3$-II phase is reported (Me is Ni, Co, or Mn). The single crystals are synthesized in a high-pressure diamond synthesis unit. A phase *P-T* diagram of $CaCO_3$ is plotted, and the reaction cell filling arrangement is presented. The X-ray diffraction patterns of the resulting single crystals in Fe radiation and their refractive indices are summarized. Spectral analysis and refraction data show that isomorphous impurities of metal carbonates vary within 10-40 percent; crystal lattice parameters are calculated on the basis of X-ray diffraction data. It is speculated that stabilized $CaCO_3$-II and -III forms can be found in kimberlites, carbonatites, and other rock formed under high pressures. Figures 3; tables 2; references 6: 3 Russian, 3 Western.

Lightweight Mullite Refractory

937D0039B Moscow RAZVEDKA I OKHRANA NEDR in Russian No 9, Sep 92 pp 16-17

[Article by Ye.G. Yarotskaya, V.P. Golenko, V.A. Vanyshev, M.Ye. Andreyev, V.G. Yarotskiy, Ye.V. Polyanskiy; UDC 549.057:666.762.14]

[Abstract] A new lightweight crystal mullite refractory developed at the Research Institute for Synthetic Materials (VNIISIMS) meets the requirements imposed on modern lining materials; its production is a mullitization process based on the interaction of aluminum fluoride with silicon, aluminum, and vanadium oxides under heating to a 1,200° C temperature. The production technology is outlined, and a block diagram of silicon tetrafluoride recovery is cited. The chemical reactions involved in the refractory production are examined. Refractory 150x170x220 mm bricks are produced for use as lining. Brick sections are examined in transmitted and reflected light under a POLAM-R-211 polarization microscope; the study shows that the material has an intertwined filamentary microcrystalline structure with 7-15 μm long mullite crystals with a 1-3 μm diameter, making the material tough and strong. The new refractory is machinable and has a good absorptance. It is recommended for use as lining for electric furnaces operating at a temperature of up to 1,600° C and is promising for use as ceramic filters and absorbers. Figures 2; references 1.

Growth and Physical Properties of Rare Earth Aluminum Garnets With Scandium

937D0039C Moscow RAZVEDKA I OKHRANA NEDR in Russian No 9, Sep 92 pp 17-19

[Article by L.I. Kazakova, V.S. Kovalenko, V.M. Dubovskaya, S.V. Bykova; UDC 549.057:622.375]

[Abstract] The mechanism of scandium atom injection in the matrix of rare earth aluminum garnets and the outlook for using gadolinium-scandium aluminum garnets (GSAG) doped with Nd^{3+} and Cr^{3+} ions as an efficient laser (OKG) working medium or as scintillation materials for simultaneous detection of low- and high-energy electromagnetic radiation and neutrons and charged particles are discussed. Growth of GSAG crystals by the methods of vertical and horizontal oriented crystallization in a vacuum in molybdenum containers at a 1.55-8 mm/h crystallization front rate is reported. The component ratios were manipulated and the X-ray phase analysis was carried out in a DRON-2 unit in *C* and K_α radiation while optical absorption spectra were examined in a Specord M40 unit within a broad 50,000-10,000 cm^{-1} range. The photoluminescence spectra are recorded by an SDL-2 spectral unit in a 200-800 nm band. The temperature dependence of magnetic susceptibility, the dependence of the effective magnetic moment and lattice cell parameter on the scandium concentration, and the temperature dependence of reciprocal magnetic susceptibility are plotted. A study of the lattice cell parameter shows that as the Sc concentration rises, the crystal lattice widens, attesting to the fact that Sc ions take octahedral positions in the lattice. X-ray data and magnetic properties indicate that Tb and Sc ions are partially redistributed in octahedral and dodecahedral positions in the $Tb_3Sc_xAl_{2-x}Al_3O_{12}$ system. The magnetic susceptibility increases slightly with the scandium concentration at room temperature. The findings confirm that GSAG is a very practicable material suitable for doping with elements having a large ionic radius. The need for further studies of the physical properties of this garnet doped with light rare earth element (RZE) ions is stressed. Figures 2; tables 1; references 5: 2 Russian, 3 Western.

High-Speed $Bi_4Ge_3O_{12}$:Yb Radiation Resistant Scintillating Single Crystals

937D0039D Moscow RAZVEDKA I OKHRANA NEDR in Russian No 9, Sep 92 pp 21-23

[Article by B.I. Zadneprovskiy, M.V. Korzhik, V.I. Moroz, V.A. Nefedov, P.V. Nefedov, V.B. Pavlenko, A.A. Fedorov; UDC 535.372]

[Abstract] The increasingly stringent requirements imposed by the new generation of accelerators (e.g., UNK, LHC, and SSC) and the lack of a unified concept of total absorption detector material selection prompted a search for ways of improving existing scintillators, and in particular upgrading the characteristics of single crystals of bismuth trigermanate (BGO). It is speculated that the radiation resistance of BGO scintillators can be increased and their de-excitation time shortened by additionally doping them with ytterbium. The spectroscopic and scintillation characteristics of BGO single crystals doped with Yb are investigated. The scintillation kinetics of BGO and BGO:0.05 percent Yb single crystals at 300K, absorption spectra of BGO:0.05 percent Yb and crystals grown from identical charge without the activator, and the dependence of the ratio of scintillation effects before and after irradiation on the dose absorbed by BGO crystals with various Yb contents are plotted. Yb^{3+} ions may quench excitation due to the radiation-stimulated recharging. The findings show that Yb-doping of BGO crystals in the amount of no

more than 0.1 percent leads to an increase in their radiation resistance to 10^6 Gr. Combined with the short de-excitation component, this makes it possible to regard BGO:Yb single crystals as promising scintillation materials for total absorption detectors in experiments with high-energy particle recording. Figures 3; references 7: 3 Russian, 4 Western.

Lithium Tetraborate: Promising Piezoelectric Material for Making Band-Pass Filters

937D0039E Moscow RAZVEDKA I OKHRANA NEDR in Russian No 9, Sep 92 pp 27-29

[Article by K.V. Shestopalov, V.A. Nefedov, B.I. Zadneprovskiy; UDC 621.372.54]

[Abstract] The increasing importance of wide-band filters with a 1.0-2.5 percent transmission band in modern integrated circuitry and the high cost and poor temperature stability of existing materials prompted the development of a synthetic piezoelectric material—lithium tetraborate (TBL)—which can be used in surface acoustic (PAV) and bulk acoustic wave (OAV) devices. The properties of domestically synthesized TBK ($Li_2B_4O_7$) with a tetragonal syngony and 4*mm* symmetry class are examined. The crystals under study are Czochralski grown in platinum crucibles in an air medium at a 940° C maximum melt temperature. The single crystal is sliced into polished piezoelectric *Y*-cuts rotated by 51°. The spectral and temperature-frequency characteristics of a TBL-based resonator, the spectral response of a two-resonator structure and the temperature-frequency characteristics of its symmetric and antisymmetric acoustic modes, and the amplitude-frequency and temperature-frequency characteristics of a TBL-based band-pass filter are plotted. The resonators and two-resonator structures (DS) developed on the basis of 51° rotated *Y*-cuts have parabolic temperature-frequency characteristics (TChKh) with an inflection point in the area of room temperature whose position on the temperature axis depends on the slicing angle and electrode dimensions as well as the oscillation mode. The findings confirm the possibility of using TBL for making band-pass filters with a 1.0-2.5 percent transmission band. The need to analyze the optimum topological dimensions of resonator structures and develop a filter design procedure allowing for the piezoelectric element orientation and geometrical dimensions of the electrodes is stressed. Figures 3; references 4: 2 Russian, 2 Western.

Deep Treatment of Sewage From Cryolite and Aluminum Plants To Remove Fluorine by the Carbonization Method

937D0069E Moscow TSVETNYYE METALLY in Russian No 10, Oct 92 pp 34-35

[Article by V.A. Morozova and G.I. Kirillova, Physics Institute, All-Union Scientific Research and Design Institute of the Aluminum, Magnesium, and Electrode Industry; UDC 628.3:669.71]

[Abstract] The maximum permissible concentration of fluorine in water reservoirs used for fishing purposes is 0.75 mg/dm^3 (including the background concentration). Diluting the fluorine concentrations of typical sewage generated in the production of aluminum and cryolite is economically unfeasible. Several methods for deep treatment of such sewage, including reagent, ion exchange, sorption, and electrochemical methods, have been developed as an alternative. A study was conducted to determine the degree of defluorination of wastewater as a function of the calcium oxide dose, carbonization time, and number of treatment stages. The studies were performed at a temperature of 22-23° C on a unit consisting of a reactor with a mechanical mixer and a tank filled with carbon dioxide. One-hundred milliliters of water was treated, and a carbon dioxide flow rate of 200 ml/min with a severalfold calcium oxide surplus were used. The water was treated as follows: Calcium oxide was added, and the mixture was stirred for 10 minutes. Carbon dioxide was then fed into the reaction mixture (without removal of the precipitate that had formed) for 30 minutes. The fluorine concentration in the starting water was only reduced from 3 to 2.47 mg/dm^3 and from 12 to 10.26 mg/dm^3. Three water treatment cycles with a total carbonization time of 90 minutes and mixing after the addition of the calculated amount of calcium oxide in fractions over a 30-minute period did produce positive results, however. The deepest degree of defluorination was achieved in cases of a starting fluorine concentration of 3 mg/dm^3, a calcium oxide dose of 4 to 4.5 g/dm^3, and a carbonization time of 90 minutes. The residual fluorine content ranged from 0.7 to 0.4 mg/dm^3. When water with a starting fluorine concentration of 12 mg/dm^3 was treated, the calcium oxide dose rate was increased to 10 g/dm^3, thereby resulting in a decrease in fluorine concentration to 0.37 mg/dm^3. The efficiency of removing fluorine from sewage was thus directly dependent on the calcium oxide dose and carbonization time. The standard comparative cost of treating 1 cubic meter of sewage is 0.29 rubles. Figure 1, table 1.

The Development of a Gas Scrubbing System for the Flue Gases of Calcining Furnaces Used in Electrode Production

937D0069F Moscow TSVETNYYE METALLY in Russian No 10, Oct 92 pp 35-37

[Article by A.G. Aryanin, E.V. Kalinin, A.I. Lutkov, and V.A. Prokhorov, Graphite Scientific Research Institute; UDC 669.184.152.4]

[Abstract] A new gas scrubbing system has been designed to treat the flue gases of calcining furnaces used in electrode production. The new system is based on the technique of thermocatalytic neutralization of gases in a layer of mullite-silica fiber material filter heated to a temperature of 400-450° C by a burner mounted at the point where the flue gases enter the reactor. First, the mullite-silica fiber material is heat-treated in a calcining furnace at a temperature of 950° C and then activated by impregnation with a saturated solution of acetic acid copper. The mullite-silica fiber material was in the form of 20-mm-thick felt. Filter packs of alternating pieces of the mullite-silica fiber material felt and filter framework were assembled. The gas scrubbing unit tested had a capacity of 8,000 nm^3/h, a filtration surface of 36 m^2, and a mullite-silica fiber material layer thickness of 0.02 to 0.03 m. A total of 12 filter layers was used. The temperature of the scrubbed gas at the inlet to the reactor unit ranged from 100 to 170° C and reached 400° C at the outlet. The unit has a neutralization efficiency of at least 99.9 percent. The tests conducted thus confirmed the feasibility of scrubbing the flue gases from multiple-batch calcining furnaces by using movable (by a crane or by mounting it on rails) or stationary thermocatalytic reactors with a burner and layer of activated mullite-silica fiber material. The heat of the scrubbed gases may be used to heat water by installing heat exchangers in the collecting flue at the point where the gases leave the furnace. Figures 2; references 5: Russian.

Gas Chromatography in the Analytic Testing of Flue Gases in Titanium-Magnesium Production

937D0069G Moscow TSVETNYYE METALLY in Russian No 10, Oct 92 pp 39-42

[Article by A.I. Boyko, V.M. Pryakhina, L.F. Shelekhova, V.V. Bigma, and A.A. Shcherbina (deceased), Titanium Institute; UDC 543.544.26:669.295.015.7]

[Abstract] A series of studies was conducted for the purpose of developing a method of gas chromatography-based analytic testing of the composition of the process and flue gases resulting from the manufacture of titanium and magnesium products. Flue gases generated during the production of magnesium-titanium products and electrolysis chlorine gas formed during the manufacture of magnesium products were used as study objects. The gases studied contained chlorine, hydrogen chloride, sulfur and carbon oxides, organic impurities, moisture, and water vapors. The main direction of the development effort was that of breaking the corrosion analysis compounds down into noncorrosion derivatives so that their concentrations could subsequently be measured by a chromatographic detector so as to avoid problems typically encountered when corrosive substances are analyzed (i.e., corrosion of instruments, decreases in instrument sensitivity, and frequent instrument failures). The conditions for gas chromatographic isolation of flue gas components were determined. Satisfactory results were achieved in a column filled with type S-80 silochrome silanized with hexamethyldisilazane and in a column filled with chromaton rinsed with acid and silanized with hexamethyldisilazane with trifluoropropylmethylsilicon applied to it in the amount of 10 percent of the mass of the carrier. The resultant gas chromatographic separation of components was sufficient to completely eliminate any mutual effect of oxygen, chlorine, and hydrogen chloride. The best separation of

CO and CO_2 was achieved in a column filled with S-80 silanized silochrome. The silochrome did need to be regenerated frequently because of its high-adsorption properties and high retention of traces of moisture. The best results related to reaction-gas chromatographic determination of HCl were obtained by using lithium carbonate as a reagent. The chlorine and hydrogen chloride contents of the flue gases studied could be obtained by the amount of carbon dioxide released. Detection of components based on heat conduction was used in cases of high concentrations of Cl_2, HCl, CO, CO_2, and SO_2. In cases of low concentrations of CI_2, HCl, CO, CO_2, and SO_2, determination sensitivity was increased by hydrogenating the separated oxides and carbon dioxide and using highly sensitive and selective detection of their components. Low concentrations of sulfur dioxide in the study flue gases were determined by using high-sensitivity selective flame-photometric detection. The optimal flow rate conditions for this process were established as follows (cm^3/min): helium gas coolant, 50; hydrogen, 60; air, 120. The studies performed thus established the promise of the method of gas chromatography analytic testing of the composition of process and flue gases generated during the production of titanium and magnesium products. Tables 3.

NTIS
ATTN PROCESS 103
5285 PORT ROYAL RD
SPRINGFIELD VA 22161

2

Foreign Broadcast Information Service (FBIS) and Joint Publications Research Service (JPRS) publications contain political, military, economic, environmental, and sociological news, commentary, and other information, as well as scientific and technical data and reports. All information has been obtained from foreign radio and television broadcasts, news agency transmissions, newspapers, books, and periodicals. Items generally are processed from the first or best available sources. It should not be inferred that they have been disseminated only in the medium, in the language, or to the area indicated. Items from foreign language sources are translated; those from English-language sources are transcribed. Except for excluding certain diacritics, FBIS renders personal names and place-names in accordance with the romanization systems approved for U.S. Government publications by the U.S. Board of Geographic Names.

Headlines, editorial reports, and material enclosed in brackets [ ] are supplied by FBIS/JPRS. Processing indicators such as [Text] or [Excerpts] in the first line of each item indicate how the information was processed from the original. Unfamiliar names rendered phonetically are enclosed in parentheses. Words or names preceded by a question mark and enclosed in parentheses were not clear from the original source but have been supplied as appropriate to the context. Other unattributed parenthetical notes within the body of an item originate with the source. Times within items are as given by the source. Passages in boldface or italics are as published.

SUBSCRIPTION/PROCUREMENT INFORMATION

The FBIS DAILY REPORT contains current news and information and is published Monday through Friday in eight volumes: China, East Europe, Central Eurasia, East Asia, Near East & South Asia, Sub-Saharan Africa, Latin America, and West Europe. Supplements to the DAILY REPORTs may also be available periodically and will be distributed to regular DAILY REPORT subscribers. JPRS publications, which include approximately 50 regional, worldwide, and topical reports, generally contain less time-sensitive information and are published periodically.

Current DAILY REPORTs and JPRS publications are listed in *Government Reports Announcements* issued semimonthly by the National Technical Information Service (NTIS), 5285 Port Royal Road, Springfield, Virginia 22161 and the *Monthly Catalog of U.S. Government Publications* issued by the Superintendent of Documents, U.S. Government Printing Office, Washington, D.C. 20402.

The public may subscribe to either hardcover or microfiche versions of the DAILY REPORTs and JPRS publications through NTIS at the above address or by calling (703) 487-4630. Subscription rates will be provided by NTIS upon request. Subscriptions are available outside the United States from NTIS or appointed foreign dealers. New subscribers should expect a 30-day delay in receipt of the first issue.

U.S. Government offices may obtain subscriptions to the DAILY REPORTs or JPRS publications (hardcover or microfiche) at no charge through their sponsoring organizations. For additional information or assistance, call FBIS, (202) 338-6735,or write to P.O. Box 2604, Washington, D.C. 20013. Department of Defense consumers are required to submit requests through appropriate command validation channels to DIA, RTS-2C, Washington, D.C. 20301. (Telephone: (202) 373-3771, Autovon: 243-3771.)

Back issues or single copies of the DAILY REPORTs and JPRS publications are not available. Both the DAILY REPORTs and the JPRS publications are on file for public reference at the Library of Congress and at many Federal Depository Libraries. Reference copies may also be seen at many public and university libraries throughout the United States.